AN ABSTRACT OF THE THESIS OF

Stephen P. Hendricks for the degree of Doctor of Philosophy in Biochemistry and Biophysics presented on March 12, 1998.

Title: Regulation of Ribonucleotide Reductase Analyzed by Simultaneous Measurement of the Four Enzyme Activities.

Abstract approved: Redacted for Privacy

Christopher K. Mathews

The first committed step in DNA biosynthesis occurs by direct reduction of ribonucleotides. This reduction is catalyzed by ribonucleotide reductase (RNR), an enzyme which uses a unique radical mechanism to facilitate the transformation. All four DNA precursors are synthesized by a single enzyme. Therefore, an intricate pattern of regulation has evolved to insure that RNR generates the proper quantity of each deoxyribonucleotide. It is this regulation, and conditions that influence this regulation, that are the central focal points of this dissertation.

The studies described in this thesis have been aided by the development of a novel RNR assay. Unlike the traditional assay, this new procedure permits the simultaneous monitoring of all four RNR activities. This four-substrate assay was used to investigate whether the four enzyme activities of RNR were differentially sensitive to inhibition by the radical scavenger, hydroxyurea. The assay results, along with the results of a technique that measured enzyme inhibition as a function of radical decay, suggest that all activities of

RNR are equally inhibited by hydroxyurea. Instead of differential inhibition, it appears that the activity level of RNR determines the relative sensitivity to hydroxyurea.

The effects of nucleotide effectors and substrates on the relative turnover rates of the vaccinia virus and T4 phage RNR were also investigated by use of the four-substrate assay. When physiological concentrations of the allosteric effectors and substrates were added to the reaction mixtures, both enzyme forms produced dNDPs in ratios that approximate the nucleotide composition of their respective genomes. Non-physiological nucleotide concentrations generated significantly different product profiles, indicating that RNR has evolved to function within a defined nucleotide environment. Interestingly, the substrate component of the nucleotide environment proved to be as important as the allosteric effectors in modulating the reaction rates. Although the allosteric effects of nucleoside triphosphates have been known for some time, little attention has been given to the potential role that substrates play in the regulation of RNR. The results from my research suggest that the regulation of RNR *in vivo* results from a complex interplay between the enzyme and its substrates, products, and allosteric effectors.

Regulation of Ribonucleotide Reductase Analyzed by Simultaneous Measurement of the Four Enzyme Activities

by

Stephen P. Hendricks

A THESIS

submitted to

Oregon State University

in partial fulfillment of
the requirements for the
degree of

Doctor of Philosophy

Completed March 12, 1998
Commencement June, 1998

Doctor of Philosophy thesis of Stephen P. Hendricks presented on March 12, 1998

APPROVED:

Redacted for Privacy

Major Professor, representing Biochemistry and Biophysics

Redacted for Privacy

Chair of Department of Biochemistry and Biophysics

Redacted for Privacy

Dean of Graduate School

I understand that my thesis will become part of the permanent collection of Oregon State University libraries. My signature below authorizes release of my thesis to any reader upon request.

Redacted for Privacy

Stephen P. Hendricks, Author

Acknowledgements

I would like to thank my advisor, Dr. Christopher K. Mathews, for giving me the opportunity to work on such an exciting project. He has been a good friend and mentor. I would also like to thank my committee members, Drs. Pui Shing Ho, Victor L. Hsu, William H. Gerwick, and Russel H. Meints for the time and effort that they spent on my thesis. Special thanks go to Drs. Gary F. Merrill, Kevin Ahern, and Indira Rajagopal for their support, advice, and friendship during my time at Oregon State University.

Of course, none of this would have been possible had it not been for my parents, Thomas P. and Maria M. Hendricks. I thank them with all my heart. I also want to acknowledge my brothers, Thomas P. and Mark P. Hendricks, for the support that they have given me through the years. Finally, I wish to thank Cynthia S. Du Puy for encouraging me to go back to school and supporting me throughout the process.

Table of Contents

Table of Contents (Continued)

List of Figures

List of Figures (Continued)

List of Tables

Regulation of Ribonucleotide Reductase Analyzed by Simultaneous Measurement of the Four Enzyme Activities

Chapter 1

The Structure and Function of Ribonucleotide Reductase

Stephen P. Hendricks

Introduction

With the exception of the RNA-containing viruses, the genetic material of all organisms on Earth is DNA. In the 1950s, Arthur Kornberg accurately predicted that, like other biosynthetic processes, DNA synthesis was driven energetically by the polymerization of activated substrates. These substrates were determined to be in the form of 2´-deoxyribonucleoside 5´-triphosphates (dNTPs). Kornberg's laboratory later purified the enzyme responsible for the polymerization of DNA and made the observation that all four dNTPs were required in the process (Lehman *et al.*, 1958).

Since the time that the general properties of the enzymatic synthesis of DNA were first described, much has been learned about the process. One important aspect of DNA synthesis is the amazing fidelity with which the template is replicated, and much is now known about the factors that affect this fidelity. Indeed, for DNA to serve as an effective medium for encoding the genetic instructions of the cell, a nearly perfect copy must be produced every time cell division occurs. The error frequency for DNA replication is on the order of 10^{-6} to 10^{-10} per nucleotide replicated depending on the organism (Drake, 1991). Much of the fidelity of DNA synthesis can be attributed to the enzymes which catalyze the polymerization of dNTPs. However, other factors also contribute to the replication accuracy of the cell. One such factor is proper maintenance of the supply of substrates to the replication enzyme. Not only are all four dNTPs required for the reaction to proceed, as Kornberg and coworkers demonstrated, we now know that the fidelity of DNA replication is highly dependent on the relative amounts of these precursors (Kunz *et al.*, 1994).

Many enzymes contribute to the synthesis of dNTPs, and a large portion of these are regulated in a way which assures that the synthesis rates of all four nucleotides reflect the quantities required by the polymerase. The first step in the *de novo* synthesis of dNTPs is

catalyzed by one of these highly regulated enzymes—ribonucleotide reductase (RNR)—and it is this enzyme which is the focus of this thesis.

In 1958, Peter Reichard observed that the conversion of ribose to deoxyribose occurred at the nucleotide level (Reichard, 1958). Later work determined that the deoxyribonucleotides that were used in the production of DNA were produced by the direct reduction of ribonucleoside 5′-diphosphates (rNDPs). Eventually it was determined that a single enzyme, RNR, was ultimately responsible for the *de novo* synthesis of all four of the deoxyribonucleotides needed for DNA replication.

Figure 1 provides a general overview of the pathways for the *de novo* biosynthesis of the dNTPs in eukaryotes and many prokaryotes. Three of the four dNTPs, 2′-deoxycytidine 5′-triphosphate (dCTP), 2′-deoxyadenosine 5′-triphosphate (dATP), and 2′-deoxyguanosine 5′-triphosphate (dGTP), are produced exactly as determined by Reichard, by reduction of the corresponding ribonucleoside diphosphates. In the first step shown in Figure 1, RNR produces the 2′-deoxyribonucleoside 5′-diphosphates (dNDPs) by reducing the 2′-carbon of the rNDP substrate. The dNDPs are subsequently phosphorylated to the triphosphate level by the enzyme nucleoside diphosphate kinase (NDPK).

The production of thymidine 5′-triphosphate (dTTP) is slightly more complicated and proceeds through two distinct pathways. The primary source of dTTP comes from the deamination of 2′-deoxycytidine 5′-monophosphate (dCMP) produced by the dephosphorylation of deoxycytidine diphosphate (dCDP). Deamination of dCMP produces 2′-deoxyuridine 5′-monophosphate (dUMP), which is the substrate for thymidylate synthase (TS). In a reaction which utilizes N^5,N^{10}-methylene tetrahydrofolate as the source of the one-carbon unit, TS converts dUMP to thymidine 5′-monophosphate (dTMP). dTMP is then phosphorylated to the deoxyribonucleoside triphosphate by two distinct nucleotide kinases. The other pathway leading to dTTP goes through 2′-deoxyuridine 5′-diphosphate (dUDP) produced by the RNR-catalyzed reduction of uridine

5′-diphosphate (rUDP). As a result of reactions which culminate in the net loss of one phosphate, dUDP is converted to dUMP. The dUMP produced by this pathway is further metabolized to dTTP in the same manner that the dUMP produced from dCMP deamination is metabolized.

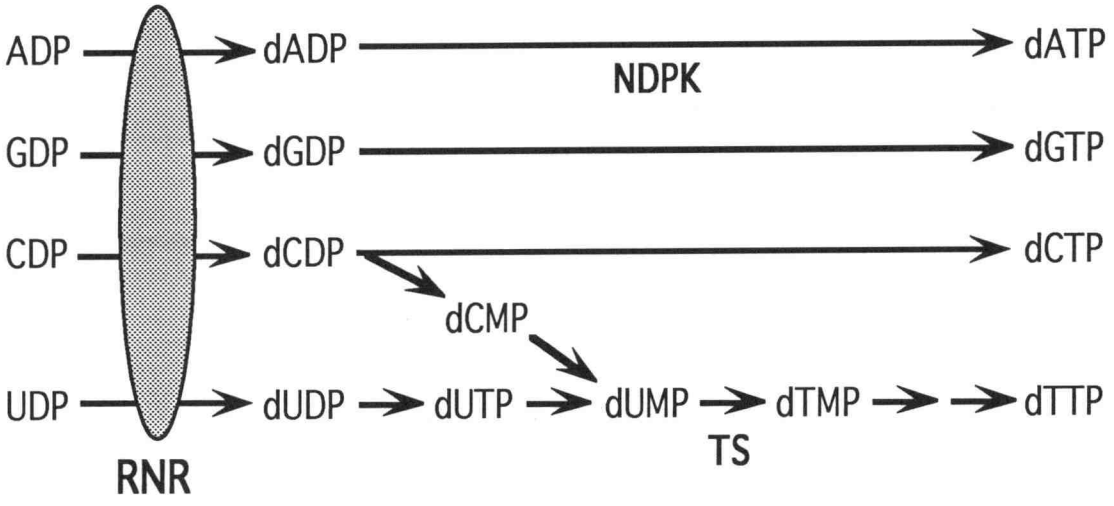

Figure 1 **Overview of DNA precursor (dNTP) biosynthesis.** The enzymes pertinent to this introduction are RNR, ribonucleotide reductase; NDPK, nucleoside diphosphate kinase; and TS, thymidylate synthase.

A concept fundamental to the understanding of the role of RNR in dNTP biosynthesis is that the same protein produces all four deoxyribonucleotide products. Furthermore, the products of RNR are used exclusively for the production of dNTPs—the building blocks for DNA synthesis. Therefore, Nature has evolved a highly sophisticated pattern of regulation to control the reactions catalyzed by RNR. To insure that a proper balance of the four products is maintained, the substrate specificity of RNR is allosterically regulated. Maintaining a proper ratio of the products of RNR may be required to insure that all four of the dNTPs are efficiently supplied to DNA polymerase, at the time at which they are needed. In light of the evidence that indicates that dNTP pool imbalances can lead to

mutagenesis (Kunz *et al.*, 1994), the maintenance of the proper RNR product ratio may be of critical importance to the long-term survival of a species. In many forms of RNR, the overall activity of the enzyme is controlled as well. This may be accomplished allosterically, as in the case of substrate specificity, or may be mediated through synthesis or degradation of the protein itself. The control of overall RNR activity has probably evolved to limit the production of dNTPs to times when DNA is being replicated or repaired.

Interestingly, in most mammalian cell lines and tissues that have been studied, the dNTP pools are not truly balanced. Instead, the relative amounts of the four common dNTPs are asymmetric in a way that doesn't necessarily reflect the genomic base composition. In general, the DNA precursor pools are heavily biased toward dTTP and dATP. The dGTP pool is normally underrepresented and in many cases may represent as little as 5-10% of the total dNTPs (Mathews and Ji, 1992; Traut, 1994).

The cause of this natural imbalance, however, remains elusive. One obvious possibility for the source of this dNTP pool asymmetry is RNR. Because RNR reduces all four rNDPs in a highly regulated way, it is possible that this intricate control is responsible for the pool asymmetries. It is also possible that this asymmetry is created by the dNTP biosynthetic machinery downstream of RNR or by the salvage pathway enzymes. In order to address the possible role of RNR in the generation of the dNTP pool asymmetry in mammalian cells, I have performed experiments which will be described in later chapters.

RNR is categorized into three primary classes. These classes vary considerably at all four levels of protein structure, require different cofactors for activity, and have substrate requirements which differ based on the level of phosphorylation (i.e. rNDPs vs. rNTPs). Despite these differences, a unique radical-dependent mechanism of catalysis appears to be common to all three classes of RNR. In addition, the pattern of allosteric regulation, specifically in terms of substrate specificity, is almost identical for all the classes. The similar catalytic mechanism and allosteric behavior have led to the belief that all of the

classes of RNR have evolved from a common ancestor through divergent evolution. According to this belief, although the proteins have changed significantly in sequence, mutations which disrupt the regulation of substrate specificity or change the mode of catalysis have been selected against (Reichard, 1993).

Class I

The enzymes that form the Class I RNRs are characterized by having a stable tyrosyl radical and an oxygen-linked diferric iron center. The Class I RNRs are found in all higher organisms and most prokaryotes examined to date. The enzyme from *Escherichia coli* is the best characterized of all RNRs and serves as the prototype for the Class I enzymes. The active holoenzyme structure of the prototypical Class I enzyme is an $\alpha_2\beta_2$ heterotetramer (Brown and Reichard, 1969a). According to convention (Fontecave *et al.*, 1992), the larger α_2 homodimer is usually referred to as R1 and the smaller β_2 homodimer is called R2. This nomenclature will be used from this point on when referring to the individual homodimers.

The smaller β_2 homodimer, R2, contains the stable tyrosyl radical, which is required for enzyme activity, and a closely associated dinuclear iron center. Each protomer of the R2 from *E. coli* is composed of 375 amino acids. The total molecular weight of the dimer is 86.7 kDa. Each functional dimer contains 4 atoms of iron (2 per protomer) and one tyrosyl radical, on average. The iron center participates together with molecular oxygen to generate and stabilize the tyrosyl radical (Fontecave *et al.*, 1992; Bollinger *et al.*, 1991). This class of RNR is functional only under aerobic conditions due to the requirement for molecular oxygen. The presumed function of R2 is to provide the tyrosyl radical, which is used by the larger homodimer R1, for activation of the ribose ring of the substrate in the first step of ribonucleotide reduction.

Each *E. coli* R1 protomer consists of 762 amino acids (85.7 kDa) and contains three nucleotide binding sites. One of these sites functions as the active site where the ribonucleotide substrates bind (von Döbeln and Reichard, 1976), which in the case of the Class I enzymes, are ribonucleoside diphosphates (rCDP, rUDP, rADP, and rGDP). The other two nucleotide binding sites are allosteric sites, both of which function through the binding of ATP or certain dNTPs (Brown and Reichard, 1969b). One of these allosteric sites controls the overall activity of the enzyme and is therefore called the activity site. Binding of ATP to this allosteric site results in general activation of the enzyme. Binding of dATP to this site results in general inhibition of the enzyme. Traditionally, this site was called the low-affinity site, since dATP was found to bind with less affinity to this site than the second allosteric site. The second allosteric site, historically referred to as the high-affinity site, controls the relative substrate specificity of the enzyme and is now generally referred to as the specificity site. Binding of nucleoside triphosphates to this site modifies the substrate preference of the enzyme. For example, when dGTP binds to the specificity site, the protein undergoes a conformational change to a conformer which prefers rADP as substrate. Binding of dTTP to the specificty site results in an enzyme conformer with a preference for rGDP reduction. Binding of either ATP or dATP to this site on R1 stimulates reduction of rCDP and rUDP. Interestingly, dCTP does not act as an allosteric effector of RNR.

Table 1 summarizes the general allosteric behavior for most forms of the Class I RNRs. Some evidence, both published (Chang and Cheng, 1979; Cory *et al.*, 1985) and presented in Chapter 4 of this thesis, suggests that allosteric regulation may also occur by the binding of nucleoside diphosphates to one, or both, of these nucleotide binding sites. In addition to the stable tyrosyl radical of R2, the activity of the holoenzyme requires the participation of five highly conserved, cysteine residues found in the R1 subunit. These cysteines have been shown to act in concert to carry out the reduction process (Thelander, 1974; Mao *et*

al., 1992a-c). Ribonucleotide reduction requires an input of two electrons per catalytic event. This supply of electrons, or reducing equivalents, is shuttled to the active site via

Table 1 *Regulation of the activities of Class Ia RNR*

Nucleotide bound in **activity site**	Nucleotide bound in **specificity site**	Activates reduction of	Inhibits reduction of
ATP	dATP or ATP	rUDP and rCDP	
ATP	dGTP	rADP	rUDP and rCDP
ATP	dTTP	rGDP	rUDP and rCDP
dATP	any one		all

four of these five cysteine residues, which function in redox-active pairs. In the *E. coli* R1 protein, one of these cysteine pairs is located in the active site (C225 and C462) and participates directly in the reduction of substrate. The other pair (C754 and C759), functions to shuttle the reducing equivalents from the exogenous electron source to the cysteine pair at the active site. The fifth required cysteine, C439, has been implicated as the protein residue which forms a transient cysteinyl radical responsible for initiating catalysis (see mechanism below).

In vivo, the ultimate source of electrons used to reduce ribonucleotides comes from NADPH. During substrate turnover the active site cysteines, C225 and C462, are oxidized to a disulfide. To enter another round of catalysis, this newly formed cystine must be reduced. The reducing equivalents for this reduction are shuttled via the second pair of cysteines, C754 and C759, to the active site cystine. Cysteine residues 754 and 759 receive their electrons from either thioredoxin or glutaredoxin, two small multifunctional redox-active proteins, which interact with RNR (Holmgren, 1988). Thioredoxin is

reduced by thioredoxin reductase, which in turn gets its electrons directly from NADPH. Glutaredoxin gets its electrons by oxidizing a pair of glutathiones. The oxidized glutathione is reduced by glutathione reductase which uses NADPH as its electron source.

In vitro, the electrons can be supplied by small dithiol-containing molecules like dithiothreitol (DTT). These dithiol compounds, however, are not as effective in serving as reductants of RNR as the protein-based redox systems and therefore the rate of substrate turnover is generally much lower when they are used as the source of reducing equivalents. For example, when DTT is used, the rate of rCDP reduction by the T4 bacteriophage RNR is 10% of the rate obtained when glutaredoxin is present (Berglund, 1972). By comparing the enzyme activities of a series of cysteine-to-serine site-directed mutants, it was determined that DTT can bypass the redox-active cysteine pair, C754 and C759, and directly reduce the cysteines at the active site after each catalytic event (Mao *et al.*, 1992). Glutaredoxin, on the other hand, was unable to supply electrons to C754S and C759S mutants, corroborating that glutaredoxin functions as an electron source for RNR through interactions with the C754 and C759 cysteine pair.

Recently, the Class I enzymes have been further divided into two subclasses, Class Ia and Ib (Jordan *et al.*, 1996). The new subdivision, Class Ib, is made up of proteins with properties very similar to the Class Ia enzymes and are found in enterobacteriaceae including *E. coli*. Like the Class Ia proteins, the Class Ib enzymes reduce ribonucleoside diphosphates, the functional holoenzyme form is an $\alpha_2\beta_2$ heterotetramer, and the β_2 dimer contains an iron center and tyrosyl radical (Jordan *et al.*, 1994). However, the Class Ib enzymes do differ significantly from the Class Ia enzymes in their regulation of overall activity: they are not inhibited by dATP (Eliasson *et al.*, 1996). In the case of the Class Ib enzyme from *Salmonella typhimurium*, dATP stimulates reduction of rCDP at concentrations which completely inhibit the Class Ia enzymes. The regulation of substrate specificity, on the other hand, is essentially the same as for the Class Ia RNRs.

All known Class Ib R1 proteins lack the last 50 to 60 N-terminal amino acids which are present in the Class Ia R1 proteins. Since the Class Ib enzymes also functionally lack the dATP inhibition, it has been proposed that the activity site may be located in this region of the Class Ia proteins. In support of this proposal is the finding that the Class Ib protein from *S. typhimurium* contains two, rather than three, nucleotide binding sites (Eliasson *et al.*, 1996). One of these sites is the active site where the rNDP substrates bind, and the other is the Class Ib equivalent of the specificity site which controls substrate specificity through the binding of dNTP effectors. The function of this subclass of RNR in organisms like *E. coli* which also encode and express the Class Ia enzyme is unknown.

Class II

The Class II enzymes are found only in microorganisms and are classified as the adenosylcobalamin-dependent RNRs. The first example of an RNR which required adenosylcobalamin for activity was found in the microorganism *Lactobacillus leichmannii* (Blakley and Barker, 1964). The enzyme is a functional monomer with a molecular weight (89.1 kDa) similar to the R1 protomer of *E. coli.* Unlike Class I, in this class of RNRs both the substrates and allosteric modulators are nucleoside triphosphates. The enzyme from *L. leichmannii* converts rNTPs to the corresponding dNTPs and is therefore referred to as a ribonucleoside triphosphate reductase. Like the Class I enzymes, the substrate specificity is regulated by the binding of dNTPs to a single allosteric site on the protein. Thus, two of the products of the Class II RNRs (dATP and dGTP) are immediately able to act as allosteric effectors for regulation of this enzyme. This class of RNR is not inhibited by dATP as the Class Ia enzymes are. Presumably, the lack of dATP-mediated inhibition is due to the absence of a second allosteric nucleotide binding site analogous to the activity site of the Class Ia enzymes (Chen *et al.*, 1977).

The function of adenosyl cobalamin in the Class II RNRs is similar to the function of the R2 homodimer in the Class I enzymes—it is the coenzyme which generates the radical required for enzyme activity (Hamilton *et al.*, 1972). Like the Class I enzymes, five cysteine residues have been implicated by site-directed mutagenesis to be involved in ribonucleotide reduction by the *L. leichmannii* RNR. Four of these cysteines shuttle electrons to the substrate and are maintained in the reduced state by transthiolation with either thioredoxin or glutaredoxin (Booker *et al.*, 1994). The last cysteine of this group has recently been demonstrated to be the residue which forms a transient cysteinyl radical, a critical component of the catalytically-active enzyme (Licht *et al.*, 1992).

Class III

The generation of the tyrosyl radical and iron-oxo center in the Class I RNRs is oxygen dependent and therefore Class I enzymes are inactive under conditions of anaerobiosis. The Class II enzymes utilize S-adenosylcobalamin as the cofactor for radical generation and are active under either aerobic or anaerobic conditions. The Class III RNRs are found in organisms which can grow anaerobically but do not encode the S-adenosylcobalamin-dependent enzyme. Organisms which contain this form of RNR include *E. coli* (Fontecave *et al.*, 1989) and the bacteriophage T4 (Young *et al.*, 1994).

Similar to the $\alpha_2\beta_2$ structure of the Class I enzymes, the Class III RNRs consist of two closely associated homodimeric proteins. The smaller homodimer, like the R2 dimer of the Class I enzymes, functions to generate the radical required for enzyme activity. However, this protein contains an iron-sulfur cluster instead of the oxygen-linked dinuclear iron center in R2 (Ollagnier *et al.*, 1996). Activation of this enzyme occurs by an S-adenosyl-methionine-dependent reaction resulting in formation of an oxygen-sensitive glycine radical in the large homodimer. In *E. coli* this radical forms at Gly681 and in T4 bacteriophage the glycine radical occurs at position 580 (Young *et al.*, 1996).

Like the Class II enzymes, the Class III anaerobic RNRs require rNTPs as substrates. The allosteric regulation of this class is very similar to the Class Ia enzymes in that there are two allosteric sites which control specificity and overall activity. However, these sites cannot be distinguished as being either an activity site or a specificity site. Instead, one site is referred to as the purine site and one the pyrimidine site. Binding of ATP to the pyrimidine site activates the enzyme for reduction of rCTP and rUTP. At the purine site, dGTP binding stimulates ATP reduction and dTTP binding stimulates GTP reduction. Binding of dATP to either site results in inhibition (Eliasson *et al.*, 1994). Although the function of these two allosteric sites differs from the function of the allosteric sites in the Class Ia enzymes, the final outcome is the same: dATP is a general inhibitor of enzyme activity, and the other allosteric effectors act to specifically enhance the reduction of a particular substrate.

Unlike the other two classes, the source of reducing equivalents for the Class III enzyme from *E. coli* is not the cysteine thiols of glutaredoxin or thioredoxin. Instead, the *E. coli* Class III RNR uses formate as the source of electrons for the reduction of ribonucleotides (Mulliez *et al.*, 1995). Thus, *E. coli* uses completely different enzymes and electron donors for the production of dNTPs during anaerobic and aerobic growth. This strengthens the speculation that the Class III enzymes arose early during evolution and may be the closest ancestor of the first enzyme used to reduce ribonucleotides.

As mentioned previously, it has been proposed that the three classes of RNR have evolved through divergent evolution. According to this proposal, the common ancestor of the modern RNRs most closely resembled the Class III enzyme (Reichard, 1993). This proposal is based on the two assumptions. The first assumption is that ribonucleotide reduction requires a radical mechanism, and the second is that DNA evolved prior to photosynthesis and the advent of an oxygen-rich atmosphere. The Class III enzymes require adenosylmethionine and anaerobic conditions to generate the protein radical. The lack of oxygen in the primordial environment makes this mechanism of radical formation a

logical choice for the original RNR. Such a radical-generating mechanism is also used by pyruvate formate lyase, a key enzyme in anaerobic energy metabolism. It is speculated that the glycyl radical mechanism may have arisen early during evolution as a means for anaerobic energy metabolism and the first RNR may have exploited it for the reduction of ribonucleotides. As the oxygen concentration in the atmosphere increased, the oxygen-sensitive glycyl radical became inoperative. Therefore, new ways of generating a stable protein radical were required to compensate for the increasing oxygen. This requirement led to major changes in protein structure and the evolution of the Class I and II enzymes.

Probably the best evidence in support of divergent evolution is the similar allosteric behavior common to all three types of RNR. Specifically, the allostery which determines substrate specificity is highly conserved within all classes of RNR: ATP (and dATP when it is not inhibitory) always activates reduction of the pyrimidine substrates, dGTP activates reduction of the adenosine nucleotide substrates, and dTTP activates reduction of the guanosine nucleotide substrates.

Reaction mechanism of ribonucleotide reduction

All three classes of ribonucleotide reductase catalyze the reduction of ribonucleotides using a unique radical mechanism—a fact which is consistent with the idea that the different forms of RNR have arisen through divergent evolution. In the early 1970s a mechanism for ribonucleotide reduction by the *E. coli* enzyme was proposed (Thelander, 1974). In this paper, it was demonstrated that the *E. coli* RNR holoenzyme catalyzed the reduction of ribonucleotides at the expense of sulfhydryls in R1. Using the *in vivo* reducing system, thioredoxin and thioredoxin reductase, the kinetics of RNR catalysis was shown to be consistent with a ping-pong mechanism. This meant that the enzyme alternated between two forms, a reduced catalytically active form and an oxidized inactive form. The mechanism which was proposed to explain these data is as follows. In the reduction of

ribonucleotides, thioredoxin binds to R1, reduces the catalytically active sulfhydryls, and then dissociates from the enzyme. A ribonucleotide substrate then binds to the enzyme and is reduced at the expense of R1 oxidation in a radical-dependent reaction. Finally, the newly formed deoxyribonucleotide is released from the enzyme, completing the cycle.

To probe the mechanism further, nucleoside analogs were prepared in which the 2′ or 3′ position was substituted with various substituents. Two separate laboratories reported that incubation of RNR with one such analogue, [3′-^{3}H] 2′-chloro-2′deoxyuridine 5′-diphosphate (CldUDP), resulted in production of uracil, chloride ion, inorganic pyrophosphate, and substoichiometric quantities of ^3H_2O, and was accompanied by inactivation of the enzyme (Thelander *et al.*, 1976; Stubbe and Kozarich, 1980). Then, in one of the biggest breakthroughs in the understanding of ribonucleotide reduction, it was found that incubation of substrate containing tritium at the 3′-position, specifically [3′-^{3}H] rUDP, resulted in a 1° isotope effect on conversion to dUDP (Stubbe and Ackles, 1980). A similar isotope effect was also observed when [3′-^{3}H]rADP was converted to its deoxyribonucleotide product. The observation of an isotope effect during the reduction of these 3′-tritiated substrates indicates that the 3′-C–H bond is cleaved in the reaction and that the breaking of this bond is the rate-determining step. But how does the cleavage of the 3′-C–H facilitate the reduction of the 2′-carbon? To answer this question, a working hypothesis was developed which included the results obtained using the chloro analogue (CldUDP) and the observed isotope effect. In this hypothesis, cleavage of the 2′-C–OH bond of the substrate is activated by prior cleavage of the 3′-C–H bond. In the case of CldUDP, interaction with RNR results in cleavage of the 3′-hydrogen and conversion of the analogue to 3′-keto-2′-deoxyuridine diphosphate. The hydrogens of this intermediate which are alpha to the 3′-keto functionality are substantially more acidic than a normal C–H bond. Dissociation of one of these protons results in a rearrangement of electrons within the molecule culminating in the elimination of uracil and inorganic pyrophosphate and generation of a highly reactive species which was later identified as 2-methylene-3-

furanone. Nucleophilic attack on this reactive furanone by a side chain in the active site would then result in inactivation of the protein. This hypothesis also explained the small amount of ^3H_2O released when this analogue was incubated with the enzyme. Apparently, the tritium which is abstracted from the 3′-carbon of the analogue in the intial step of the reaction is occasionally accompanied by loss of label to solvent.

In these experiments with CldUDP, the amount of tritium which appeared in H_2O was low—only about 1%. Mechanistically, it is important to determine the location of the remainder of the label. To determine the fate of the 3′-hydrogen which was abstracted by RNR, rUDP deuterated at the 3′-carbon was prepared and the location of the deuterium before and after the reaction was determined by NMR (Stubbe *et al.*, 1983a). Analysis of the NMR spectra of the deuterated substrate and purified product indicated that the deuterium at the 3′ position of substrate was returned to the 3′ position in the product. Evidence for 3′-C–H bond cleavage and reformation was also found in the Class II enzyme from *L. leichmannii* using similar analogues and techniques (Stubbe *et al.*, 1983b). Since that time, similar results have been seen using the enzyme from herpes simplex virus (Ator *et al.*, 1986).

Based on the available evidence, the reaction mechanism is thought to be initiated by formation of an oxidized cysteinyl radical at the active site (C439 in *E. coli* R1 and C408 in the *L. leichmannii* Class II enzyme). Just recently, direct evidence for the existence of this transient cysteinyl radical in the Class II enzyme from *L. leichmannii* was demonstrated using electron paramagnetic resonance (Licht *et al.*, 1996). This transient radical species is thought to be generated through hydrogen abstraction of the cysteinyl thiol by another radical in the enzyme. In *E. coli*, this is presumably the stable tyrosyl radical of R2. In the current model of the Class I holoenzyme complex from *E. coli*, the distance between the tyrosyl radical in R2 and the active site in R1 is 35-40 Å (Sjöberg, 1994). The abstraction event is proposed to occur via long range electron transfer through a highly conserved hydrogen bonded network which spans the distance from the R2 radical to the active site

(Nordlund *et al.*, 1993). Once formed, this transient thiolyl radical abstracts the hydrogen from the 3′ position of the ribose ring creating a protein-bound substrate radical (see Figure 2). The 2′-hydroxyl of the ribose is then protonated by an active site residue. Protonation of the 2′-hydroxyl is followed by loss of H_2O from this position resulting in the formation of a radical cation intermediate. A hydride equivalent (a proton + two electrons) is then transferred to the 2′ position of the radical cation intermediate from active site cysteines. In the *E. coli* enzyme, the hydride is thought to be donated by the C225/C462 pair of redox-active cysteines. The reaction is completed by the return of the originally abstracted hydrogen back to the 3′ position of the substrate resulting in regeneration of the protein radical.

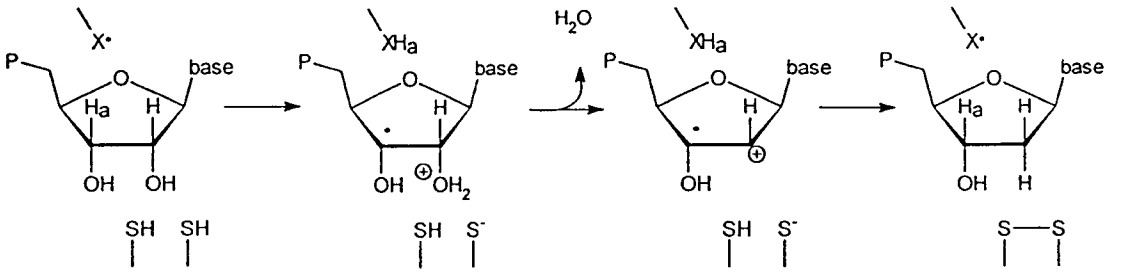

Figure 2 **The proposed reaction mechanism of RNR** (adapted from Stubbe, 1990).

The rest of this chapter, like my studies, will focus on the Class I RNRs.

Protein R2

Primary sequence homology

Although the *E. coli* R2 has served as a model for the protein in eukaryotes, there are a number of significant differences between the proteins from *E. coli* and higher organisms. The amino acid sequences of the *E. coli* and mouse proteins are only 25% identical (Thelander & Gräslund, 1994). Sequence alignments of the Class I small subunits comprise three groups of homology, each consisting of at least 50% identical amino acids. The eukaryotic proteins, including the protein from vaccinia virus, make up one group, the herpes virus proteins the second, and the *E.coli* and bacteriophage T4 proteins form the third. The R2 sequences among the three groups are highly divergent with only 16 residues being conserved for all species. Among these conserved residues in the three groups are the tyrosine residue which forms the stable radical and the iron ligands.

The eukaryotic R2 proteins form a highly homologous group of sequences to which the vaccinia and African swine fever viruses belong. As an example of the conservation within this group, the vaccinia virus amino acid sequence is ~80% homologous to the mouse R2 while the vaccinia and herpesvirus proteins are only 27% homologous (Slabaugh *et al.*, 1988). The greatest divergence in similarity among this group of R2 proteins is in the length of the amino terminus. The amino acid sequences from mammals and yeast average about 50 residues longer than the sequences from plants and viruses. These extra N-terminal residues are thought not to be involved in enzyme activity since they are missing from the R2 sequences in many species. Furthermore, N-terminal truncation of the mouse R2 does not significantly affect the activity of the holoenzyme (Mann *et al.*, 1991). Instead, the N-terminus may be involved in some aspect of R2 protein activity or turnover. Ser20 in the mouse R2 was recently shown to be phosphorylated in a cell-cycle-dependent

manner by a cdc2-related protein kinase (Chan *et al.*, 1993). The role of this kinase in cell cycle progression and the fact the the mouse R2 was phosphorylated by this enzyme during S-phase is consistent with the notion that phosphorylation may play a role in the cell cycle regulation of ribonucleotide reduction and therefore DNA synthesis.

The C-terminus of R2 is involved in protein-protein interactions with the larger R1 subunit and is essential for formation of the active holoenzyme. The sequence of the C-terminus is highly species-specific and in many cases the formation of the holoenzyme, and therefore enzyme activity, can be inhibited by peptides with a sequence corresponding to the R2 C-terminus. The ribonucleotide reductase from *E. coli* can be inhibited by the addition of a 20-mer corresponding to the terminal twenty residues of the R2 sequence, and a truncated version of the R2 protein lacking the last thirty C-terminal residues is unable to bind R1 (Sjöberg *et al.*, 1987). An interesting example of the importance of the interaction between the R2 carboxy terminus and the R1 protein was found when the R1 protein was prepared for crystallographic studies. In order to obtain X-ray quality crystals of the R1 subunit, researchers found that a 20-mer with the same sequence as the R2 carboxy-terminus was a required component of the mother liquor (see discussion on R1 structure). Furthermore, the peptide co-crystalized with the *E. coli* R1 at the site of the proposed R2 interaction surface (Uhlin & Eklund, 1994).

As in *E. coli* , the herpes simplex viral RNR proteins provide another example of the importance of the C-terminal region of R2 structure in the interaction between the R1 and R2 dimers, which is required for holoenzyme formation. A potent peptidomimetic inhibitor has been derived from the herpes R2 C-terminal sequence which shows promising *in vivo* efficacy against the herpes virus (Liuzzi *et al.*, 1994). By competing with the herpes simplex R2 for binding to R1, this peptide can inhibit holoenzyme assembly and thus inhibit viral RNR activity.

In the mouse protein, the last seven C-terminal residues of R2 have been shown to be essential for dimer-dimer interaction. Nuclear magnetic resonance (NMR) has been used to

study the mobility and conformation of the C-terminus of the mouse R2 in the presence and absence of R1 (Lycksell *et al.*, 1994). In the ^{1}H NMR spectrum of mouse R2, a number of sharp proton resonances were observed with significantly narrower line widths than the majority of resonances in the spectrum. By the use of two-dimensional NMR techniques, these resonances were assigned to the carboxy-terminal residues of R2 by comparison with the cross-peak patterns of peptides of the same sequence as the R2 carboxy-terminus, and lack of those resonances in a C-terminal truncated version of R2. One interpretation of these data is that this segment of R2 is highly mobile and essentially unstructured in solution. Upon addition of the mouse R1 protein to the R2 solution, these sharp resonances become significantly broadened, suggesting that the mobility of this portion of R2 becomes severely restricted by the heterodimer interactions responsible for holoenzyme assembly. Presumably, the flexible C-terminal tail recognizes a particular surface on the large subunit, promoting holoenzyme formation and concomitant structuring of the R2 C-terminus. It is suggested that this form of protein-protein recognition may fit into the model in which unstructured domains give rise to increased rates of specific macromolecular associations (Pontius, 1993). It has also been reported that the NMR spectrum of the small subunit of herpes simplex virus contains a number of resolved resonances corresponding to the C-terminus (LaPlante *et al.*, 1993).

In Chapter 4 of this thesis I shall provide evidence indicating that similar R2 carboxy-terminal sequences can allow for interspecies RNR activity, specifically in the case of the vaccinia virus and mouse proteins.

Structure of the R2 protein

The crystal structure of the small subunit from *E. coli* has been determined to 2.2 Å resolution (Nordlund *et al.*, 1990). The three-dimensional structure not only demonstrated what a beautiful job Nature has done in creating a protein environment which can produce,

capture, and subsequently harbour a normally highly reactive and unstable free electron, it also provided new insight into the mechanics of the reaction mechanism. The generally accepted view prior to publication of the structure was that the tyrosyl radical directly abstracted the hydrogen from the substrate, activating the ribose ring for the subsequent steps in the reaction. From the crystal structure it was obvious that this tyrosyl radical could not directly abstract the hydrogen from the substrate since this particular tyrosine residue is buried deep in the protein, 10 Å from the closest surface. Instead, it was postulated that electron transfer from the substrate to the stable tyrosyl radical occurs via a hydrogen-bonded array of highly conserved residues. These conserved residues, along with one of the irons in the iron center, provides a route for the electron to be transferred back and forth between the storage site and the active site where catalysis occurs. The proposed electron transport chain is described in greater detail in a later section.

Helices make up about 70% of the R2 protein from *E. coli*. The protein has only one β-sheet region, which forms an antiparallel hairpin turn. The main structural motif of the protein is a unique eight-helix bundle. The center of the bundle consists of a long hydrophobic helix which is surrounded by the other helices. The helices in the bundle are all relatively long, four of which comprising 30 residues or more.

The functional dimer is formed by homologous interactions between three surface helices of each subunit around the molecular two-fold axis. The helices at the subunit-subunit interface cross at an angle of approximately 140° to each other. The ellipsoidal shape of the individual subunits and the tilted interaction formed between them gives the molecule a heart shape. The tip at the bottom of the heart-shaped dimer is formed by a four-stranded sheet composed of the antiparallel β-hairpins from both subunits. Figure 3 shows the crystal structure of the R2 dimer from *E. coli* viewed from a position that emphasizes the heart-like shape of the protein.

The top lobes of the R2 dimer are believed to make up the R1 interaction surface. As discussed, it is well established that the carboxy terminus of R2 is essential for holoenzyme

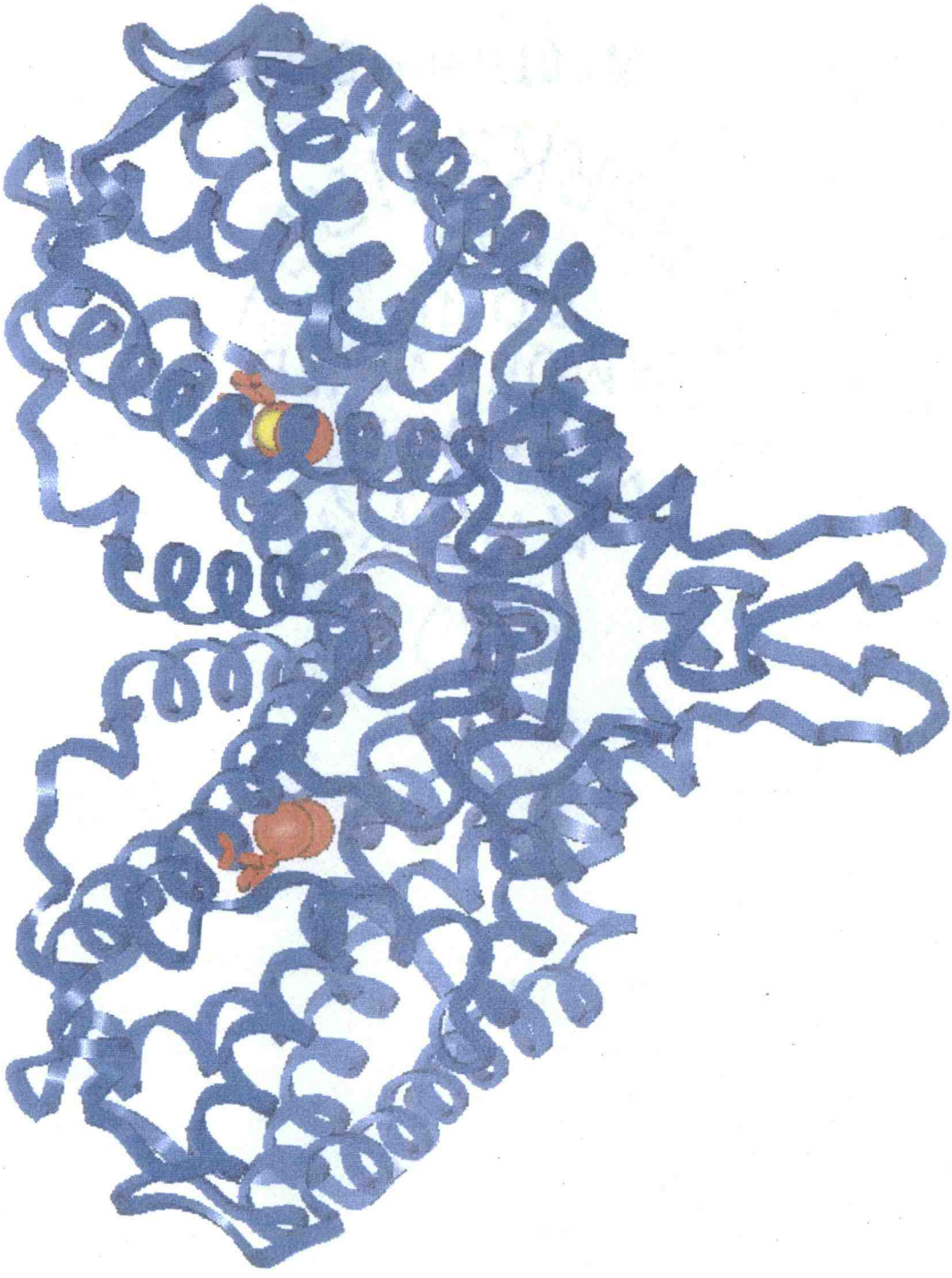

Figure 3 **Three-dimensional structure of *E. coli* R2.** The crystal structure of *E. coli* R2, shown above, was determined by Nordlund *et al.*, 1990. Indicated in the structure are the iron atoms (shown as red spheres) and the bridging oxygen atom (shown in yellow). Also highlighted in the structure is closely associated tyrosine side chain of Y122, which forms the stable phenoxy radical (shown in red).

assembly and enzyme activity. The structure of the C-terminus of R2 is not yet defined, since the last 32 residues of the protein are disordered and invisible in the crystal. However, the last resolvable C-terminal residue is located in the middle of the lobed region at the top of the R2 dimer. Thus, the carboxy terminus is located in a region consistent with the proposed R1-R2 interface. Characterization of the tertiary structure of the carboxy terminus of R2 may have to await the determination of the crystal structure of the RNR holoenzyme.

Recently, the three dimensional structure of the mammalian small subunit from mouse was determined (Kauppi *et al.*, 1996). The overall tertiary structure of the mouse protein is similar to the prokaryotic form from *E. coli*, having as its main structural motif an eight helix bundle. Like the *E. coli* structure, the mouse R2 carboxy terminus is disordered and not visible in the electron density maps. Also missing from the mouse structure are the amino terminus residues which, as discussed earlier, are not required for enzyme activity but instead may play a role in protein-protein interactions with proteins other than R1 (Mann *et al.*, 1991). The dimer interface of the mouse R2 is formed primarily by hydrophobic interactions and the residues involved in these interactions are highly conserved among the eukaryotes.

Although the overall structure is similar, there are several distinct differences between the mouse and *E. coli* R2 structures. The mouse R2 crystal structure totally lacks the β-strand motif seen in the *E. coli* protein. Thus, the tip structure seen in the *E. coli* protein is missing from the mouse protein giving it less of a heart-shaped appearance.

Relevant to this thesis, one of the more significant structural differences between the eukaryotic and prokaryotic proteins is a narrow channel, about 10 Å deep, in the mouse R2 which leads from the surface of the protein to a region within the protein interior where the tyrosyl radical and iron-oxo center are located. The channel is about 15 Å wide and lined primarily by hydrophobic amino acids. The *E. coli* R2 has a similar channel. However, in this latter case, the channel is about half the width of the channel in the mouse R2 and the

opening to the channel is blocked by the side chain of a tyrosine residue. The mouse and vaccinia virus, as well as most of the other eukaryotic proteins have a serine at this position, resulting in a larger channel opening and presumably a more accessible radical and iron center. The channel dimensions of these proteins are directly correlated with the relative ease at which radical scavenging drugs, like hydroxyurea, can inactivate the tyrosyl radical of these enzymes (Pötsch *et al.*, 1995).

Based on the high sequence homology among the eukaryotic R2 proteins, the three-dimensional structures of the other eukaryotic proteins, including the vaccinia virus R2, are expected to be very similar to the mouse protein.

The tyrosyl radical

The tyrosyl radical of the *E. coli* enzyme was the first example of a stable protein-derived free radical to be reported. EPR was used to quantitate the amount of radical, and from this measurement, a correlation between the radical content and enzyme activity was made (Ehrenberg & Reichard, 1972). The amazing stability of this protein-derived radical, when compared to model organic radicals that had been described at that time (Land *et al.*, 1961), was quite surprising. *In vitro,* the *E. coli* tyrosyl radical is stable for more than a week at 4° C. Even at 25° C, the half-life of the radical is on the order of days (Atkin *et al.*, 1973).

The surprising stability of the tyrosyl radical is no longer such an enigma since the three-dimensional structure of R2 was determined. From the structure it was obvious that the tyrosyl residue which harbours the radical is buried inside the protein and is therefore fairly inaccessible to solvent. The environment around the tyrosyl radical is primarily hydrophobic with no oxidizable residues within van der Waals contact of the radical (Nordlund *et al.*, 1992).

The stable radical is formed by a one-electron oxidation of the phenoxy ring of a specific tyrosine residue (Y122 in *E. coli* and Y177 in mouse) in a reaction between R2, iron and molecular oxygen (Atkin *et al.*, 1973; Petersson *et al.*, 1980; Bollinger *et al.*, 1991). Inactivation involves a gradual reduction of the phenoxy radical, presumably by solvent-derived reductants, resulting in formation of a normal tyrosine. In the case of the *E. coli* enzyme, the intial reduction of the radical does not change the oxidation state of the iron-oxo center and the coordination of the iron atoms is probably also unchanged (Backes *et al.*, 1989). This form of R2 is called metR2.

The iron-oxo center of R2

By the early 1970s, it was known that protein R2 was EPR-active. The R2 EPR signal was assigned to an organic radical housed in the protein and was shown to be directly correlated with enzyme activity. In addition, this organically-derived free radical was dependent on the presence of iron in the protein (Ehrenberg and Reichard, 1972). However, at that time not much was known about the chemical nature of either the organic radical or the protein-bound iron.

The initial characterization of the iron center was done using Mössbauer spectroscopy (Atkin *et al.*, 1973). The Mössbauer spectrum of *E. coli* R2 contained four lines of approximately equal intensity. The spectrum was interpreted as arising from two pairs of split absorptions which were indicative of the presence of two nonequivalent iron sites. As further evidence for this assignment, the Mössbauer spectrum of hemerythrin, a marine invertebrate oxygen-carrying protein containing a well-characterized binuclear iron center (Garbett *et al.*, 1969), was compared with the spectrum from R2. The Mössbauer spectra of the two proteins strongly resembled each other both in the number of lines and the quadrupole splitting. To further explore the nature of the iron center as it related to the radical, *E. coli* R2 was stripped of iron and then regenerated in the presence of $^{57}Fe^{+2}$.

Mössbauer and EPR spectroscopy of the ^{57}Fe-containing R2 established that the iron nuclei were diamagnetic and therefore distinct from the paramagnetic species which gave rise to the EPR signal. Resonance Raman spectroscopy was later used to determine that the non-protein ligand which bridges the two irons is an oxygen ion, specifically O^{2-} (Sjöberg *et al.*, 1982).

The positions and molar extinction coefficients of the absorbance bands in the electronic spectra of hemerythrin and R2 are also very similar. Figure 4 shows the characteristic electronic absorption spectrum of *E. coli* R2. The specific peaks of interest in the spectrum are the relatively sharp peak at 410 nm, due primarily to the tyrosyl radical, and a broad band centered at 370 nm, arising mainly from the iron center. The band centered at ~390 nm is a composite absorption due primarily to the tyrosyl radical with some overlapping absorbance from the iron-oxo center.

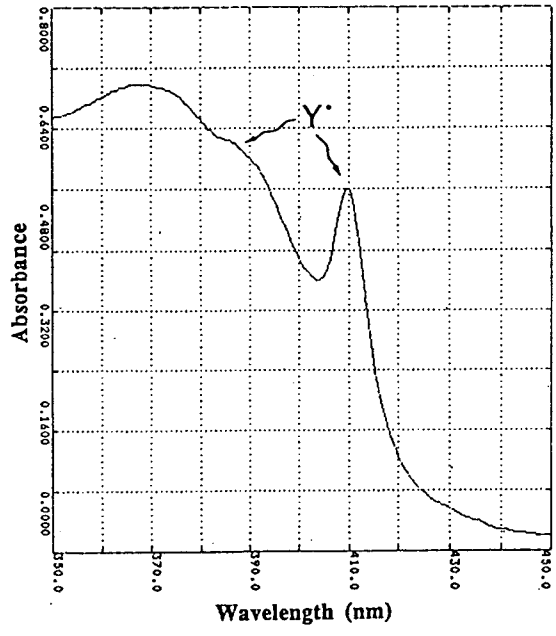

Figure 4 **Electronic absorption spectrum of *E. coli* R2.** Spectrum was recorded on a Beckman DU-64 spectrophotometer. Protein concentration was ~50 μM. The *E. coli* R2 was a gift from the laboratory of Britt-Marie Sjöberg.

The UV-vis absorption spectrum of oxyhemerythrin displays very similar iron absorption bands to the bands seen in the spectrum of *E. coli* R2. The only significant spectroscopic difference determined in this comparison was the lack of the sharp peak at 410 nm and band at 390 nm in the spectrum of hemerythrin. This was not surprising since these absorbances had already been assigned to the protein-bound radical chromophore which we know today to be the tyrosyl radical.

From these intial studies it was concluded that the iron in R2 was associated with, but not the source of, the paramagnetic entity. Instead, the paramagnetic species was assigned to a stable organic free radical (Ehrenberg and Reichard, 1972). Furthermore, it was known that destruction of the radical by treatment with NH_2OH or hydroxyurea resulted in no change in the Mössbauer or iron-associated electronic spectra, indicating that the iron center remained intact even though the protein was inactivated by this treatment (Atkin *et al.*, 1973; Ehrenberg and Reichard, 1972). What then is the function of the iron?

The electronic spectrum of R2 was not affected by the addition of reducing agents used as electron sources (thioredoxin or dithiothreitol) during enzyme catalysis. This was interpreted as meaning that the iron in R2 was not participating as an electron carrier during the catalytic cycle (Atkin *et al.*, 1973). Furthermore, other studies argued against a structural role for the iron. The apoprotein and native protein have identical electrophoretic and ultracentrifugal properties and both form 1:1 complexes with R1 (Thelander, 1973).

Instead, based on the data available at that time, it was hypothesized that the function of the iron was to generate an organic radical from a protein-bound group concomitant with binding to the apoprotein. Once the iron was bound and the radical formed, the protein-bound iron further functioned to stabilize the radical through a continued interaction (Atkin *et al.*, 1973). In the crystal structure of the *E. coli* protein, the Tyr122 is 5.3 Å from the closest iron and is located on an axis formed by the two iron atoms. Within this environment, the radical is expected to experience a significant magnetic field from the iron center and this interaction may be involved in stabilizing the radical. Studies of the

temperature dependence of EPR relaxation and line shape have verified the presence of magnetic dipolar interactions between the iron center and free radical (Sahlin *et al.*, 1987). Furthermore, when these interactions were compared in the mouse and *E. coli* R2 proteins, it was found that the effects were more pronounced for the mouse protein. This indicates that the magnetic interaction between the iron center and radical in the mouse R2 is stronger than in the *E. coli* protein.

According to this hypothesis, the iron-stabilized organic radical was the functional contribution of R2 to the active holoenzyme. A logical assumption that comes from this hypothesis is that the reduction of ribonucleotides may involve the participation of substrate- and/or protein-derived radical intermediates. This was not the first suggestion that transient radicals may be involved in the reduction of ribonucleotides. Just prior to the publishing of this hypothesis, the involvement of transient free radicals in the reduction of nucleoside triphosphates by the class II RNR from *L. leichmannii* had been proposed (Tamao and Blakley, 1973). This hypothesis remains valid today.

Ever since the iron center was first reported (Brown *et al.*, 1969b), the number of iron centers per R2 dimer has been disputed. Some data, reported prior to the publication of the crystal structure, suggested a single iron-oxo center formed at the dimer interface (Atkin *et al.*, 1973; Sjöberg *et al.*, 1987). Determination of the three-dimensional structure of R2 by X-ray crystallography put an end to this dispute, at least in the case of the protein from *E. coli* and mouse. The crystal structure of the *E. coli* R2 clearly shows that the dimer contains two equivalent iron centers. The location of these centers was confirmed by comparison with electron density maps of the iron-free, or apoR2, crystals. From the crystal structure it was determined that the iron atoms are ligated to four helices from the eight-helix bundle, two of which are located at the dimer interface.

From the crystal structure of the *E. coli* R2, a detailed description of the iron center ligands and geometry was determined. This structure is shown in Figure 5. The iron ligands consist of three glutamic acids, two histidines, one aspartic acid, two water

molecules, and the iron-linked oxygen atom. The ferric irons are bridged by two common ligands; the O^{2-} forms one bridge between the iron nuclei, and the two carboxylate oxygens of Glu115 form the second bridge. Iron 1, as denoted in Figure 5, is further ligated to His118 and both carboxylate oxygens of Asp84. The sixth ligand to Iron 1 was interpreted from the electron density to be a water molecule. Iron 2 is ligated to two glutamic acids, Glu238 and Glu204, and to His241, as well as the two common ligands. As in the case of Iron 1, a water molecule occupies the sixth coordination of Iron 2. Because both γ-oxygens of Asp84 are ligated to Iron 1, the coordination around this iron atom has the characteristics of both trigonal bipyramidal and octahedral geometries. The second iron atom lacks a bidentate ligand and therefore has a more regular octahedral geometry.

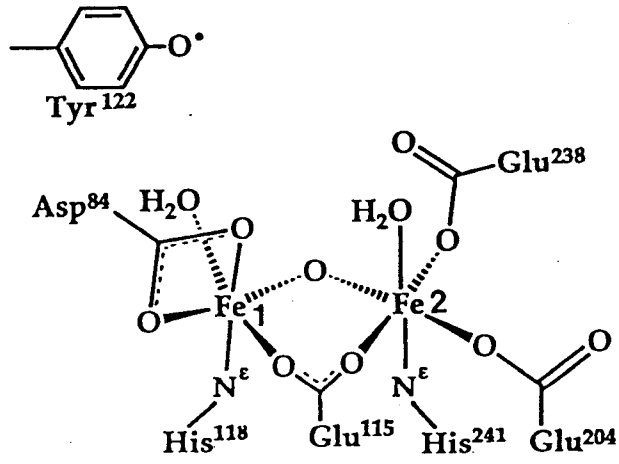

Figure 5 **Structure of the tyrosyl radical and dinuclear iron-oxo center.** This figure shows the structure of the *E. coli* R2 metal center (adapted from Nordlund *et al.*, 1990)

Sequence homologies, as discussed above, are relatively low among the R2 proteins from *E. coli* and mouse or vaccinia virus. Of the residues that are conserved within all

species are the amino acids which serve as the ligands for the iron-oxo center. Other conserved residues include the tyrosine which serves as the radical storage site, some hydrophobic residues in proximity to the radical site, and the network of amino acids which make up the putative electron transport chain.

A major distinction between the eukaryotic and *E. coli* forms of R2 is in the stability of the iron center. The mouse R2, for instance, loses 50% of its iron after 30 minutes at 37°C (Mann *et al.*, 1991), while the half-life of iron loss for the *E. coli* protein under similar conditions is on the order of several days (Atkin *et al.*, 1973).

The non-heme dinuclear iron center of R2 is found in at least two other classes of proteins and, as more metalloproteins are characterized, may prove to be a common structural motif. One of these classes which was mentioned earlier, the hemerythrins, functions as oxygen carrying proteins in certain marine invertebrates (Garbett *et al.*, 1989). Methane monooxygenases, another class of proteins containing a non-heme dinuclear iron cluster, are enzymes found in methanotrophic bacteria that oxidize methane (Fox *et al.*, 1989). In each of these three groups of proteins, the iron center functions through its reactivity with molecular oxygen. The mode of reactivity, however, is different for each protein class. In the hemerythrins, the oxygen is bound by the iron center reversibly. In the methane monoxygenases, the protein-bound ferrous irons react with molecular oxygen to form an active enzyme which catalyzes the two-electron oxidation of methane and other small saturated hydrocarbons. Finally, in R2, the diferrous iron cluster activates molecular oxygen for the one-electron oxidation of a tyrosine residue.

Assembly of the tyrosyl radical and iron center in R2

The stoichiometry for the formation of the tyrosyl radical and iron-oxo center has been extensively studied both in the mouse (Ochiai *et al.*, 1990) and the *E. coli* (Bollinger *et al.*, 1991) R2 proteins. Based on these studies, the stoichiometry is best described by the following reaction:

$$Tyr + 2\ Fe^{+2} + O_2 + e^- + 2\ H^+ \longrightarrow {}^{\bullet}Tyr + Fe^{+3}\text{–}O^{-2}\text{–}Fe^{+3} + H_2O$$

This reaction, as written, is a four-electron reduction of molecular oxygen. Two of the electrons come from the oxidation of two ferrous irons to two ferric irons. Oxidation of the tyrosine residue supplies another electron resulting in the formation of the tyrosyl radical. The source of the final electron is dependent on the experimental conditions. In the absence of other reductants, ferrous iron can provide the fourth electron. In this case, 3 moles of Fe^{+2} are oxidized per mole of tyrosyl radical formed. If ascorbate is added to the reaction, the last electron may ultimately come from this reductant. When ascorbate is present, the expected molar ratio of oxidized iron to tyrosyl radical should be 2 to 1. These theoretical values are in good agreement with the experimentally determined quantities for both the mouse and *E. coli* R2, suggesting that the formation of the iron center and tyrosyl radical is similar mechanistically in both cases. Formation of the tyrosyl radical in the mouse protein required 3.5 ± 0.5 moles of ferrous iron per mole radical, when iron was the sole reductant. When ascorbate was added, 2.6 ± 0.4 moles of iron were oxidized per mole of radical formed. For radical formation in the *E. coli* protein, the values were 3.2 ± 0.1 and 2.5 ± 0.1 moles of iron required to produce one mole of radical in the absence and presence of ascorbate, respectively.

In addition to the stoichiometry, a mechanism for the formation of the *E. coli* tyrosyl radical and iron-oxo center has been proposed (Bollinger *et al.*, 1991). A detailed

description of this reaction was made possible by the fact that the radical and iron center in the *E. coli* R2 can be removed and regenerated, and that the regeneration can be monitored by measuring the distinct spectroscopic signatures of the tyrosyl radical and iron-oxo center. Using stopped-flow absorption spectroscopy and rapid freeze-quench EPR to measure the kinetics of radical formation, two novel intermediates in the pathway leading to the active form of R2 were detected. The detection of these intermediates provided the necessary information required to deduce the mechanism.

To decipher the mechanism, the radical regeneration reaction was performed under various iron concentrations and monitored with stopped-flow absorption spectroscopy. Although the absorption spectra of the iron center and tyrosyl radical overlap, the broad band of the iron cluster centered at 370 nm and the relatively sharp band of the tyrosyl radical at 410 nm allow the kinetics of the reaction to be determined. Close examination of the time-dependent absorption spectra of the reaction revealed two critical pieces of information which were used to deduce the mechanism. First, it was determined that production of the tyrosyl radical preceded formation of the final iron-oxo center. Second, in the early spectra, recorded at time points prior to formation of the active R2, was the presence of a transient chromophore which was spectroscopically distinct from the chromophore of the final diferric iron center. This new species was designated as intermediate (U). The rate constants of the formation and decay of intermediate (U) made it kinetically competent to be a precursor of the active R2. Furthermore, since the rate constant of decay for intermediate (U) was similar to the rate constant of formation for the tyrosyl radical, it was suggested that (U) may be directly responsible for production of the radical. Under conditions of excess ferrous iron or ascorbate, this intermediate was not observed, suggesting that excess reductant prevents the intermediate from accumulating to an extent observable by normal spectroscopic techniques. Figure 6 depicts the proposed mechanism for the formation of the active form of R2 from apoR2, ferrous iron, and molecular oxygen.

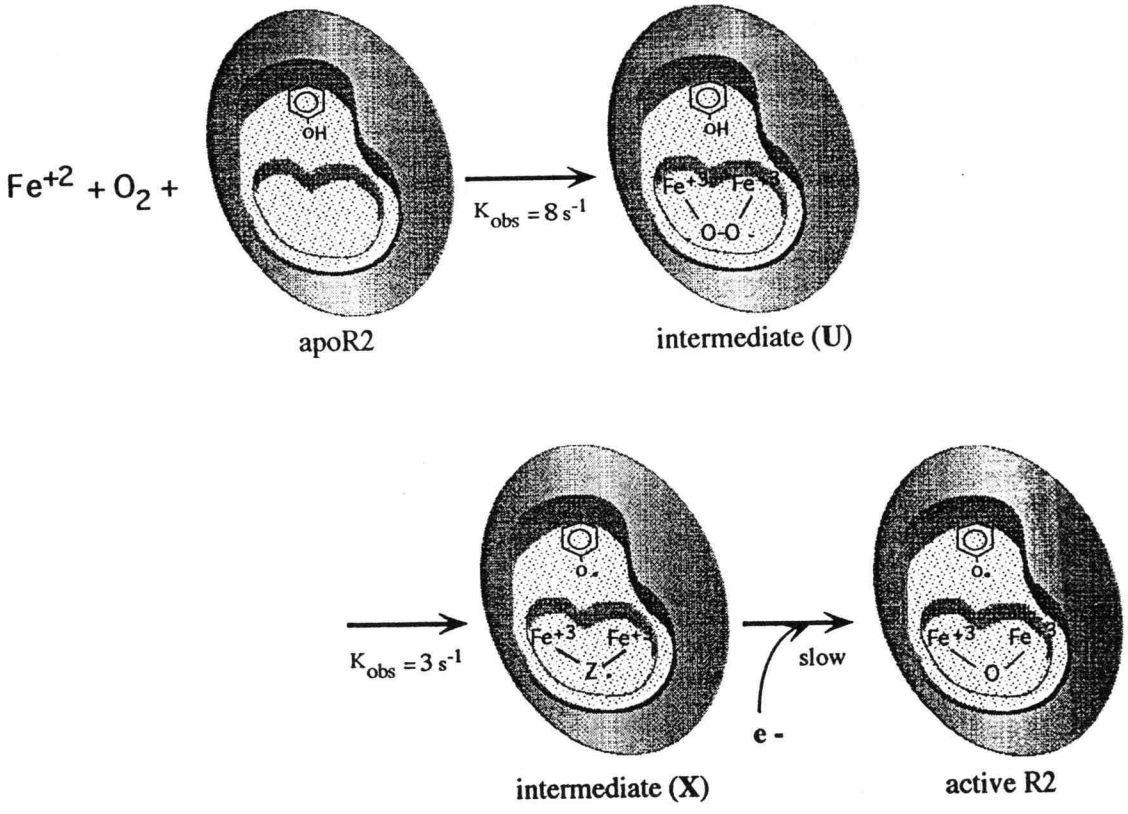

Figure 6 **Mechanism of the formation of the iron center and tyrosyl radical of R2** (adapted from Bollinger *et al.*, 1991)

To further test whether intermediate (U) was responsible for the production of the tyrosyl radical, a mutant R2, in which Tyr122 was changed to a phenylalanine, was prepared. In this Y122F mutant, the radical-generating intermediate decayed at half the rate of the intermediate in the wildtype protein. Consistent with the role of (U) as the species which generates the tyrosyl radical, the increased half-life of the intermediate in the Y122F R2 mutant was presumably due to the fact that the phenyl ring of phenylalanine is harder to oxidize than the phenoxy ring of tyrosine. Concomitant with the decay of intermediate (U) in the Y122F mutant was the appearance of a new, short-lived, signal with a λ_{max} at 410

nm. The identity of this new signal was attributed to the formation of a tyrosyl radical formed at another location in the protein, although this was not demonstrated conclusively. The short-lived nature of this new radical species is probably due to reduction by a neighboring residue or by a solvent derived-reductant.

The decay of intermediate (U) is kinetically consistent with the formation of a tyrosyl radical in both the wild-type and mutant proteins and this fact is used as evidence for the first step of the mechanism shown in Figure 6. Based on the similarity of the absorption spectra of sythetically prepared peroxodiferric organometallic compounds, the structure of the intermediate was proposed to be a μ-peroxodiferric species. Peroxo-compounds similar in structure to the μ-peroxodiferric intermediate are generally good oxidizing agents. This fact makes the proposed intermediate chemically consistent with the type of species needed to oxidize the phenoxy ring of Tyr122.

Intermediate (U) is not EPR active. However, EPR spectra of of the reaction mixture quenched at various times after the addition of iron revealed a new EPR signal, quite distinct from the tyrosyl radical spectrum, which was designated as intermediate (X). When the reaction was carried out with $^{57}Fe^{+2}$, the new EPR signal was broadened significantly, indicating that intermediate (X) is due to an iron-coupled radical. Kinetic analysis of this new EPR signal showed that it was produced at approximately the same rate as the tyrosyl radical and decayed with a rate consistent with the formation of the final iron-oxo product.

Based on the rapid freeze-quench EPR spectroscopy, stop-flow absorption spectroscopy, and the behavior of the Y122F mutant, a mechanism was proposed for the reconstitution of the radical under limiting iron conditions. In the mechanism, addition of Fe^{+3} and O_2 to apoR2 results in the rapid formation of the proposed μ-peroxodiferric intermediate (U). Intermediate (U) undergoes a one-electron reduction by Y122, resulting in the formation of the tyrosyl radical and iron-coupled radical of unknown structure, intermediate (X). In the final step of the reaction, a slow one-electron reduction of

intermediate (X) by ferrous iron or ascorbate results in formation of the final product—the active R2 protein.

The results from these spectroscopic studies corroborate, as does the spatial proximity of the two species in the crystal structure, that the iron center participates directly in formation of the tyrosyl radical. We know today that the active form of R2 contains a μ-oxo bridged binuclear ferric iron center closely associated with the tyrosyl radical. In the crystal structure of the *E. coli* R2, the tyrosyl radical is 5.3 Å from the iron-oxo center (Nordlund *et al.*, 1990). The proximity of these two species is conducive for many kinds of interactions and may facilitate the generation and stabilization of the tyrosyl radical by the iron-oxo center.

Protein R1

Primary sequence

Similar to the small subunit, the primary sequence of the large subunit from different phyla shows weak but significant sequence similarities distributed throughout the polypeptide. The amino acids which are conserved in essentially all R1 proteins are composed primarily of residues which contribute to the catalytic mechanism of RNR. These include the cysteine which is thought to form the cysteinyl radical, the redox-active cysteines which shuttle reducing equivalents to the active site, the residues which line the active site cavity, and the residues which make up the putative electron transport chain. The R1 amino acid sequences within the different phyla are significantly more conserved. For example, the amino acid sequences of the mouse and vaccinia virus R1 proteins are 72.5% identical (Tengelsen *et al.*, 1988).

Structure of the R1 protein

The crystal structure of the R1 protein from *E. coli* has been refined to an R-factor of 21% at 2.5 Å resolution (Uhlin & Eklund, 1994). Many of the structural features described in this work make it possible to describe the working mechanism of the Class I ribonucleotide reductases. In particular, the structure is supportive of the proposal that an electron transfer pathway, which connects the active site cysteinyl radical in R1 to the tyrosyl radical in R2, exists in the protein.

The tertiary structure of the R1 subunit consists of three primary domains: a ten stranded α/β-barrel of ~480 residues, the α-helical N-terminal domain composed of ~220 residues, and a 70-residue small domain.

The α/β-barrel structure of the *E. coli* large subunit is composed of two halves. Each half-barrel is composed of five parallel β-strands connected in series by four α helices. As depicted in Figure 7, the β-strands in the first half of the α/β-barrel are labeled from βA to E, and the strands in the second half are labeled βF thru J. The α-helices are labeled αA through D and αF through H, for the first and second half-barrels, respectively. The two halves come together by the formation of antiparallel β-sheets formed between the terminal strands, βA, F, E, and J, of each half-barrel. Thus, the hydrogen bonding between strands within each half-barrel is parallel while the bonding between the half-barrels is antiparallel. This gives the barrel a puesdo two-fold axis of symmetry. The number of hydrogen bonds between strands within each half-barrel ranges from three to six while the number of antiparallel hydrogen bonds formed between half-barrels is three at each junction.

The 10-stranded α/β-barrel of R1 has a larger diameter and has the β-strands arranged differently from the more common α/β-barrel of triose phosphate isomerase (TIM barrel) which is composed of eight strands arranged in a highly symmetrical parallel fashion (Uhlin & Eklund, 1996). The wider barrel of R1 allows the insertion of a finger-like loop

consisting of twenty residues. The finger is formed by a β-hairpin loop which extends into the barrel from one end, reaching clear to the opposite end, and returning to the end where it originated. Active site residues are located at the tip of this twenty-residue loop, including Cys439. Much evidence suggests that this cysteine residue is the site of the protein radical which ultimately abstracts the 3′-hydrogen from the nucleotide diphosphate substrate. Two other cysteines, which are required for enzyme activity, are located on separate β-strands of opposite half-barrels as indicated in Figure 7. These residues are Cys462, located on β-strand F, and Cys225, located on β-strand A. These cysteines have been shown to be the redox-active residues which ultimately reduce the ribose ring of the substrate (Mao et al., 1992a-c).

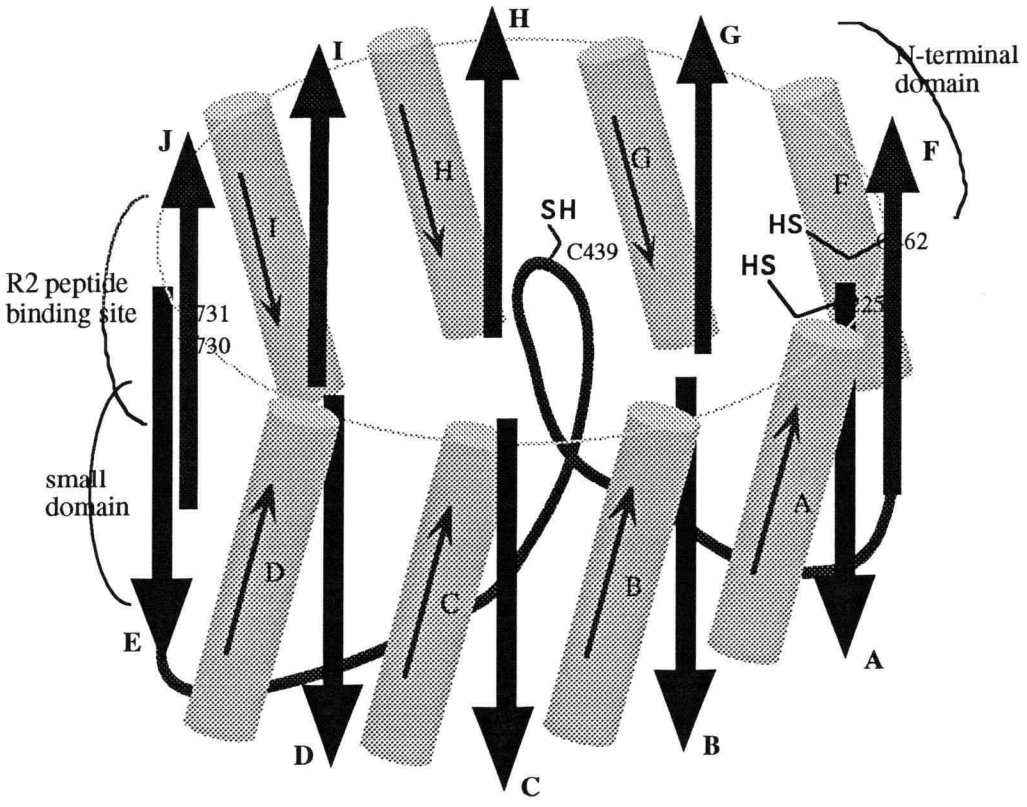

Figure 7 **The organization of the α/β barrel of *E. coli* R1.** The elements αA-αD and βA-βE belong to the first half-barrel, and αF-αI and βF-βJ to the second half-barrel. The two halves are connected by the center loop which contains, at the tip of the loop, the residue which forms the putative cysteinyl radical (C439). Also shown in this figure are the binding surfaces for the small and N-terminal domains, and the R2 C-terminal peptide.

After each catalytic event, these cysteines are oxidized to a cystine residue which must be reduced prior to the next round of catalysis. Figure 8 shows the crystal structure of the *E. coli* R1 protomer solved by Uhlin and Eklund. Highlighted in the structure are the three active site cysteines. In the crystal used to solve the R1 structure, Cys225 and Cys462 are found in the oxidized disulfide form. Although these cysteines are separated by over two hundred residues, it is clear from the three-dimensional structure of R1 that they are positioned such that the side chains extend into the active site, poised to contribute reducing equivalents to the substrate. Also highlighted in the structure is the side chain of Cys439, the active site cysteine which is thought to form the transient radical responsible for abstraction of the 3′-hydrogen of the substrate.

The hydrogen-bonded network between the internal loop and the barrel strands is quite extensive, especially at the top where the active site is found. Seven residues from different strands make side chain contacts with the loop close to the β-hairpin region. These interactions form a concave surface, presumably forming the substrate binding pocket. The position of the internal loop within the barrel is further stabilized by intra-loop hydrogen bonds as well as hydrogen bonds formed between the loop and highly conserved barrel strand residues, Glu441 and Cys225. Several water molecules also mediate the contacts between the loop and the inside of the barrel. The extensive hydrogen bonding between the loop and the barrel may be necessary to stabilize the loop and correctly position the active site cysteines. The correct spatial positioning of Cys439 may be critical for radical formation and substrate hydrogen abstraction (Sjöberg, 1994).

The contact area between the two half-barrels, on the side of the barrel where βJ and E form an antiparallel pleated sheet, is partially covered by the small domain. Also found at this region of the barrel is the putative binding site for the C-terminus of the R2 protein. Assignment of this region to the R2 binding site is based on the fact that electron density corresponding to the R2 C-terminal peptide, a required component of the crystallization mixture (Uhlin *et al.*, 1993), bound to this region in the crystal.

Figure 8 **Three-dimensional structure of *E. coli* R1.** The structure was solved by Uhlin and Eklund, 1994, and is oriented such that the viewer is looking down the center of the barrel domain. At the top of the barrel, the active site cysteines have been highlighted (carbon side chains in blue and sulfur in yellow). C225 and C462 are shown in this figure as a cystine disulfide, the form of the enzyme used to determine the crystal structure. C439, the transient cysteinyl radical, is also highlighted in the figure. The proximity of these catalytically-essential cysteines is consistent with the proposed mechanism of catalysis for RNR.

The R2 C-terminal peptide is found inserted into a narrow groove formed between two parallel α-helices. One of the helices which form the groove is part of the small domain. The other helix, barrel helix αI, provides the second face of the groove. The highly specific interaction between the R2 C-terminal peptide and this groove provides the physical link between the R1 and R2 homodimers. The R1 residues which contribute to the R2 peptide binding site are not conserved among different but related species, reflecting the species-specific nature of this protein-protein interaction. The positioning of this peptide relative to the active site is consistent with the proposal that the R2 C-terminus provides the electron transfer link between R1 and the R2 tyrosyl radical.

The N-terminal domain is composed of 12 α-helices, the first four of which form a left-handed 4-helix bundle. This 4-helix bundle packs against the barrel opposite of the surface where the small domain and R2 carboxy terminus bind. The position of the N-terminal domain against the barrel adds further definintion to the substrate binding pocket.

The R1 from *E. coli* behaves as a dimer in sedimentation equilibrium centrifugation experiments and is thought to be a homodimer in the active holoenzyme (Brown and Reichard, 1969a; Thelander, 1973). The R1 dimer interface is formed by two helices of the α/β barrel of one monomer, αA and αB, and the symmetry-related pair of the other monomer. The R1 dimer has an unusual S-shape which appears inherently flexible. This flexibility may facilitate the movement of domains and/or subunits of the R1 dimer and these intramolecular rearrangements may form the structural basis for the allosteric regulation and catalysis.

In an effort to identify the location of the allosteric sites on R1, crystals were either grown in the presence of dTTP, or soaked in a solution containing dATP and then analyzed by X-ray crystallography. Difference Fourier maps gave positive peaks corresponding to these nucleotides at the amino end of αA close to the homodimer interaction surface. Earlier studies, using R1 which had been photoaffinity-labeled with dTTP, demonstrated that this allosteric effector specifically labeled Cys289, localizing the specificity site to the

region around residues 288-294 of R1 (Eriksson *et al.*, 1986). Cys289 and the surrounding residues are part of αB of the 10-stranded α/β-barrel structure of R1. This area is directly adjacent to the amino terminus of αA, corroborating the results of the crystallographic studies done on the R1-nucleotide complex.

The location on R1 of the other allosteric nucleotide binding site, the activity site, has not yet been conclusively identified. However, it has been proposed that the activity site may be formed by the first 50-60 N-terminal residues of R1 (Eliasson *et al.*, 1996). This proposal is based on the finding that the subclass of type I RNRs, type Ib (Jordan *et al.*, 1996), lack the last 50 N-terminal residues present in the type Ia enzymes. The type Ib enzymes also lack the dATP-mediated inhibition observed by the type Ia enzymes, suggesting that the N-terminus may be involved in forming the activity site. Further support of this proposal is the finding that a D57N mutation in the mouse R1 protein makes the mutant protein insensitive to inhibition by dATP (Caras and Martin, 1988).

Modeling of the ribonucleotide reductase holoenzyme

A model for the $\alpha_2\beta_2$ holoenzyme complex can be made by superimposing the 2-fold axes of the individual three-dimensional structures of the R1 and R2 dimers and placing the complementary concave face of the R1 dimer onto the top lobes of the heart-shaped R2 dimer (Uhlin and Eklund, 1994). In this conformation, the binding site for the R2 C-terminal peptide determined by the crystallographic studies is in the right vicinity to allow docking of the flexible R2 carboxy terminus. Modelling of the complex in any other conformation will not bring Tyr122 closer to the active site of R1.

Before the crystal structures of R1 and R2 were determined the active site was thought to be located at the R1-R2 interface where the Tyr122 radical could directly interact with the substrate. However, the three-dimensional structure of the R2 protein showed that this could not be the case, since the Tyr122 was buried within the core of the protein 10 Å from

the nearest surface. Furthermore, structural changes resulting in exposure of the tyrosyl radical to the active site during complex formation are unlikely since no change in the EPR or absorbance spectra is observed upon binding of R2 to R1 (Sahlin *et al.*, 1987). In the current model of the holoenzyme, the distance between the tyrosyl radical of R2 and the active site in R1 is approximately 35-40 Å. These discrepancies led to the proposal that the radical may be transferred to the active site during catalysis via an electron transfer pathway composed of several highly conserved hydrogen-bonded residues contributed from both the R1 and R2 dimers (Nordlund *et al.*, 1990; Nordlund and Eklund,1993). The R1 structure reinforces this hypothesis.

The tyrosyl radical in R2 is an oxidized species (Backes *et al.*, 1989). Therefore, in contrast to most biological electron transfer processes which are reductive in nature, the proposed electron transfer pathway in RNR implies an oxidative transfer event. Examination of the crystal structure, as well as sequence comparisons and analysis of mutant proteins led to the selection of the following residues as participants in the transfer pathway. In the three-dimensional structure of R2, the residue which forms the stable tyrosyl radical (Y122) is hydrogen-bonded to Asp84. Asp84 is the bidental ligand of Iron-1. Another Iron-1 ligand, His118, forms a hydrogen bond with the δ-oxygen atom of Asp237. Asp237 forms a hydrogen bond to the ε-nitrogen of Trp48. Trp48 is a highly conserved residue which is located on the top lobe of the R2 structure at the proposed R1 binding site. Although Trp48 is located on the R1 binding surface, it is probably not the terminal electron transport link in R2. Two other residues located in the R2 carboxy terminus, Glu350 and Tyr356, have been implicated in the transfer of electrons between R1 and R2. This portion of the R2 protein is not defined in the crystal structure, but site-directed mutagenesis of these residues has provided compelling evidence for this assignment (Climent *et al.*, 1992). Although the sequence of the R2 C-terminus is highly species-specific, Glu350 and Tyr356 are invariant. Mutant *E. coli* R2 proteins were prepared in which either Glu350 or Tyr 356 were converted to alanine. Both of these

mutants bound R1 and substrate with binding constants very similar to wild-type R2. However, the catalytic activities of these proteins were severely impaired. The E350A mutant was 240 times less active than wild-type, while the Y356A mutant was totally inactive. These results indicate that these residues play catalytic rather than structural roles in ribonucleotide reduction and suggest that the R2 C-terminus is not only required for R1-R2 association, but that it may also function as the electron transport connection between R1 and R2.

The proposed electron transport circuit is completed by two tyrosines in the R1 structure, Tyr730 and 731. These two residues are located on β-strand J of the R1 barrel structure adjacent to the binding site for the R2 C-terminal peptide. This positioning within the R1 structure is consistent with the formation of a connection between the C-terminal R2 electron transport residues and the active site in R1. In the crystal structure of R1, Tyr731 is hydrogen-bonded to Tyr730, which is hydrogen bonded to Cys439 at the active site. To test the possible role of these residues in electron transport, site-directed mutagenesis was used to change each of these tyrosines to phenylalanine (Ekberg *et al.*, 1996). These R1 mutants were enzymatically inactive even though it was established that the three-dimensional structures were unchanged and R1-R2 complex formation as well as substrate binding were not impaired. Furthermore, the mechanism-based inhibitor 2′-azido-2′-deoxyCDP was incapable of scavenging the radical in these mutants, and no azido-CDP-derived radical intermediate was formed. Interaction of this nucleotide analogue with wild-type holoenzyme results in destruction of the tyrosyl radical (Thelander *et al.*, 1976) and concomitant generation of a nitrogen-centered substrate radical (Sjöberg *et al.*, 1983). These results indicate that disruption of the hydrogen-bonded link connecting the active site cysteine with the R2 binding surface leads to loss of electron transfer.

Thus, the electron transfer pathway in *E. coli* RNR which connects the stable tyrosyl radical in R2 to the transient cysteinyl radical in R1 is thought to involve Asp84, Iron-1,

His118, Asp237, Trp48, Glu350, Tyr356 in R2 and Tyr731 and Tyr730 in R1. Figure 9 depicts the residues from R1 and R2 which make up the putative electron transport chain.

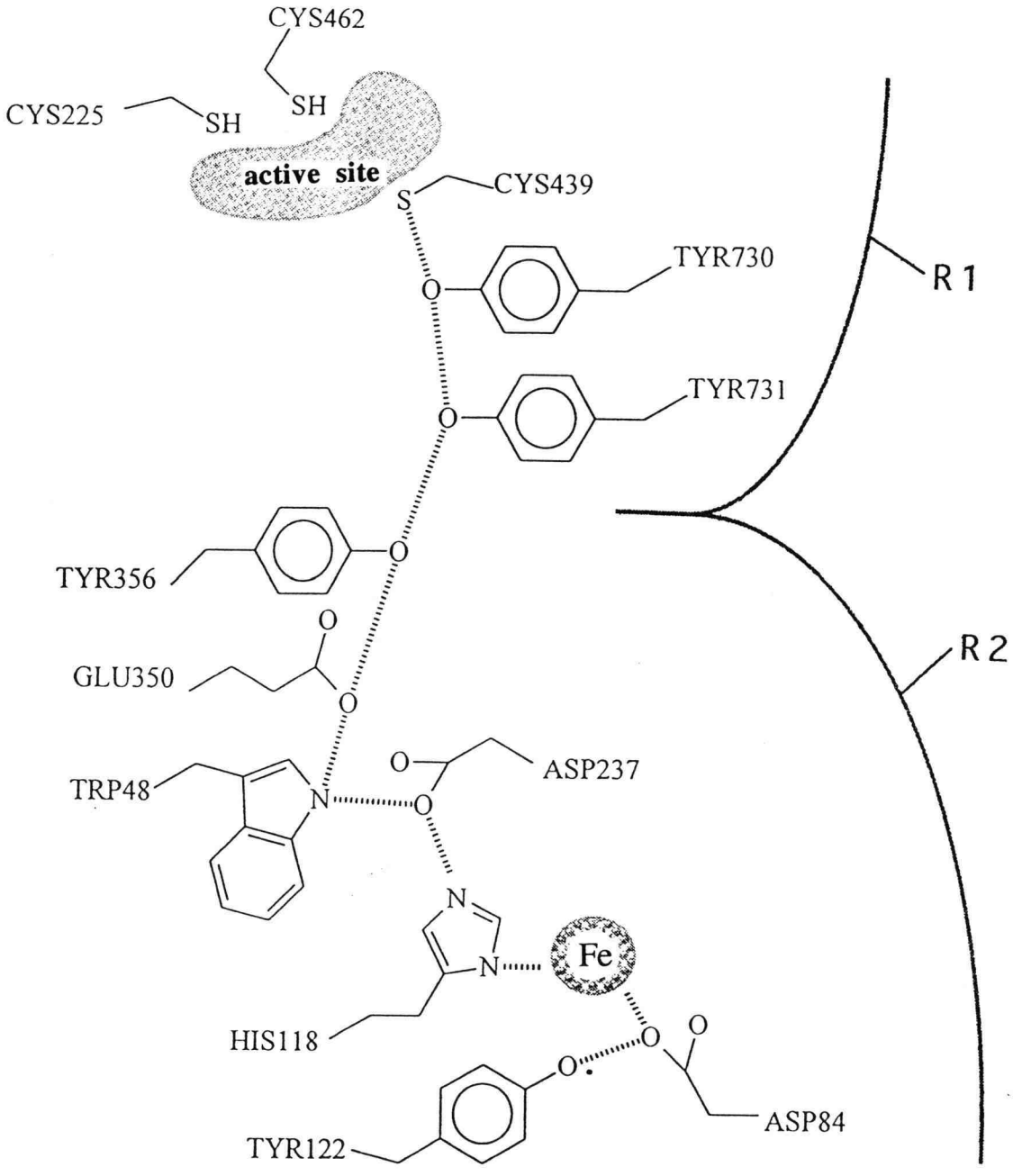

Figure 9 **The electron transfer pathway from *E. coli* RNR.** This hydrogen bonded array of highly conserved residues was proposed by Uhlin and Eklund, 1994, to shuttle the radical between the active site on R1 and Tyr122 of the R2 protein.

Inhibition of ribonucleotide reductase by hydroxyurea

Ribonucleotide reductase is an obvious target for antiproliferative agents because of the key role that it plays in DNA synthesis. Many drugs which inhibit RNR act by targeting the unique feature of the enzyme that is required for activity—the tyrosyl radical. Hydroxyurea, a drug used for many years in the treatment of chronic myelogenous leukemia (CML) and other myeloproliferative syndromes (Sather *et al.*, 1978), is the most common and best characterized example of drugs which inhibit DNA synthesis by scavenging the tyrosyl radical of RNR.

Hydroxyurea was first synthesized in 1869 (Dresler and Stein, 1869) and an inhibitory effect on leukocyte production was noted in 1928 (Rosenthal *et al.*, 1928). However, the drug received little attention until antineoplastic activity was observed in 1960 (Stock *et al.*, 1960). In 1964, a decrease in CDP reduction in hydroxyurea-treated rat and human bone marrow cells was reported (Frenkel *et al.*, 1964), localizing the effects to RNR. Then in 1972, it was demonstrated that hydroxyurea specifically inhibited RNR by destroying the free radical of the enzyme (Ehrenberg & Reichard, 1972). Hydroxyurea has been used clinically in the treatment of a wide variety of solid tumors, acute and chronic leukemia (Bolin *et al.*, 1982), and has even been used to control the proliferation of psoriasis (McDonald, 1981). Hydroxyurea enters cells by a diffusion process (Tagger *et al.*, 1987). The drug enters all tissues, including the central nervous system, with a maximal velocity that appears infinite (Morgan *et al.*, 1986).

Much work has been done using analogues of hydroxyurea to determine the structural features of the molecule required for activity, and in the attempt to design more effective and specific antiproliferative agents (Kjöller-Larson *et al.*, 1982). The general structure required for activity was found to be

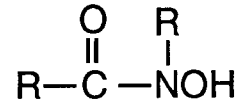

Substitution of the R_2 moiety with one- or two-carbon alkyl groups did not significantly affect activity. Substitution of the R_1 moiety, the 1° amine in hydroxyurea, with a variety of substituents had varying effects. In general, it was determined that the activity of the hydroxyurea analogue was inversely proportional to the bulk of the R_1 substituent. Based on the structure-activity relationship determined in these studies, it was estimated that the free radical of the *E. coli* enzyme was buried in a pocket approximately 4 Å wide and at least 6 Å deep. The mouse enzyme was found to be sensitive to much bulkier analogues, suggesting that the pore leading to the radical in this form of the enzyme was larger than in *E. coli*. The crystal structures of the two forms of RNR have corroborated these conclusions.

Hydroxyurea is a specific inhibitor of the iron-containing, or Class I, RNRs. It functions by quenching the tyrosyl radical, presumably through a one-electron reduction of the oxidized tyrosyl residue. Hydroxyurea reduces the tyrosyl radical of mouse R2 approximately three times as fast as the radical in the *E. coli* protein (Karlsson *et al.*, 1992; Nyholm *et al.*, 1993). In addition, the radical and iron center of the mouse protein are reduced simultaneously (Nyholm *et al.*, 1993), while the iron center of the *E. coli* protein remains intact. Interestingly, even though all forms of RNR are believed to use the radical-mediated catalytic mechanism described earlier, the adenosylcobalamin-containing Class II enzymes are resistant to the radical scavenging properties of hydroxyurea (Hamilton *et al.*, 1972).

The effects of hydroxyurea on the *E. coli* enzyme have been well characterized. When hydroxyurea reacts with the *E. coli* enzyme, only the tyrosyl radical is reduced, leaving the iron center intact. This form of the protein is known as metR2 (Sahlin *et al.*, 1989). The general features of the Mössbauer spectra of native and hydroxyurea-treated R2 are essentially the same, verifying that the iron center remains unperturbed by hydroxyurea (Petersson *et al.*, 1990). The difference spectrum, created by subtracting the spectrum of

the metR2 from that of native R2, contains the electronic spectral bands assigned to the iron-oxo center, and lacks the bands due to the tyrosyl radical.

In vitro studies done on the *E. coli* enzyme have demonstrated that during substrate turnover, the radical is several times more sensitive to hydroxyurea than when the enzyme is in a resting state (Atkin *et al.*, 1973). The increase in sensitivity to hydroxyurea which occurs in conjunction with an increase in the level of enzyme activity has also been observed for the ribonucleotide reductase from bacteriophage T4 (Berglund and Sjöberg, 1978).

The hydroxyurea sensitivity of the radical from the *E. coli* enzyme is also dependent on the regulatory state of the enzyme (Karlsson *et al.*, 1992). By indirectly measuring the tyrosyl radical half-life under various conditions, the effects of holoenzyme formation and the nucleotide environment on the susceptibility to hydroxyurea were determined. Using the half-life of the R2 protein alone as the reference, it was found that formation of the R1R2 complex reduced the hydroxyurea sensitivity of the radical 1.4 to 2.5 fold. It has been shown by EPR (Backes *et al.*, 1989) and resonance Raman (Sahlin *et al.*, 1987) spectroscopy that formation of the R1R2 complex does not influence the structure of the radical or iron centers. Thus, the decreased sensitivity to hydroxyurea of the R2 radical upon formation of the holoenzyme is thought to be due to a physical phenomena in which the R1 blocks accessibility to the radical, rather than a change in the structure of the radical center.

The susceptibility of the radical in the *E. coli* R1R2 complex is changed significantly through binding of the allosteric effectors ATP and dATP. Activation of the holoenzyme by addition of a positive effector, such as ATP or dATP at low concentration (2 μM), made the radical more susceptible to hydroxyurea. Conversely, addition of dATP at concentrations in which the enzyme is completely inhibited (100 μM), made the radical much less susceptible to hydroxyurea.

Addition of either substrate (rCDP) or product (dCDP) to the *E. coli* holoenzyme made the R2 radical three times more susceptible to hydroxyurea destruction compared to susceptibilty of the R1R2 complex without these nucleotides present. When a positive effector was added along with substrate or product, the rate of hydroxyurea inactivation increased dramatically to values which were too rapid to accurately determine in these experiments.

These results, taken together, suggest that the radical sensitivity to hydroxyurea is proportional to the activity-state of the enzyme. That is, when the enzyme is poised to reduce substrate, the radical somehow becomes more accessible to hydroxyurea.

One possible mechanism behind the increased susceptibility of the radical in the ternary complex is a conformational change in R2 which accompanies the binding of an activating allosteric effector and/or substrate/product to R1. Although it is assumed that conformational changes in R1 driven by the binding of effectors to the allosteric sites are responsible for changes in enzyme's substrate specificity and relative activity, there is no evidence that these conformational changes are propagated to the R2 protein. However, the compact structure which is formed when the holoenzyme is modeled such that the dimer axes are superimposed (Uhlin and Eklund, 1994) places the top lobes of the heart-shaped R2 dimer in contact with a large portion of the R1 surface. Part of the R1 surface which is is contact with R2 includes the last resolvable N-terminal residues, and it is this region that has been implicated as forming part of the activity site (Eliasson *et al.*, 1996). Therefore, it is feasible that allosterically driven conformational changes in R1 may also change the R2 conformation and hence hydroxyurea sensitivity of the radical center.

Another possible explanation of the increased sensitivity of the ternary complex involves the putative electron transfer pathway. This pathway is responsible for transfer, back and forth, of the electron from the substrate bound in the R1 active site to the tyrosyl radical in R2 during each catalytic cycle. It is postulated that the electron transport is triggered by binding of a nucleoside triphosphate to an allosteric site and further enhanced

by binding of substrate (or product) to the active site. This electron transport presumably creates transient radicals at residues along the hydrogen-bonded pathway. These transiently occupied sites may be more effeciently scavenged by hydroxyurea than the tyrosyl radical in R2, simply because of their proximity to bulk solvent. This may be especially true for the transport chain residues located at the interface between R1 and R2. If this model is correct, the electron transport triggered by the allosteric activation of the enzyme will increase the frequency of inactivation of the radical (decreasing the half-life) which occurs at these transiently occupied sites.

Pool size change

The effect of hydroxyurea treatment on the *in vivo* dNTP pools has been investigated in many cell types. When *E. coli* is treated with hydroxyurea, all four of the deoxyribonucleoside triphosphate pools are depressed (Neuhard, 1967), as expected for a system in which the inhibited enzyme produces all four dNTP precursors. However, in cultured mammalian cells this is not the case. Surprisingly, addition of hydroxyurea to mammalian cells results in depletion primarily of the purine dNTPs (Adams *et al.*, 1971; Skoog and Nordenskjöld, 1971; Åkerblom and Reichard, 1985; Slabaugh *et al.*, 1991). Even more surprising, in most cases the dTTP pool is elevated by hydroxyurea treatment.

Effects of hydroxyurea in combination with other compounds

The effects of various combinations of hydroxyurea with iron-chelating agents have been tested for RNR inhibition (Cory *et al.*, 1981). It was found that adding iron-chelators like EDTA, desferroxamine, and 8-hydroxyquinoline in combination with hydroxyurea

increased the inhibition of RNR activity in cultured cells. This result is consistent with the requirement for iron in the regeneration of the tyrosyl radical.

Recently, hydroxyurea has been shown to be a possible candidate for AIDS therapy, especially when used in conjunction with 2′, 3′-dideoxyinosine (ddI) (Lori *et al.*, 1994). The human immunodeficiency virus (HIV) requires dNTPs for the reverse transcriptase-catalyzed synthesis of viral DNA. Since hydroxyurea treatment leads to a depletion of dNTPs, any process which requires these precursors should be inhibited to some degree. Lori and coworkers found that, by decreasing the dNTP pools, hydroxyurea inhibits HIV DNA synthesis both in stimulated and quiescent human lymphocytes infected with HIV-1. This inhibition resulted not only in less production of viral DNA, but the DNA that was produced was in the form of incomplete chains (Gao *et al.*, 1993). Furthermore, it was found that when hydroxyurea was combined with the nucleoside analog ddI, the inhibition was greater than the additive effects of the two drugs separately. As discussed earlier, hydroxyurea treatment of cells results primarily in a decrease in the purine dNTPs. ddI is metabolized in the cell to the active form of the drug, a purine dideoxynucleoside triphosphate. The active form of ddI is then able to compete with the purine dNTPs for incorporation into viral DNA. Once incorporated, the growing DNA strand can no longer elongate, since the incorporated nucleotide analog lacks the 3′-hydroxyl required for the next polymerization step. The basis for the synergistic effect of hydroxyurea and ddI is presumably due to the increased utilization of the metabolized form of ddI by reverse transcriptase required to compensate for the depressed dATP pool (and to a lesser extent dGTP) resulting from the hydroxyurea treatment. Results obtained using the thymidine analog, azidothymidine(AZT) instead of ddI support this presumption. Cells treated with AZT plus hydroxyurea show severalfold less inhibition of viral DNA synthesis compared to treatment with ddI plus hydroxyurea. Because the dTTP pool in hydroxyurea-treated cells is not depressed to any significant extent in most cell types, the active metabolite of AZT will not compete as effectively for incorporation into viral DNA as the ddI metabolite

can. Thus, one sees the synergistic effect of hydroxyurea and nucleoside analog only when that analog competes with the dNTP pool which is specifically depressed by hydroxyurea. Furthermore, because hydroxyurea targets a host cell enzyme rather than inhibiting the virus directly, the high rate of formation of drug-resistant forms of HIV commonly observed with conventional antiviral drugs should not be a problem.

References

Adams, R. L. P., Berryman, S., and Thompson, A. (1971) *Biochem. Biophys. Acta* **240**, 455-462

Åkerblom, L., and Reichard, P. (1985) *J. Biol. Chem.* **260**, 9197-9202

Atkin, C. L., Thelander, L., Reichard, P., and Lang, G. (1973) *J. Biol. Chem.* **248**, 7464-7472

Ator, M.A., Stubbe, J. A., and Spector, T (1986) *J. Biol. Chem.* **261**, 3595-3599

Backes, G., Sahlin, M., Sjöberg, B.-M., Loehr, T. M., and Sanders-Loehr, J. (1989) *Biochemistry* **28**, 1923-1929

Berglund, O. (1972) *J. Biol. Chem.* **247**, 7270-7275

Berglund, O., and Sjöberg, B.-M. (1978) *J. Biol. Chem.* **254**, 253-254

Blakley, R. L. and Barker, H. A. (1964) *Biochim. Biophys. Res. Commun.* **16**, 301

Bolin, R. W., Robinson, W. A., Sutherland, J., and Hamman, R. F. (1982) *Cancer* **50**, 1683-1686

Bollinger, J.M., Edmonson, D.E., Huynh, B. H., Filley, J., Norton, J.R., and Stubbe, J. (1991) *Science* **253**, 292-298

Booker, S., Licht, S., Broderick, J. and Stubbe, J. (1994) *Biochemistry* **33**, 12676-12685

Brown, N. C., Eliasson, R., Reichard, P., and Thelander, L. (1969) *Eur. J. Biochem.* **9**, 512-518

Brown. N. C. and Reichard, P. (1969a) *J. Mol. Biol.*, **46**, 25-38

Brown. N. C. and Reichard, P. (1969b) *J. Mol. Biol.*, **46**, 39-55

Caras, I. W., and Martin, D. W. J. (1988) *Mol. Cell Biol.* **8**, 2698-2704

Chan, A. K., Lichfield, D. W., and Wright, J. A. (1993) *Biochemistry*, **32**, 12835-12840

Chang C.-H., and Cheng, Y.-C. (1979) *Cancer Res.* **39**, 5081-5086

Chen, A. K., Bhan, A., Hopper, S., Abrams, R., and Frazen, J. S. (1977) *Biochemistry* **13**, 654-661

Climent, I., Sjöberg, B.-M., and Huang, C. Y. (1992) *Biochemistry* **31**, 4801-4807

Cori, J. D., Lasate, L., and Sato, A. (1981) *Biochem. Pharm.* **30**, 979-984

Cori, J. D., Rey, D. A., Carter, G. C., and Bacon, P. E. (1985) *J. Biol. Chem.* **260**, 12001-12007

Drake, J. (1991) *Proc. Natl. Acad. Sci. USA* **88**, 7160-7164

Dresler, W. F. C., and Stein, R. (1869) *Justus Liebigs Ann. Chem. Pharmacol.* **150**, 242-252

Ehrenberg, A., and Reichard, P. (1972) *J. Biol. Chem.* **247**, 3485-3488

Ekberg, M. Sahlin, M., Eriksson, M., and Sjöberg, B.-M. (1996) *J. Biol. Chem.* **271**, 20655-20659

Eliasson, R., Pontis, E., Jordan, A., and Reichard, P. (1996) *J. Biol. Chem.* **271**, 26582-26587

Eliasson, R., Pontis, E., Sun, X., and Reichard, P. (1994) *J. Biol. Chem.* **269**, 26052-26057

Eriksson, S., Sjöberg, B.-M., Jörnvall, H., and Carlquist, M. (1986) *J. Biol. Chem.* **261**, 1878-1882

Fontecave, M., Eliasson, P., and Reichard, P. (1989) *Proc. Natl. Sci. U.S.A.* **86**, 2147-2153

Fontecave, M., Nordlund, P., Eklund, H., and Reichard, P. (1992) *Adv. Enzymol. Relat. Areas Mol. Biol.* **65**, 147-183

Fox, B. G., Surerus, K. K., Münck, E., and Lipscomb, J. P. (1989) *J. Biol. Chem.* **263**, 10553

Frenkel, E. P., Skinner, W. N., and Smiley, J. D. (1964) *Cancer Chemother. Rep.* **40**, 19-22

Gao, W.-Y., Cara, A., Gallo, R. C., and Lori, F. (1993) *Proc. Natl. Acad. Sci. USA* **90**,825

Garbett, K., Darnell, D. W., Klotz, I. M., and Williams, R. J. P. (1969) *Arch. Biochem. Biophys.* **135**, 419

Hamilton, J. A., Tamao, Y., Blakley, R. L. and Coffman, R. E. (1972) *Biochemistry* **11**, 4696-4705

Hendricks, S. P., and Mathews, C. K. (1997) *J. Biol. Chem.* **272**, 2861-2865

Holmgren, A. (1988) *Bioch. Soc. Trans.* **16**, 95-96

Jordan, A., Pontis, E., Atta, M., Krook, M., Gilbert, I., Barbé, J., and Reichard P. (1994) *Proc. Natl. Acad. Sci. U.S.A.* **91**, 12892-12896

Jordan, A., Pontis, E., Åslund, F., Hellman, U., Gilbert, I., and Reichard P. (1996) *J. Biol. Chem.* **271**, 8779-8785

Karlsson, M., Sahlin, M., and Sjöberg, B.-M. (1992) *J. Biol. Chem.* **267**, 12622-12626

Kauppi, B., Nielsen, B. B., Ramaswamy, S., Larsen, I. K., Thelander, M., Thelander, L., and Eklund, H. (1996) *J. Mol. Biol.*, **262**, 706-720

Kjöller-Larson, I., Sjöberg, B.-M., and Thelander, L. (1982) *Eur. J. Biochem.* **125**, 75-81

Kunz, B. A., Kohalmi, S. E., Kunkel, T. A., Mathews, C. K., McIntosh, E. M., and Reidy, J. A. (1994) *Mutat. Res.* **318**, 1-64

Land, E. J., Porter, G., and Strachan, E. (1961) *Trans. Faraday Soc.* **57**, 1885-1893

LaPlante, S. R., Aubry, N., Moss, N., and Liuzzi, M. (1993) *J. Cell. Biochem.* **S17C**, 307

Lehman, I. R., Bessman, M. J., Simms, E. S., and Kornberg, A. (1958) *J. Biol. Chem.* **233**, 163-170

Liuzzi, M., Deziel, R., Moss., N., Beaulieu, P., Bonneau, A. M., Bousquet, C., Chafouleas, J. G., Garneau, M., Jaramillo, J., Krogrud, R. L., Lagace, L., McCollum, R. S., Nawoot, S. and Guindon, Y. (1994) *Nature* **372**, 695-698

Lori, F., Maly, K. H., Cara, A., Sun, D., Weinstein, J. N., Lisziewicy, J., and Gallo, R. C. (1994) *Science* **266**, 801-805

Lycksell, P. O., Ingemarson, R., Davis, R., Gräslund, A., and Thelander, L. (1994) *Biochemistry* **33**, 2838-2842

Mann, G. J., Gräslund, A., Ochiai, E. I., Ingemarson, R., and Thelander, L. (1991) *Biochemistry* **30**, 1939-1947

Mao, S. S., Holler, T. P., Bollinger, J. M., Yu, G. X., Johnston, M. I., and Stubbe, J. (1992b) *Biochemistry* **31**, 9744-9751

Mao, S. S., Holler,T. P., Yu, G. X., Bollinger, J. M., Booker, S., Johnston, M. I., and Stubbe, J. (1992a) *Biochemistry* **31**, 9733-9743

Mao, S. S., Yu, G. X., Chalfoun, D., and Stubbe, J. (1992c) *Biochemistry* **31**, 9752-9759

Mathews, C. K. and Ji, J. (1992) *Bioessays* **14**, 295-301

McDonald, C. J. (1981) *Pharmacol.Ther.* **14**, 1-24

Menage, S., Brennan, B. A., Juarez-Garcia, C., Münck, E., and Que, L. (1990) *J. Am. Chem. Soc.* **112**, 6423-6425

Moore, E. C. and Hurlbert, R. B. (1985) *Pharmac. Ther.* **27**, 167-196

Morgan, J. S., Creasey, D. C., and Wright, J. A. (1986) *Biochem. Biophys. Res. Commun.* **134**, 1254-1257

Neuhard, J. (1967) *Biochem. Biophys. Acta* **145**, 1-6

Nordlund, P., Sjöberg, B.-M., and Eklund, H. (1990) *Nature* **345**, 593-598

Nordlund, P., and Eklund, H. (1993) *J. Mol. Biol.* **232**, 123-164

Nyholm, S., Thelander, L., and Gräslund, A. (1993) *Biochemistry* **32**, 11569-11574

Ochiai, E.-I., Mann, G. J., Gräslund, A., and Thelander, L. (1990) *J. Biol. Chem.* **265**, 15758-15761

Ollagnier, S., Mulliez, E., Gaillard, J., Eliasson, R., Fontecave, M., and Reichard, P. (1996) *J. Biol. Chem.* **271**, 9410-9416

Petersson, L., Gräslund, A., Ehrenberg, A., Sjöberg, B.-M., and Reichard, P. (1980) *J. Biol. Chem.* **255**. 6706-6712

Pontius, B. W. (1993) *Trends Biochem. Sci.* **18**, 181-186

Pötsch, S., Sahlin, M., Langelier, Y., Gräslund, A., and Lassmann, G. (1995) *FEBS Letters* **374**, 95-99

Reichard, P. (1958) *Biochim. Biophys. Acta* **27**, 434-435

Reichard, P. (1993) *Science* **260**, 1773-1777

Rosenthal, F., Wislicki, L., and Koller, L. (1928) *Klin. Wochstr.* **7**, 972-977

Sahlin, M., Gräslund, A., Petersson, L., Ehrenberg, A., and Sjöberg, B.-M. (1989) *Biochemistry* **28**, 2618-2625

Sahlin, M., Petersson, L., Gräslund, A., Ehrenberg, A., and Sjöberg, B.-M., and Thelander, L. (1987) *Biochemistry* **26**, 5541-5548

Sanders-Loehr, J. (1989) in *Iron Carriers and Iron Proteins* (Loehr, T. M., ed) pp. 375-466, VHC Publishers Inc., New York

Sather, M. R. Weber, C. E., Preston, J. D., Lyman, G. H., and Sleight, S. M. (1978) *Cancer Chemotherapeutic Agents: Handbook of Clinical Data* 69-71, G.K. Hall & Co.; Boston

Sjöberg, B.-M. (1994) *Structure* **2**, 793-796

Sjöberg, B.-M., Karlsson, M., Jörnvall, H. (1987) *J. Biol. Chem.* **262**, 9736-9743

Sjöberg, B.-M., Loehr, T. M., and Sanders-Loehr, J. (1982) *Biochemistry* **21**,96-102

Sjöberg, B.-M., Reichard, P., Gräslund, A., and Ehrenberg, A (1977) *J. Biol. Chem.* **252**, 536-541

Skoog, L., and Nordenskjöld, B. (1971) *Eur. J. Biochem.* **19**, 81-89

Slabaugh, M. B., Roseman, N., Davis, R., and Mathews, C. K. (1988) *J.Virol.* **62**, 519-527

Slabaugh, M. B., Howell, M. L., Wang, Y., and Mathews, C. K. (1991) *J. Virol.* **65**, 2290-2298

Stock, C. C., Clarke, D. A., Philips, F. S., Barclay, R. K., and Myron, S. A. (1960) *Cancer Res.* **20**, 193-382

Stubbe, J. A., and Ackles, D (1980) *J. Biol. Chem.* **255**, 8027-8030

Stubbe, J. A., Ator, M. A., and Krenitsky, T (1983a) *J. Biol. Chem.* **258**, 1625-1630

Stubbe, J. A., and Kozarich, J. W. (1980) *J. Am. Chem. Soc.* **102**, 2505-2507

Stubbe, J. A., Smith, G. and Blakley, R. L. (1983b) *J. Biol. Chem.* **258**, 1619-1624

Tagger, A. Y., Boux, J., and Wright, J. A. (1987) *Biochem. Cell. Biol.* **65**, 925-929

Tamao, Y. and Blakley, R. L. (1973) *Biochemistry* **12**, 24-34

Tengelsen, L. A., Slabaugh, M. B., Bibler, J. K., and Hruby, D. E. (1988) *Virology* **164**, 121-131

Thelander, L. (1973) *J. Biol. Chem.* **248**, 4591-4601

Thelander, L. (1974) *J. Biol. Chem.* **249**, 4858-4862

Thelander, L., Larsson, A., Hobbs, J., and Eckstein, F. (1976) *J. Biol. Chem.* **251**, 1398-1405

Thelander, L., and Gräslund, A. (1994). Ribonucleotide reductase in mammalian systems. In *Metal Ions in Biological Systems* (Sigel, H. and Sigel, A., eds), pp. 109-129, Marcel Dekker, Inc., New York.

Timson, J. (1975) *Mutat. Res.* **32**, 115-131

Traut, T. (1994) *Mol. Cell. Biochem.* **140**, 1-22

Uhlin, U. and Eklund, H. (1994) *Nature* **370**, 533-539

Uhlin, U. and Eklund, H. (1996) *J. Mol. Biol.* **262**, 358-369

Uhlin, U., Uhlin, T., and Eklund, H. (1993) *FEBS Letters* **336**, 148-152

von Döbeln, U. and Reichard, P. (1976) *J. Biol. Chem.* **251**, 3616-3622

Young, P., Öhmann, M., Xu, M. Q., Shub, D. A., and Sjöberg, B.-M. (1994) *J. Biol. Chem.* **269**, 20229-20232

Young, P., Andersson, J., Sahlin, M., and Sjöberg, B.-M. (1996) *J. Biol. Chem.* **271**, 20770-20775

Chapter 2

Inactivation of Vaccinia Virus Ribonucleotide Reductase by Hydroxyurea

Stephen P. Hendricks and Christopher K. Mathews

Summary

Hydroxyurea inhibits DNA synthesis by destroying the catalytically essential tyrosyl radical of Class I ribonucleotide reductase, thereby blocking the *de novo* synthesis of deoxyribonucleotides. Unexpectedly, in mammalian cells, including cells which are infected by vaccinia virus, this block results in a differential decrease in the pools of the four DNA precursors. This led to the suggestion that the four activities of ribonucleotide reductase may be differentially sensitive to hydroxyurea. Two independent methods were developed to test this idea; a spectroscopic technique was used to directly measure the hydroxyurea-induced decay of the radical/iron center chromophore, and a biochemical technique that was used to measure the hydroxyurea inhibition as a function of enzyme activity. Neither technique seemed to indicate that any one of the four ribonucleotide reductase activities was more sensitive than any other to hydroxyurea. However, other factors that influence the sensitivity of the radical and iron center were identified. Specifically, the sensitivity of the radical and iron center to hydroxyurea appeared to be dependent upon the activity level of the enzyme. When no allosteric effectors were present, the holoenzyme was most resistant to hydroxyurea. When the enzyme was activated for substrate turnover by the addition of nucleoside triphosphate effectors, the half-life of the tyrosyl radical/iron center chromophore in the presence of the inhibitor was significantly reduced. Futhermore, addition of substrate to the activated holoenzyme further sensitized the enzyme to hydroxyurea.

Introduction

Hydroxyurea (HU) inhibits DNA replication in cells that use the Class I form of ribonucleotide reductase (RNR) by inactivating the tyrosyl radical required for enzyme activity (Ehrenberg and Reichard, 1972). This inhibition is also observed in viruses, like vaccinia, which code for a Class I RNR. For example, when vaccinia virus-infected BSC_{40} monkey kidney cells are treated with HU, the synthesis of viral DNA is inhibited. HU inhibits the *de novo* synthesis of deoxyribonucleotides, thereby starving the host cell and viral replication complexes for precursors. One might expect that the inhibition of RNR by a drug like HU should result in an equivalent decrease in the rate of formation of all four products of the enzyme. However, when the triphosphate forms of these products, the 2′-deoxyribonucleoside 5′-triphosphates (dNTPs), were measured in vaccinia-infected cells, it was found that hydroxyurea treatment led to a differential decrease in the four dNTP pools. In particular, the concentration of the 2′-deoxyadenosine 5′-triphosphate (dATP) pool was decreased to the greatest extent (Slabaugh *et al.*, 1991).

Specifically, when vaccinia-infected BSC_{40} cells were treated with 0.5 mM HU, the dATP pool was depressed to 10% of the value from the control. At higher HU concentrations (2 and 5 mM), the dATP pool was reduced to less than 5% of the control. The other dNTP pools were not affected as much. At 0.5 mM HU, the 2′-deoxycytidine 5′-triphosphate (dCTP) and 2′-deoxyguanosine 5′-triphosphate (dGTP) pools were both reduced to approximately 50%, and at 2.0 mM these pools were reduced to approximately 30%, of the control. Surprisingly, the 2′-deoxythymidine 5′-triphosphate (dTTP) pool nearly doubled at all hydroxyurea concentrations studied (0.5 to 5 mM) (Slabaugh *et al.*, 1991; Figure 5). This trend in HU-induced dNTP pool changes, in particular the enigmatic increase in the dTTP concentration, has been observed in studies done on numerous other mammalian cell types (Bianchi *et al.*, 1986a; Nicander and Reichard, 1985a; Adams *et al.*, 1971; Skoog and Nordenskjöld, 1971).

Consistent with the finding that dATP was the most depleted dNTP, Slabaugh and coworkers found that the addition of deoxyadenosine (dAdo), the corresponding nucleoside of dATP, to the vaccinia-infected cells could reverse the HU-mediated inhibition of viral DNA synthesis. None of the other deoxyribonucleosides, deoxyguanosine (dGuo), deoxycytidine (dCyd), or deoxythymidine (dThd), were capable of reversing the effects of hydroxyurea, nor did they augment the dAdo effect. It is important to note for the purpose of later discussion that the dAdo rescue was observed only when erythro-9-(2-hydroxyl-3-nonyl) adenine (EHNA), a potent inhibitor of adenosine deaminase, was added in conjunction with the nucleoside.

A hypothesis that was developed to explain these data presumes that the differential changes that occur in the dNTP pools after HU treatment are the result of RNR being differentially sensitive to the radical scavenging properties of the drug. According to this hypothesis, the relative sensitivity will depend on which allosteric effector is bound, and therefore, which substrate the enzyme is activated to reduce. The fact that the largest decrease occurs in the dATP pool suggests that the most sensitive conformation occurs when the enzyme is stimulated to reduce adenosine 5′-diphosphate (rADP). In other words, when the allosteric activator for rADP reduction, dGTP, is bound to the specificity site, the enzyme adopts a conformation that makes the tyrosyl radical most accessible to HU. This will result in inhibition of the enzyme primarily when poised to reduce rADP, resulting in a greater depletion of the 2′-deoxyadenosine 5′-diphosphate (dADP) pool. The decreased dADP flux will then be translated down the *de novo* pathway, resulting in the experimentally observed depletion of the dATP pool. The dCTP, dTTP, and dGTP pools should be less affected by HU because the RNR conformations associated with the rCDP-, rUDP-, and rGDP-reducing activities will be less sensitive to the drug. I joined the Mathews laboratory to test this hypothesis.

This chapter describes two independent *in vitro* techniques I have developed to test this hypothesis, and the results of studies done using these techniques. The first technique is a

physical method which monitors the HU-induced decay of the radical directly, and the second technique is an enzymatic assay which follows the destruction of the radical as a function of the relative enzyme activities.

The physical method I used to determine the relative sensitivity of RNR takes advantage of a chromophore that arises from the tyrosyl radical and iron-oxo center of R2. The Class I RNRs, which include the *Escherichia coli*, mouse and vaccinia enzymes, are characterized as having an iron-oxo center that is closely associated with a catalytically essential tyrosyl radical. These species give rise to unique chromophores that absorb light in the visible region of the electromagnetic spectrum. In the *E. coli* R2 protein, the tyrosyl radical chromophore gives rise to a peak at 410 nm and a broad band centered at approximately 390 nm. The iron-oxo center has an absorbance band centered at approximately 370 nm and contributes some overlapping absorbance to the 390 and 410 nm absorbance bands (Ehrenberg and Reichard, 1972). The tyrosyl radical and iron-oxo chromophores of the mouse and vaccinia proteins absorb light at slightly lower energy, giving a relatively sharp peak at 417 nm. Treatment of the *E. coli* enzyme with HU or NH_4OH results in destruction of the 410 and 390 nm absorbances with little or no change in the iron-oxo bands. The mammalian forms of R2 behave differently when treated with these inhibitors. Treatment of the mouse or vaccinia R2 with HU results in destruction of both the tyrosyl radical and iron-oxo center absorbance bands on a similar time scale (Nyholm *et al.*, 1993; Howell *et al.*, 1992). In addition, at least in the case of the mouse R2, the destruction of these chromophores is accompanied with release of iron from the protein (Nyholm *et al.*, 1993). The different behaviors of the *E. coli* and mammalian proteins with respect to HU inactivation may reflect a more exposed iron center in the mammalian R2, or may be related to different redox potentials of the iron centers.

To test whether the radical was differentially sensitive, HU was mixed with purified vaccinia RNR and the decay of the absorbance at 417 nm was monitored over time. By comparing the chromophore decay rates of the enzyme in the presence of different dNTP

effectors, the relative sensitivity of the radical and iron-oxo center was determined under different allosteric conformations. In addition, the chromophore decay was measured while the enzyme was turning over substrate in order to determine whether the overall activity of the enzyme altered its sensitivity to HU.

Although this technique proved useful for investigating the radical sensitivity, the results were not very reproducible due primarily to practical problems associated with the vaccinia RNR proteins. The highly variable decay rates made it difficult to determine whether any of the four activities was more sensitive than the others to HU. Therefore, I sought an additional, more reproducible technique to answer the question. One obvious way to approach this problem is to follow the inhibition as a function of the enzyme activity. For this purpose, it would be useful to have the ability to simultaneously measure all four RNR activities under physiological effector concentrations in order to mimic the *in vivo* nucleotide environment of the enzyme. However, the routine method used to assay RNR activity uses a single substrate, usually tritiated cytidine diphosphate ([^{3}H]rCDP), and thin-layer chromatography (TLC) to separate the substrate from the product. The TLC separation does not have satisfactory resolution to resolve the four possible 2′-deoxyribonucleoside 5′-diphosphate (dNDP) products. Therefore, most of the data regarding RNR enzyme activity, including substrate specificity and allosteric effects, collected prior to this report were obtained using single substrate assays.

To better address the question of differential sensitivity, I developed a novel assay in which the four activities of RNR can be simultaneously monitored in a single reaction vial. This four-substrate assay, as we refer to it, can be used to determine how perturbations of RNR effect each of the four activities under identical conditions (Hendricks and Mathews, 1997). I used this assay to determine the extent that HU inhibited each of the four vaccinia RNR activities. In addition, the method has also proved useful for studying other aspects of RNR enzyme activity. For example, the assay can be performed using any desired combination of allosteric effectors and substrates in order to study the role of the allosteric

environment in the regulation of RNR activity. The following chapters describe such studies done using the recombinant enzymes from T4 bacteriophage and vaccinia virus. Chapter 3 describes the assay in more detail and Appendix I gives the step by step procedure. This chapter summarizes the results of the HU inhibition of vaccinia RNR obtained using both the physical and enzymatic techniques.

Materials and Methods

Overexpression and Purification of Recombinant Subunits—Both subunits of vaccinia ribonucleotide reductase were previously cloned into IPTG-inducible pET expression vectors and were overexpressed as described (Slabaugh *et al.*, 1993; Howell *et al.*, 1992).

The purification procedure for the R2 subunit was essentially as reported (Howell *et al.*, 1992) except for the incorporation of an additional radical reactivation step. In this step, recombinant apoR2 was activated to form the tyrosyl radical and iron-oxo center by addition of ferrous iron under anaerobic conditions. The reactivation was accomplished during gel exclusion chromatography by addition of ferrous ammonium sulfate to extensively degassed column buffer. Once the size exclusion column was equilibrated with this solution, partially purified R2 was applied, allowed to bind iron, and then eluted as normal. The tyrosyl radical was formed when the protein eluted from the anaerobic environment of the column and was exposed to air in the fraction collector.

Purification of the R1 protein was based on the protein's affinity for dATP. A dATP-Sepharose affinity resin was synthesized by coupling 2'-deoxyadenosine-5'-(γ-4-aminophenyl)-triphosphate (USB), via the aminophenyl moiety, to cyanogen bromide-activated Sepharose (Pharmacia Biotech). Details of the coupling procedure can be found in Appendix II. Routinely, 3-5 g of cells containing overexpressed vaccinia R1 were lysed in a French press and centrifuged at 12,000 rpm for 20 minutes. The clarified lysate was filtered and applied to a column packed with 1.0 ml of dATP-Sepharose resin, and the

column was washed extensively with column buffer composed of 50 mM N-[2-hydroxyethyl]piperazine-N′-[2-ethanesulfonic acid] (HEPES), 100 mM KCl, 1mM dithiothreitol (DTT), pH 8.2. After washing the column back to baseline with column buffer, a 7.0 ml-wash of column buffer containing 5 mM ATP was used to elute any *E. coli* R1, or other bound proteins resulting from the expression system. Finally, the recombinant vaccinia R1 protein was eluted with column buffer containing 75 mM ATP. Centricon-30 centrifugation devices (No. 4209; Amicon Inc., Beverly, MA) were used to concentrate the purified R1 and remove the ATP used in the elution step.

Hydroxyurea-Mediated Radical Decay Assays—Purified holoenzyme, or R2 alone, plus the appropriate effectors and substrates, were mixed with HU at time = 0 and the change in absorbance at 417 nm over time was recorded on a Beckman DU-64 spectrophotometer. Typically, assays were done in 50 mM HEPES, pH 8.2, containing 15 μM R2, 20 μM R1, 800 μM dNTP effector, 1 mM rNDP substrate, and 20 mM DTT, in a final volume of 75 μl. R1 was added in excess to assure that most of the R2 would be bound in the holoenzyme form. HU was added to a final concentration of either 3 or 20 mM.

Ribonucleotide Reductase Four-Substrate Assay—The assay was performed essentially as described in Hendricks and Mathews, 1997 (see Chapter 3). The assay is composed of two chromatographic steps. The first step, boronate affinity chromatography, separates the RNR products (dNDPs) from the substrates (rNDPs). In the second step of the assay, the dNDPs are resolved into individual nucleotides by high performance liquid chromatography (HPLC). Vaccinia R2 was added to the reaction in a two- to four-fold molar excess over vaccinia R1. In all reactions, vaccinia R1 was present at 1.0 μM final concentration. ATP and DTT were present in all reaction mixtures at 2.0 mM and 50 mM, respectively. Except as indicated, all four rNDP substrates were added to the reactions at equimolar concentrations, usually 0.15 mM each. In the inhibitor-treated samples, the final HU concentration ranged from 0.2 - 2.5 mM.

Results

Purification of the Recombinant Proteins—The results of a typical purification of the R2 and R1 subunits of the vaccinia RNR are shown in Figures 2.1 and 2.2, respectively. As the gels indicate, the purification procedures used in these studies are effective at generating homogeneous proteins.

Electronic Spectra of R2—Figure 2.3 shows the UV-vis spectra from 350 to 450 nm of three different forms of R2. Panel A is the spectrum of R2 from *E. coli*. Several peaks of interest arising from the iron-oxo and/or tyrosyl radical can be seen in the spectrum. Most notable is the relatively sharp absorbance at 410 nm. This peak is due primarily to the tyrosyl radical chromophore. The broad band or shoulder centered at ~370 nm is due to the iron-oxo center and has been assigned to the iron-oxygen bond stretching. A second band or shoulder, centered at ~390 nm, is attributed primarily to the tyrosyl radical but contains some overlapping absorbance from the iron center chromophore (Ehrenberg and Reichard, 1972). The assignment of these peaks was based initially on spectroscopic data including comparison to the spectrum of the 2,4,6-tri-*tert*-butylphenoxy radical, a model phenoxy radical produced chemically (Land *et al.*, 1961), and the optical spectrum of hemerythrin (Garbett *et al.*, 1969), an oxygen-binding protein containing a well characterized non-heme iron center.

Figure 2.3, panel B, shows the spectrum of the recombinant R2 protein from mouse. The tyrosyl radical of the mouse protein gives rise to a shoulder at 395 nm and a peak at 417 nm instead of the 390 nm shoulder and 410 nm peak observed in the *E. coli* R2 protein. As well as the shift of the peak to lower energy, the shape of the radical peak at 417 nm of the mouse protein is broader than the corresponding peak in the spectrum of the *E. coli* protein. The different shapes and positions of these peaks probably reflect differences in the protein structure surrounding the tyrosyl radical. As well as the differences in the residues found in this region of the protein, the distance, and hence the

Vaccinia R2 purification procedure:

streptomycin-SO_4 ppt.

↓

$(NH_4)_2SO_4$ ppt.

↓

Superose (size exclusion) FPLC

↓

MonoQ (ion exchange) FPLC

Typical results:

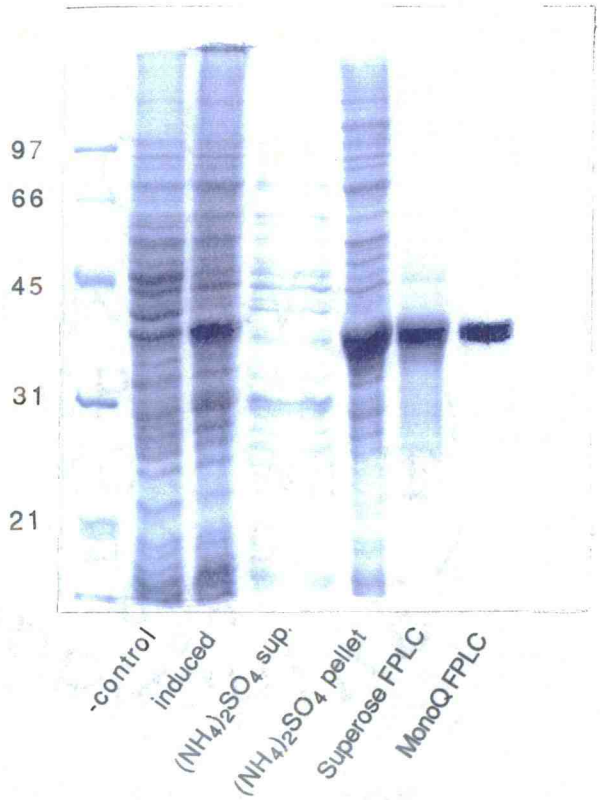

Figure 2.1 **Purification of the vaccinia R2 subunit.** The purification scheme used for the recombinant vaccinia and mouse R2 proteins is shown at the top of this figure. The gel shown at the bottom of this figure shows the results of a typical vaccinia R2 purification. Final yields from this procedure were routinely 3-5 mg of R2 per liter of induced cells. The radical content of purified vaccinia R2, which was estimated using the mouse R2 radical extinction coefficient of 3400 M^{-1} cm^{-1} (Thelander *et al.*, 1985), was found to be slightly less than 0.5 radicals per polypeptide chain, or approximately 1 radical per R2 dimer.

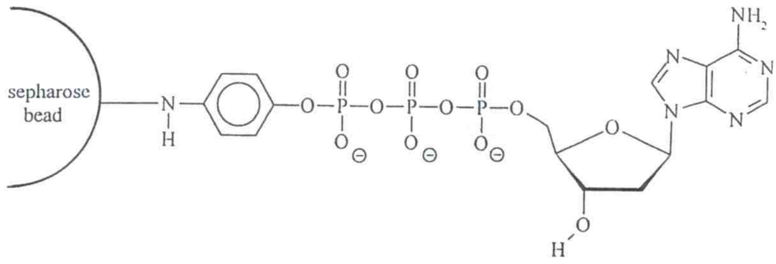

dATP - sepharose

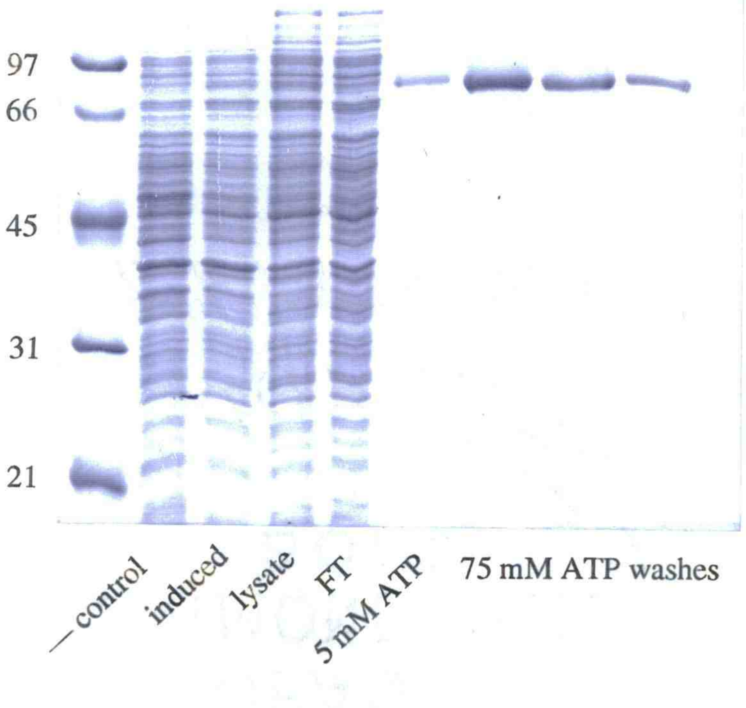

Figure 2.2 **Purification summary gel of vaccinia R1.** The gel shows the results of a typical purification of recombinant vaccinia R1. Typically, this purification procedure yielded 1.0 mg of vaccinia R1 per liter of induced cells. The structure of the dATP-Sepharose affinity resin used to purify the R1 is shown above the gel.

energy of the interaction, between the radical and iron center in the *E. coli* and mouse proteins is different. The distance between the tyrosyl radical and the closest iron atom in the *E. coli* protein is 5.3 Å (Nordlund *et al.*, 1990). The corresponding distance in the mouse R2 is slightly shorter (Kauppi *et al.*, 1996).

The iron center of the mouse protein gives rise to a shoulder centered at 370 nm, similar to the iron-oxo band in the *E. coli* R2 spectrum, and contributes some overlapping absorbance to the tyrosyl radical peaks (Thelander *et al.*, 1985). The similar position of the iron-related band at 370 nm of the R2 from mouse and *E. coli* suggests that the iron-oxo centers of these proteins are similar in structure. Indeed, comparison of the crystal structures of these proteins corroborates the similarity of the iron centers. Both the ligands, as well as the geometry of those ligands around the iron atoms, of the two centers are almost identical (Kauppi *et al.*, 1996).

The electronic absorption spectrum of vaccinia virus R2, shown in Figure 2.3, panel C, is almost identical to the absorption spectrum of the tyrosyl radical and iron-oxo center of the mouse R2. Based on sequence homologies, the vaccinia and mouse R2 proteins are predicted to be very similar in structure (Nordlund *et al.*, 1990) and this is reflected in the electronic absorption and electron paramagnetic resonance (EPR) spectra of the two proteins (Howell *et al.*, 1992). The electronic absorbance bands of the iron center and tyrosyl radical of the vaccinia R2 are virtually superimposable on the absorbance bands of the mouse R2 spectrum.

Hydroxyurea-mediated chromophore decay—Figure 2.4 shows the visible spectra of the vaccinia R2 protein taken at approximately 90 second intervals following the addition of HU. These spectra illustrate the simultaneous decay of both the tyrosyl radical and iron-oxo chromophores that occurs in the mammalian forms of protein R2.

Figure 2.3 **Light absorption spectra of R2 from three different species.** The electronic spectra, recorded from 350 to 440 nm, of the *E. coli* (*panel A*), mouse (*panel B*), and vaccinia (*panel C*) R2 proteins are shown on the following page. Protein concentrations of the samples used for these measurements were ~50 μM each. *E. coli* R2 was a gift from the laboratory of Dr. Britt-Marie Sjöberg. The mouse and vaccinia proteins were overexpressed and purified according to Material and methods. Spectra were recorded using a Beckman DU-64 spectrophotometer.

Figure 2.3 (Continued)

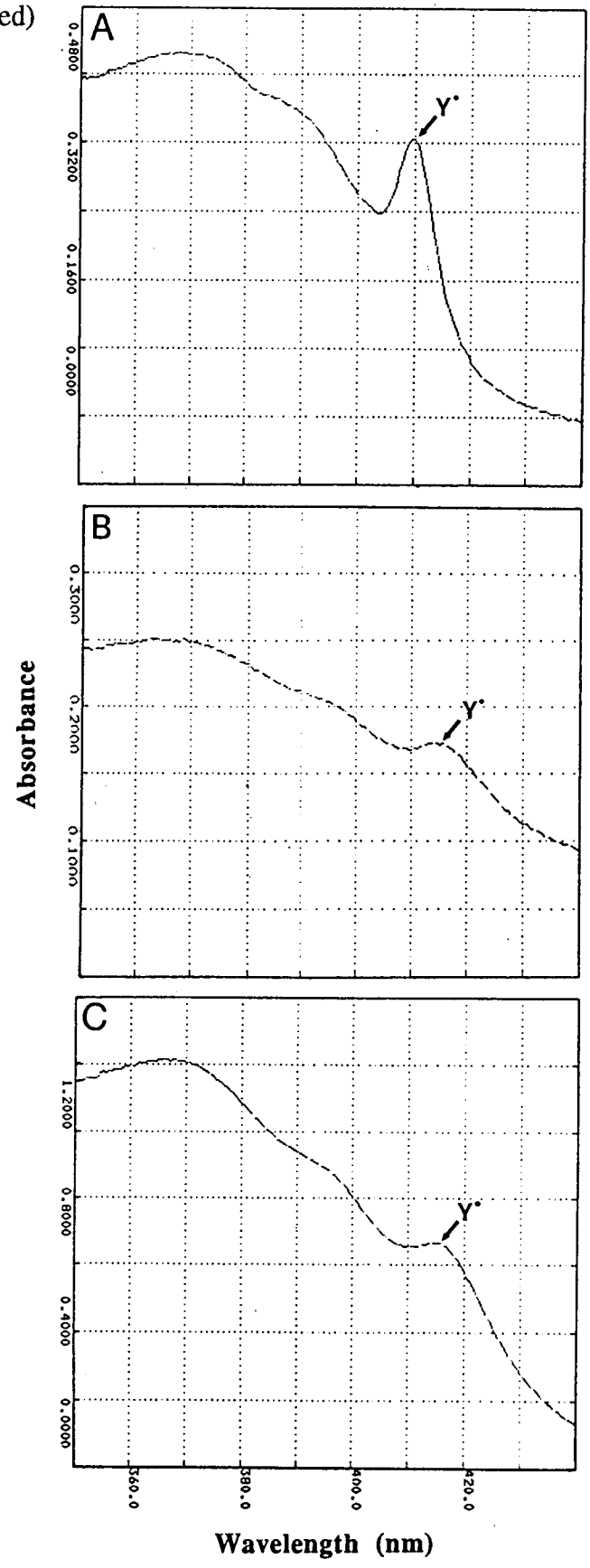

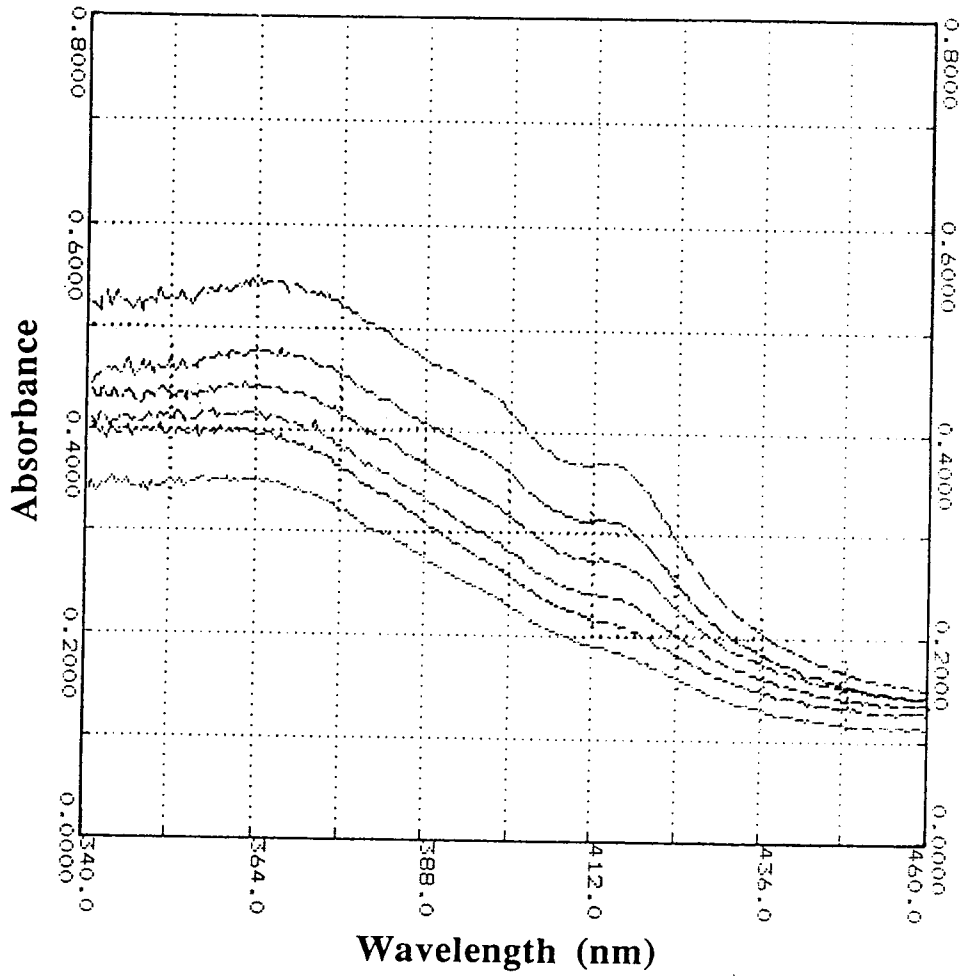

Figure 2.4 **Hydroxyurea-mediated decay of the vaccinia R2 tyrosyl radical and iron-oxo chromophores.** Time course of the chromophore decay of vaccinia R2 after treatment with HU. The upper tracing was recorded just prior to HU addition. Each successive spectrum was recorded at ~90 second intervals following addition of HU. This figure illustrates the simultaneous decay of the radical and iron-oxo center absorbance bands.

Figure 2.5 shows the results of a HU-mediated radical decay experiment. The curves represent the loss of signal at 417 nm after treatment of enzyme with 10 mM HU. Comparison of the decay rates of R2 alone (second curve from top) and R2 plus R1 (top curve) suggest that the presence of R1 protects the R2 tyrosyl radical and iron-oxo center from HU. This protection was lost once allosteric effectors were added to the holoenzyme (two lower curves).

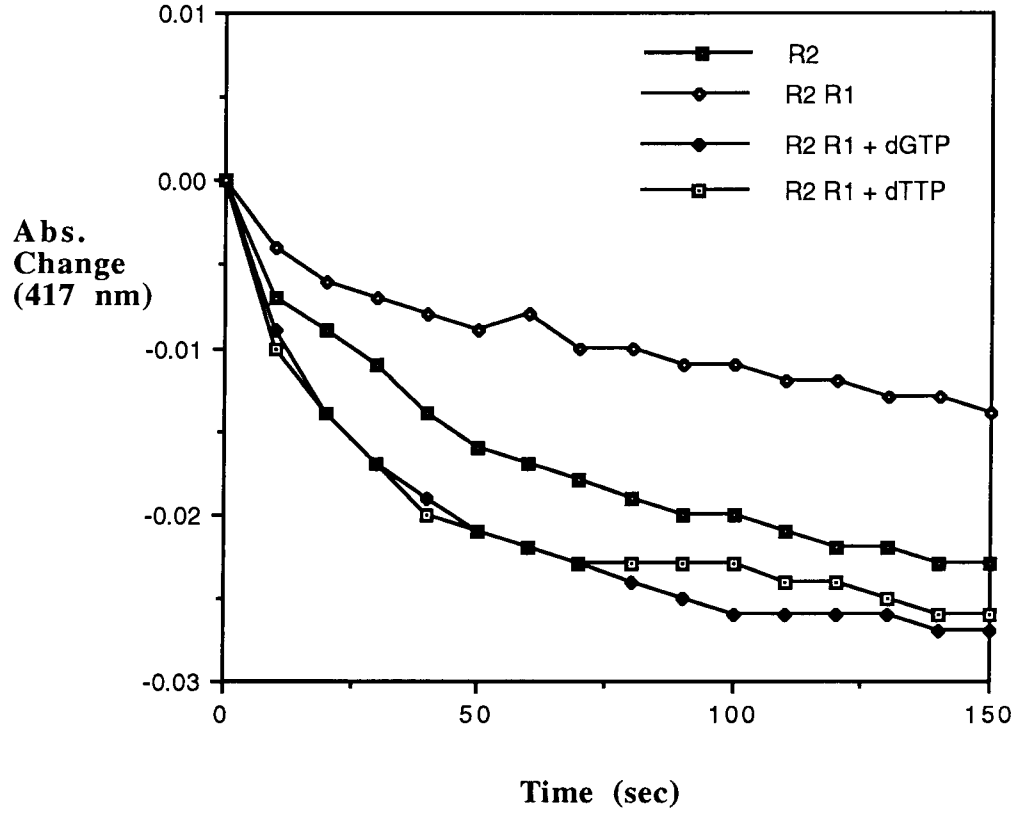

Figure 2.5 **Hydroxyurea-mediated radical decays of R2 in different states.** Experimental conditions were: 60 mM HU, 15 μM R2, 20 μM R1, and 800 μM dNTP.

The decay rate of the 417 nm chromophore was further examined at lower hydroxyurea concentrations and different allosteric states. Figure 2.6 shows the exponential decay of the chromophore when the holoenzyme was combined with one effector (dTTP or dGTP), plus or minus the appropriate substrate (rGDP or rADP). When either dTTP or dGTP was added to the enzyme solution, the chromophore decayed according to the two upper curves.

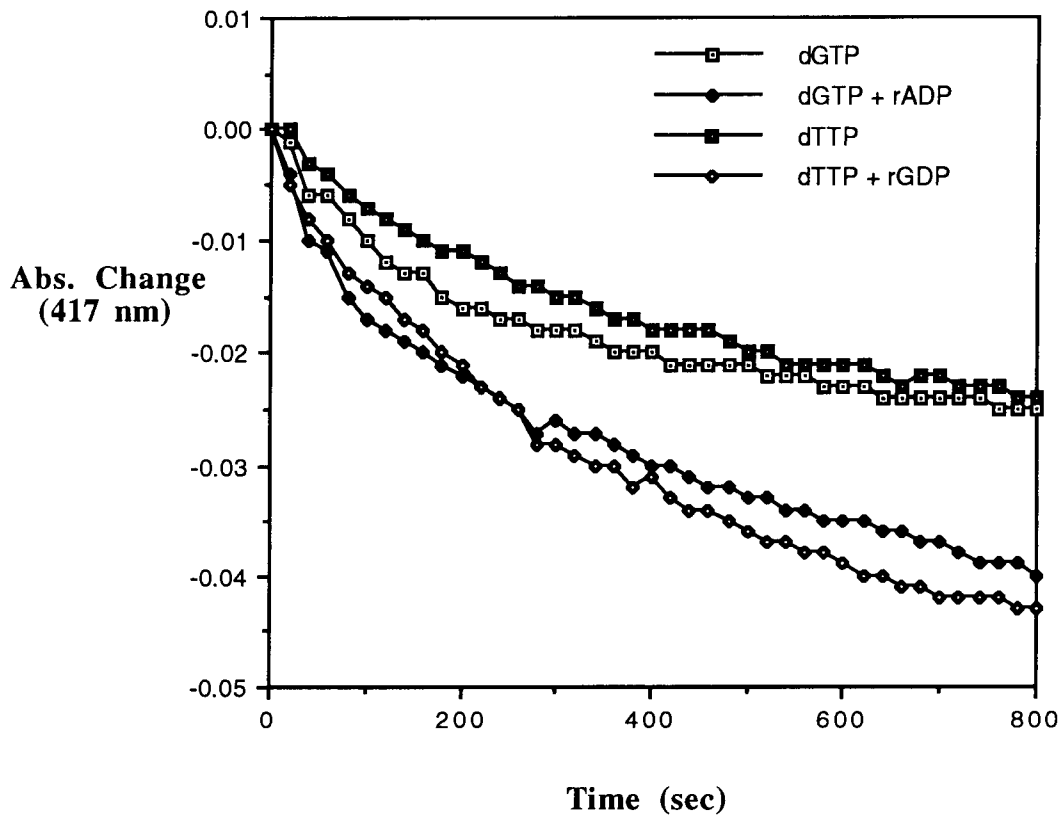

Figure 2.6 **The tyrosyl radical/iron-oxo center is more sensitive to hydroxyurea during substrate turnover.** 3 mM hydroxyurea and 1 mM rNDP substrate were used in these experiments. All other conditions were the same as those in Figure 2.5.

Interestingly, when substrate was added (0.1 mM) to this mixture, the radical and iron-oxo center became even more susceptible to hydroxyurea, as indicated by the decreased

half-life seen in the lower curves. This phenomenon was also observed when ATP and rCDP were added to the reaction mixture. The decay rates for two different effector/substrate combinations are plotted on the same graph in order to illustrate what was observed in most experiments: the half-lives of the radical in the presence of either effector were indistinguishable and the same was true when substrates were added. The curves from Figures 2.5 and 2.6 were from experiments done on the same day, using the same enzyme preparation. These were selected as figures because they best illustrate the common trends consistent within each experiment. However, the obvious differences in half-lives shown in Figures 2.5 and 2.6 were generally not as extreme as these graphs depict. Furthermore, data obtained on different days, or obtained using different enzyme preparations, were hard to compare as the variability of the decay rates was large (see discussion). Although the absolute value of the rate constants varied greatly between experiments, the trends on a given day were consistent with what is shown in Figures 2.5 and 2.6: R1 appeared to protect the radical and iron-oxo center when compared to the decay rate of the R2 protein without added R1. This effect was observed until the addition of effectors, at which point the radical and iron-oxo center became increasingly more sensitive to hydroxyurea. Furthermore, as illustrated in Figure 2.6, the addition of substrate further increased the rate of chromophore decay.

Measurement of HU-Inhibition using the Four-Substrate Assay—Figure 2.7 shows the results of a typical four-substrate assay. In these experiments, duplicate reactions containing identical levels of enzyme, substrates, and allosteric effectors were prepared. HU was added to one of the samples at time = 0 and the reaction mixtures were incubated at 37° C. After a short incubation (6 minutes in this case) the reactions were quenched and processed according to the assay procedure. The difference between the peak areas for each dNDP product in the treated and untreated samples gives the amount of product formation inhibited by HU.

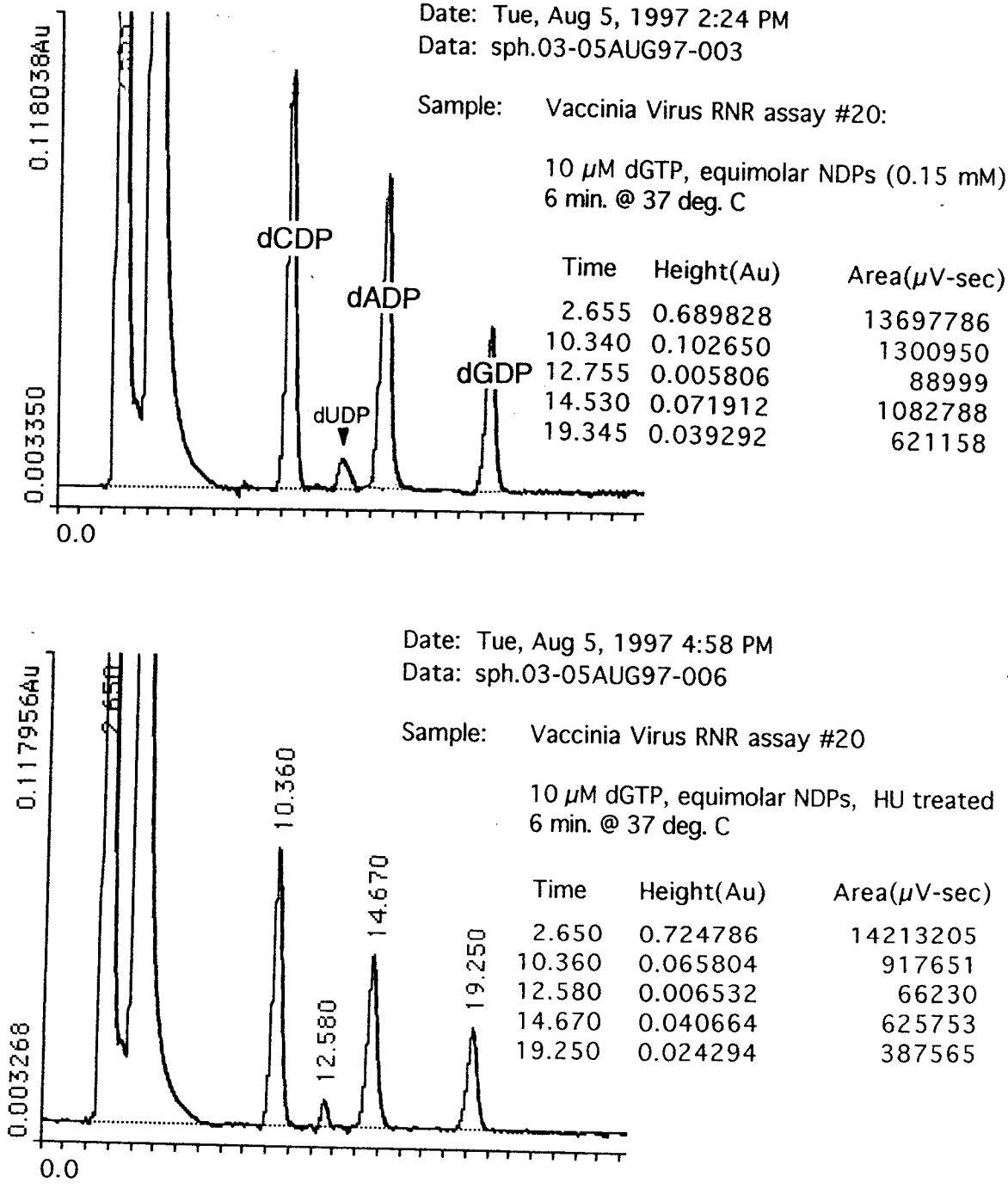

Figure 2.7 **HPLC chromatograms showing the results of vaccinia RNR assays ± HU.** The top chromatogram shows the results of the untreated control vaccinia RNR assay, and the lower chromatogram is the results from the assay which included 2.5 mM HU. Typical assays contained 1 μM R1, 4 μM R2, 2 mM ATP, and 0.15 mM each of the four rNDP substrates. In this particular experiment, the allosteric effector dGTP was added to 10 μM final concentration.

Tables 2.1 thru 2.3 contain the results of the four-substrate assay performed under the allosteric environments indicated at the top of each table. In these experiments, the HU-mediated inhibition was determined for each of the RNR activities by comparing the peak areas of each dNDP in the samples treated with the inhibitor and the corresponding peak areas of the untreated controls. The values in each column represent the percentage of the control activity remaining after the sample was treated with HU. All experiments were performed with 2.0 mM ATP present in the reaction mixture. ATP is a general activator of RNR and its presence was necessary to activate the enzyme to levels detectable by the assay. The results for the inhibition of the rUDP reductase activity were not included because the turnover of this substrate is very low even under optimal allosteric conditions (Hendricks and Mathews unpublished; see Chapter 4). At early time points, the peak area corresponding to dUDP was close to the noise level of the method, making it difficult to accurately measure the difference between the HU-treated and untreated samples.

The values from a given column of Tables 2.1, 2.2, and 2.3 represent the percentage of the control that each of the individual dNDP formation rates were inhibited by HU. A comparison of the values from a given column indicates that, in virtually every case, the percent inhibition was approximately the same for each substrate within the experimental error of the four-substrate assay (estimated at approximately 5% error, see Appendix V) indicating that no differential inhibition was detected by this method.

Table 2.1 *Effects of hydroxyurea on the activities of the vaccinia RNR when allosterically activated by ATP only*

% inhibition of reduction of	[HU] (mM)				
	0.5	1.0	1.5	2.0	2.5
rCDP	8	15	24	37	46
rADP	7	21	27	36	44
rGDP	5	18	36	41	49

Table 2.2 *Effects of hydroxyurea on the activities of the vaccinia RNR when allosterically activated by ATP + a single dNTP effector*

dNTP present (10 μM)	dGTP		dATP		dTTP	
[HU] (mM)	1.0	2.5	1.0	2.5	1.0	2.5
% inhibition of reduction of						
rCDP	21	35 ± 6	17	44 ± 5	31	48 ± 6
rADP	14	38 ± 4	22	38 ± 4	29	39 ± 2
rGDP	20	41 ± 3	16	37 ± 2	26	44 ± 3

Experiments performed in presence of 2.5 mM HU were done in duplicate. The results from these experiments are reported as the mean ± (range/2).

Table 2.3 *Effects of hydroxyurea on the activities of the vaccinia RNR when allosterically activated by ATP, dTTP, dATP, and dGTP*

% inhibition of reduction of	[HU] (mM)		
	1.5	0.5	0.2
rCDP	32 ± 3	14	7
rADP	28 ± 3	9	10
rGDP	24 ± 5	11	4

In these experiments, the dNTPs were added to 10 μM each and ATP was added to 2.5 mM. Experiments done at 1.5 mM HU were done in duplicate. The results of these experiments are reported as the mean ± (range/2).

Discussion

This chapter describes experiments designed to test the idea that the allosteric state of RNR is directly related to the HU sensitivity of the enzyme. The results obtained from both the spectroscopic method and four-substrate assay appear to indicate that the sensitivity of vaccinia RNR was not dependent on the identity of the bound dNTP. However, the decay rates of the chromophore at 417 nm measured using the spectroscopic method suggest that the sensitivity of the enzyme was directly proportional to the overall enzymatic activity. That is, when the enzyme was activated to reduce substrate by the binding of allosteric effectors, it was more susceptible than when no effectors were bound. Furthermore, when substrate was supplied, the enzyme became even more susceptible to the radical scavenger. These results are consistent with similar studies done on the *E. coli* RNR in which the rate of inhibition was determined by measuring the rCDP reductase activity remaining after treatment with HU (Karlsson *et al.*, 1992). The repeatability and sensitivity of the spectroscopic method was greatly limited by the low solubility of vaccinia R1 and the variable radical and iron content of R2. In order to have a reasonable absorbance change (usually 0.04-0.05 absorbance units), the radical/iron-oxo concentration was required to be approximately 10 μM. The radical content of the purified R2 used in these experiments ranged from 30-50% (2 radicals per R2 equals 100%). Therefore, these experiments required 10 to 15 μM R2. In order to assure that a majority of the R2 was bound in the holoenzyme form, an excess of R1 was required. The molecular weight of vaccinia R1 dimer is 175 kDa and thus, a 20 μM solution of R1 corresponds to ~3.4 mg/ml. Routinely, the vaccinia R1 protein would precipitate from solution when the concentration went much above 2 to 3 mg/ml. Therefore, in order to get enough sensitivity from this technique, I was constantly working on the fringe of the R1 solubility limit. To increase the solubility of R1, numerous buffer conditions were used, including various types and concentrations of buffer salts, dithiothreitol concentrations from 1 to 50 mM,

addition of nucleotide effectors, and addition of the vaccinia R2 during the concentration step. None of these conditions significantly improved the solubility of vaccinia R1. The results obtained by this technique were further complicated by the R2 radical and iron content, which varied with each preparation.

When no effectors were added to the protein solutions, the presence of R1 seemed to protect R2 from HU compared to the rate of chromophore decay when no R1 was present. Although this finding is interesting, it may have no physiological significance since within the cell the holoenzyme is probably always in contact with some level of dNTPs. From the standpoint of the electron transport system, the series of residues proposed to be involved in the transfer of the catalytic electron between R1 and R2, the result is especially intriguing. However, the decay rates determined without the addition of nucleotides had the largest variability. A possible contribution to this variability may be the presence of different levels of residual nucleotide in the R1 samples. A relatively high concentration of ATP (75 mM) was used to elute the R1 protein from the affinity column during the purification. Therefore, there was probably some residual nucleotide remaining in the R1 preparation despite attempts to remove it. The removal of nucleotide from the purified R1 was made technically difficult by the tendency of the protein to precipitate from solution. Again, the finicky solubility of vaccinia R1 proved to be a problem for the repeatability of the spectroscopic technique.

Similar to the radical decay experiments, the results from the four-substrate assay showed no obvious difference in the HU-sensitivity of any of the RNR enzyme activities. Table 2.1 shows the amount of each RNR activity inhibited by HU when only the general allosteric activator, ATP, was present in the reaction mix. This set of experiments was designed to function as a control. The assumption I made was that no differential sensitivity should be observed in these experiments since ATP was the only allosteric effector present and therefore, RNR should be in essentially one conformation. Although

this assumption may or may not be valid, the results show that none of the activities are statistically more sensitive to HU than any others.

Table 2.2 shows the results of experiments designed to mimic the radical decay experiments. The decrease in each activity after HU treatment is tabulated in columns according to which dNTP was added to the reaction mix (ATP was also present in these experiments at 2.0 mM). These experiments were performed in the presence of a single dNTP in order to test the sensitivity of each activity while RNR was activated to preferentially reduce a specific substrate. The assumption was that if a certain dNTP effector produced a conformation which was especially sensitive to HU, then this should be apparent from the percentage of inhibition for that activity relative to the control. However, within the experimental error, none of the effectors made any of the enzyme activities more or less sensitive to HU.

The four-substrate assay proved to be a nice system for these studies because it allowed the HU-induced changes in each of the individual turnover rates to be monitored while the enzyme was exposed to any combination of nucleotides desired. This enabled me to look for differential sensitivity within an allosteric environment designed to be similar to what the enzyme may be exposed to *in vivo*. Under these conditions, this assay provides a relatively good *in vitro* approximation of the *in vivo* system we seek to explain. Table 2.3 summarizes the four-substrate assay results from experiments done in an *in vivo*-like nucleotide environment consisting of the allosteric effectors ATP, dATP, dGTP, and dTTP. As these data indicate, none of the RNR activities seem to be statistically more or less sensitive to HU inhibition at the concentrations tested.

Although the results from these studies suggest that none of the activities of RNR are differentially sensitive to HU, it is still quite possible. I may have not been able to detect the difference in sensitivity because of the time scale of my experiments. The four-substrate assay indicates only the extent of inhibition which has occurred several minutes after the addition of drug. If the enzyme is differentially sensitive to HU, evaluation of the

inhibition at very short time points may be required in order to detect the difference. This may be necessary since the allosteric effectors rapidly equilibrate between the enzyme-bound and unbound states on a time scale several orders of magnitude less than the time scale of the experiment. When several effectors are present, the enzyme probably undergoes rapid conformational changes as different nucleotides bind to the allosteric sites. By the time the experiment has been completed, any short term differential effects may become undetectable as the enzyme rapidly converts between less sensitive and more sensitive allosteric states.

Relevant to this discussion, there may be another very important distinction between the *in vivo* and *in vitro* behavior of the HU-mediated radical decay. In *E. coli*, it has been demonstrated that there is an enzyme system, composed of a flavin reductase and a second poorly defined protein fraction, which is capable of regenerating the tyrosyl radical (Covés *et al.*, 1993). An *E. coli* strain lacking the flavin reductase component is more sensitive than wildtype to HU treatment, indicating that this enzyme system provides a protective function against loss of the tyrosyl radical. Furthermore, it has been suggested that this system may play a role in regulating RNR activity by controlling the radical content of protein R2 (Fontecave *et al.*, 1989). If eukaryotic cells possess a similar system, which is likely, then during HU treatment there may be a competition between radical decay and enzymatic radical regeneration. In this case, the increased inhibition of any enzyme activity which is associated with a more sensitive conformer may become evident only after enough time has passed for the cycle of decay and regeneration to repeat numerous times. This may be especially relevant if the relative sensitivities of the four reactions differ only slightly.

If the results of these *in vitro* studies on the susceptibility of RNR also apply to the behavior of the enzyme *in vivo*, then an alternate explanation for the observed dNTP pool changes is necessary. One possible explanation involves the activities of several enzymes and therefore, a brief review of deoxyribonucleotide metabolism may aid this discussion.

A surprising feature of dNTP metabolism is its dynamic nature. Once formed, the dNTPs do not remain in a static pool, sequestered somewhere in the cell, waiting to be utilized for DNA synthesis. Instead, the dNTP pools appear to undergo a continuous cycle of synthesis and degradation which results from the interplay between the *de novo* synthetic pathway and the activities of catabolic and salvage enzymes. For example, in mouse 3T6 fibroblasts the half-lives for the turnover of the dATP and dTTP pools are 4 and 5 minutes, respectively (Bianchi *et al.*, 1992; Nicander and Reichard, 1985a). Much of this turnover in cultured cells, at least in the case of pyrimidine dNTPs, results in the excretion of the nucleotide breakdown products into the surrounding media. In exponentially growing 3T6 cells for example, 28% of the *de novo*-synthesized dCDP is degraded to the nucleoside and excreted (Nicander and Reichard, 1985b).

Figure 2.8 shows the overall metabolism of deoxyribonucleotides in mammalian cells. Metabolism of deoxyribonucleotides can be separated into three distinct pathways, the *de novo* pathway, the salvage pathway, and a catabolic pathway. In the first reaction of the *de novo* synthesis of deoxyribonucleotides, rNDPs are reduced by RNR to the corresponding dNDPs. The dNDPs rapidly equilibrate, through the action of several nucleotide kinases, between the mono- and triphosphate deoxyribonucleotides. Although the concentration of a particular deoxyribonucleotide may vary considerably depending on the particular conditions, the ratio between the mono-, di-, and triphosphate deoxyribonucleotides remains relatively constant (Reichard, 1988). Therefore, as dNTPs are removed from the nucleotide pool for the synthesis of DNA, a net phosphorylation of the dNMP pool allows the equilibrium to be maintained.

As well as being phosphorylated to the triphosphate level, dNMPs can be dephosphorylated to their corresponding deoxyribonucleosides by the action of specific 5′-nucleotidases. In general, the relative activities of these nucleotidases towards a given dNMP are directly proportional to the concentration of that nucleotide (Reichard, 1988). Once formed, the deoxyribonucleosides have many possible fates. Deoxyribonucleosides

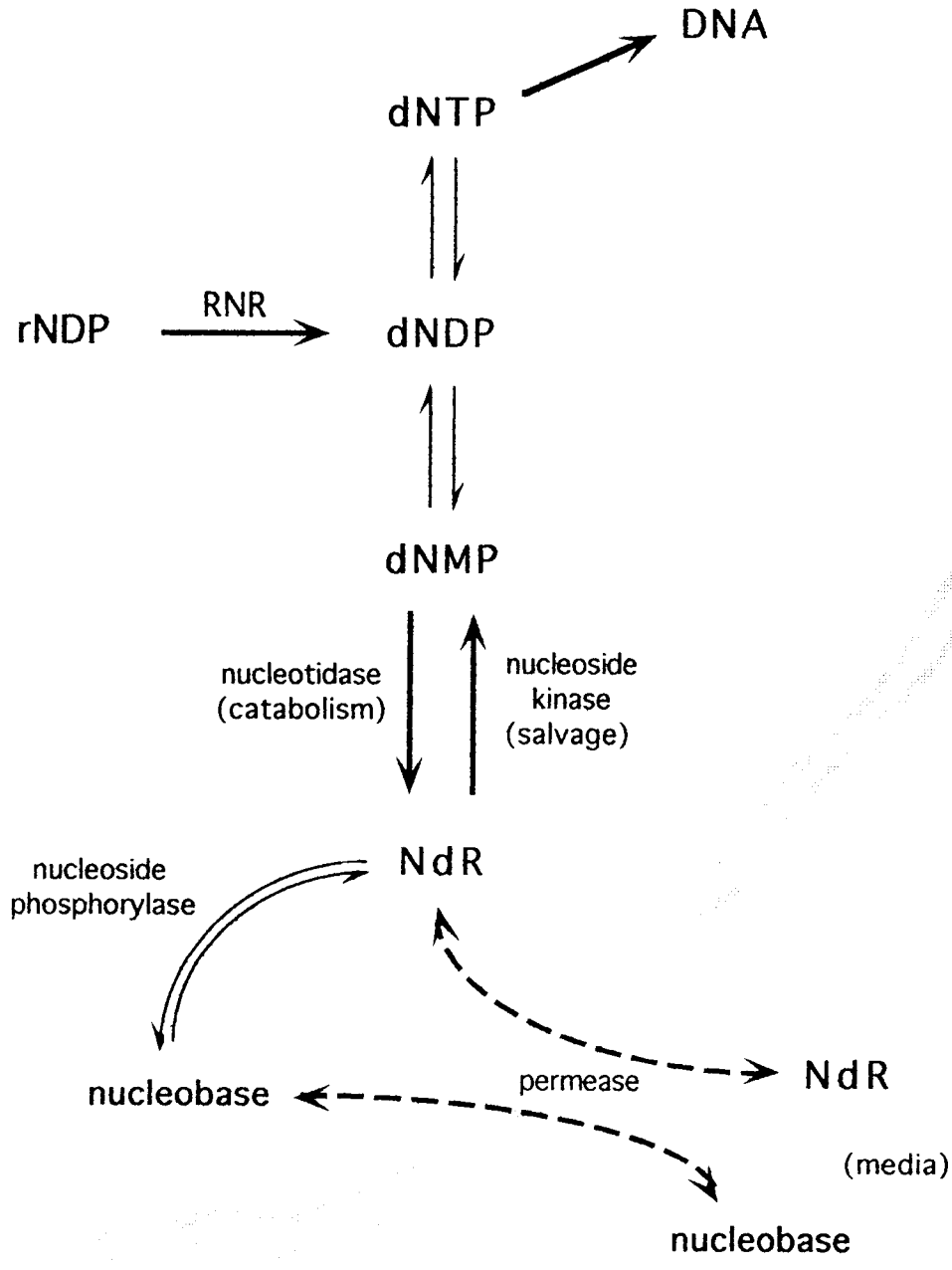

Figure 2.8 **Overview of deoxyribonucleotide metabolism.**

may be cleaved to the nucleobase and deoxyribose-1-phosphate by nucleoside phosphorylases. Various pyrimidine-nucleoside phosphorylases cleave deoxyuridine (dUrd) and dThd, and purine-nucleoside phosphorylase (PNP) cleaves deoxyinosine (dIno) and dGuo. Loss of the catabolic activity of PNP in human lymphocytes results in elevated concentrations of the purine dNTPs to levels capable of inhibiting T cell proliferation. This results ultimately in a form of immunodeficiency (Zannis *et al.*, 1978).

Generally, dAdo and to a lesser extent dCyd are enzymatically deaminated to dIno and dUrd, respectively, before being cleaved by nucleoside phosphorylase (Plagemann and Erbe, 1973a). Deoxyadenosine is readily deaminated by adenosine deaminase (ADA), and the resulting dIno may then be further degraded by PNP. In most mammalian cells, the activity of ADA is high, which keeps the intracellular concentration of dAdo low. Similar to the PNP deficiency, a lack of ADA activity also results in an immunodeficiency syndrome (Daddona and Kelley, 1977). This form of immunodeficiency, called severe combined immunodeficiency syndrome (SCIDS), is associated with an elevated concentration of dATP in lymphocytes. The accumulation of dATP in these cells presumably blocks the *de novo* synthesis of deoxyribonucleotides, resulting in the inhibition of B and T lymphocyte proliferation.

As stated earlier, a significant amount of nucleosides produced from the breakdown of *de novo* synthesized deoxyribonucleotides are excreted into the culture medium. Deoxyribonucleoside-specific permease proteins facilitate the reversible transfer of nucleosides across the cell membrane. The transfer process appears to be a form of facilitated diffusion and therefore, the transport of deoxyribonucleosides flows along any concentration gradient which may form as dNTP metabolism changes (Plagemann *et al.*, 1988). In general, the transfer of the pyrimidine deoxyribonucleosides is more efficient than the transfer of the purine deoxyribonucleosides. This fact is reflected in the apparent K_ms for the transport process which are one to two orders of magnitude lower for the pyrimidine deoxyribonucleosides (Plagemann and Erbe, 1973b). In mammalian cells, the

excretion rate of the purine deoxyribonucleosides, in particular dAdo, is much less than the corresponding rate for the pyrimidine deoxyribonucleosides. The excretion of dAdo from most cultured cells may be negligible because of the high activities of enzymes, like ADA, which catabolize the purine deoxyribonucleosides (Plagemann and Erbe, 1973b). In human lymphoblasts and hamster fibroblasts, for example, only 0.05 and 4.0%, respectively, of the dATP synthesized from the reduction of rADP is excreted into the media (Bianchi *et al.*, 1994). Instead of being excreted as dAdo, this deoxyribonucleoside is quickly deaminated to dIno which is then excreted, or cleaved to hypoxanthine by PNP. The hypoxanthine can be shuttled back into ribonucleotide synthesis by hypoxanthine-guanine phosphoribosyltransferase (HGPRT), or may undergo further degradation. In contrast, as much as 28% of the *de novo* synthesized dCTP is excreted from mouse fibroblasts in the form of deoxyribonucleosides (Nicander and Reichard, 1985b). Most of this deoxycytidine is excreted in its deaminated form, leading to an accumulation of dUrd in the medium. In addition, high levels of dCyd and dThd may also accumulate in the media of cultured cells (Bianchi *et al.*, 1986a; Nicander and Reichard, 1985b; Slabaugh *et al.*, 1991).

The last fate of deoxyribonucleosides shown in Figure 2.8 is the rephosphorylation of the nucleoside back to the dNMP level. In mammalian cells, thymidine kinase is responsible for the phosphorylation of dUrd and dThd. This kinase is feedback inhibited by dTTP (Cheng, 1978). The other prominent deoxyribonucleoside kinase activity in mammalian cells is deoxycytidine kinase. This broad specificity kinase phosphorylates dCyd and is also the major purine deoxyribonucleoside-phosphorylating activity in mammalian cells (Sarup and Fridland, 1987). The K_m values for the phosphorylation of dCyd by deoxycytidine kinase are 100-200 times less than for the phosphorylation of dAdo and dGuo. The enzyme is strongly inhibited by dCTP, and phosphorylation of the purine deoxyribonucleosides can be inhibited by dCyd (Hurely *et al.*, 1983). The greater activity of these kinases towards the pyrimidine deoxyribonucleosides may explain, at least in part,

why dNTP pools are more readily labeled by exogenous pyrimidine rather than purine deoxyribonucleosides (Plagemann and Erbe, 1973a).

The catabolism of dNMPs by the 5′-nucleotidases and the salvage of deoxyribonucleosides by the nucleoside kinases represent opposing reactions, and form a substrate cycle which has been proposed to be a regulatory mechanism for the maintenance of dNTP pool size (Nicander and Reichard, 1985b). The regulation of the *de novo* pathway through allostery of enzymes like RNR is well appreciated as a means for maintaining the proper levels of the dNTPs. In addition to this regulation, the ratio of the deoxyribonucleosides and their corresponding monophosphates may also play a significant role in maintaining proper levels of the dNTPs. The cycle of phosphorylation and dephosphorylation is schematically illustrated in Figure 2.9.

According to the substrate cycle proposal, the balance between these two opposing reactions sets the intracellular concentration of a given deoxyribonucleoside and its monophosphate. When dNTP pools start to drop, a net phosphorylation of the nucleoside pool results in an increase in the dNMP concentration (Figure 2.9, right arrow). The increase in dNMP concentration results in transfer of nucleotide to the dNTP pools through the action of the nucleoside mono- and diphosphate kinases. Thus, the drop in dNTP concentration is compensated for by an increased rate of flux through the phosphorylation phase of the substrate cycle and a decrease in the excretion of deoxyribonucleosides. When the utilization of dNTPs is blocked, a net dephosphorylation of the dNMP pool by the nucleotidase activity results in increased levels of the deoxyribonucleosides (Figure 2.9, left arrow). This increase in concentration is accompanied by increased catabolism and/or transport of the deoxyribonucleoside (or nucleobase) out of the cell.

Support for the substrate cycle hypothesis has come from studies on mutant cell lines defective in some aspect of dNTP metabolism and from studies done on normal cells exposed to inhibitors of dNTP metabolism. Pyrimidine dNTP metabolism was studied in a mutant hamster V79 cell line lacking a functional dCMP deaminase, to evaluate the role that

Figure 2.9 **dNMP/deoxyribonucleoside substrate cycle**. The cycle shown on the following page is proposed to function as a regulator of dNTP metabolism through the action of two opposing reactions. The balance of these two reactions sets the intracellular concentration of a given nucleoside and determines whether that nucleoside will move into the cell, promoting the synthesis of dNTPs, or out of the cell, promoting dNTP degradation. Deoxyribonucleosides are phosphorylated by the nucleoside kinases, whose activities are allosterically regulated by their respective dNTPs. The activities of the 5′-nucleotidases, which catalyze the opposing reaction, depend largely on the concentration of the dNMP substrate. The equilibrium of the substrate cycle is also affected by the activities of other catabolic and salvage enzymes. For instance, the deaminases and phosphorylases catalyze the degradation of deoxyribonucleosides, thereby increasing the excretion of nucleosides and nucleobases. The nucleotide kinases promote the anabolism of nucleosides, resulting in a net increase in the import of extracellular deoxyribonucleosides.

Figure 2.9 (Continued)

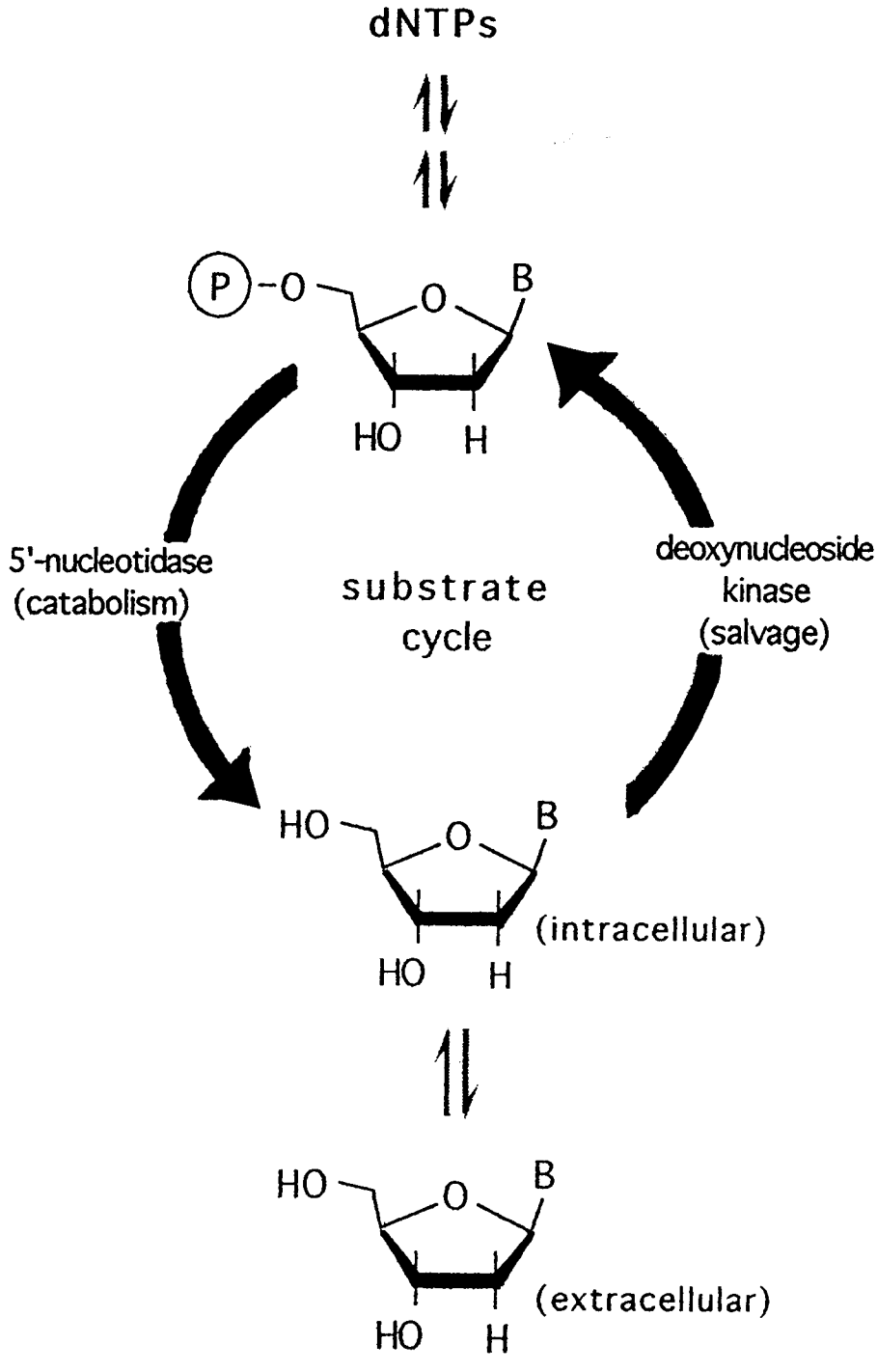

substrate cycles play in compensating for the lost enzyme activity (Bianchi *et al.*, 1987). Normal V79 cells derive more than 80% of their dTTP from the deamination of dCMP. Not surprisingly then, the dCMP deaminase-minus mutants had a significantly lower dTTP pool and an elevated dCTP pool. The elevated dCTP pool can be explained by the decreased conversion of dCMP to dUMP and to an increase in the rCDP reducing activity resulting from a decrease in the dTTP-mediated inhibition of RNR. The changes in the dNTP concentrations which were observed in these mutant cells were accompanied by an increase in the rate of dCyd excretion and a corresponding increase in the rate of dUrd uptake from the media. According to the hypothesis, the uptake of dUrd and excretion of dCyd results from an attempt by the substrate cycle to compensate for the dNTP pool changes through adjustments of the dNMP/deoxyribonucleoside ratio.When mouse 3T6 fibroblasts were treated with aphidocholin, the resulting block in DNA synthesis did not change the turnover rate of the pyrimidine dNTPs, but did increase the rate of dThd excretion (Nicander and Reichard, 1985a). Therefore, although DNA polymerization had stopped in these cells, dTTP was still being synthesized. According to the substrate cycle hypothesis, the increased excretion of dThd was a direct result of the increased flux of dTTP through the catabolic phase of the cycle. In this way, the substrate cycle can compensate for the decreased utilization of dTTP by DNA polymerase.

When the *de novo* synthesis of dNTPs was blocked in 3T6 cells by treatment with hydroxyurea, the flux of pyrimidine deoxyribonucleotides through the substrate cycle was reversed relative to the case above in which DNA polymerase was inhibited by aphidocholin. Under these conditions, the turnover of the pyrimidine dNTP pools decreased 5- to 50-fold due to a significant drop in the rate of dNTP degradation. In these cells, the dCTP pool was maintained by a net influx of dCyd from the medium, and the dTTP pool was fed by a net influx and phosphorylation of dUrd in addition to the continued deamination of the deoxycytidine nucleotide pool (Nicander and Reichard, 1985a; Bianchi *et al.*, 1986b).

When 3T6 cells are treated with HU, the dNTP pools are depleted in a manner similar to the changes which occur in vaccinia-infected cells. In both cases, HU treatment primarily depletes the purine dNTPs, especially dATP, and to a lesser extent reduces the dCTP pool. The dTTP pool, on the other hand, increases to 150% and 200% of controls in 3T6 and vaccinia-infected BSC_{40} cells, respectively. One explanation which has been proposed to explain these dNTP pool changes in HU-treated 3T6 cells centers around the substrate cycle hypothesis (Bianchi *et al.*, 1986a). According to this explanation, the dTTP pool continued to increase after HU treatment because the pool was fed by a net influx and phosphorylation of dUrd. In addition, the deamination of dCMP followed by the action of thymidylate synthase maintained the anabolic flux of pyrimidine deoxyribonucleotide into the dTTP pool. An influx of dCyd from the medium contributed to the maintenance of the dCTP pool. Therefore, when the *de novo* synthesis of deoxyribonucleotides is blocked, the substrate cycles respond by increasing the flux through the salvage phase of the cycle in an attempt to compensate for the decreasing dNTP concentrations. However, this response is capable of replenishing the pool only if the deoxyribonucleoside substrate is available for phosphorylation. The levels of the purine deoxyribonucleosides in the media, which by many accounts may approach zero (Plagemann and Erbe, 1971a; Reichard, 1988; Plagemann *et al.*, 1988), are too low to support any appreciable salvage-mediated synthesis of dATP or dGTP. The high rate of purine deoxyribonucleoside catabolism effectively reduces the concentrations of dAdo and dGuo and therefore, when dNTPs are measured in HU treated cells these pools appear to be depleted to the greatest extent.

A complication arises when one attempts to extend this explanation to the HU-induced dNTP pool changes in vaccinia-infected cells as observed by Slabaugh *et al.*, (1991). In these experiments, the culture medium was replaced with fresh medium containing dialyzed fetal calf serum at the time that HU was added. Presumably then, any deoxyribonucleosides that had accumulated in the medium prior to the addition of HU would have been removed from the extracellular environment at the same time that the *de*

novo synthesis was being inhibited. This fact seems to suggest that a mechanism other than the substrate cycle hypothesis may be responsible for the observed HU-induced dNTP pool changes observed in these studies. This led to a suggestion that perhaps HU preferentially inhibits the reduction of the purine rNDPs, especially the reduction of rADP.

However, Slabaugh and coworkers performed another experiment in conjunction with the dNTP pool measurements that gave results which seem to contradict the notion that the medium was free from deoxyribonucleosides. In an effort to measure the effects of HU on the *in vivo* flux through RNR, vaccinia-infected cells were treated with HU and then exposed to a tracer amount of tritiated ribonucleoside ([^{3}H]Cyd, [^{3}H]Guo, or [^{3}H]Ado). Like in the dNTP pool determinations, the media was changed at the point of HU treatment and then again when labeled ribonucleoside was added. After a labeling period of 1 hour, the cells were harvested and the intra- and extracellular fractions were examined to determine how much of the labeled ribonucleoside was converted to deoxyribo-containing molecules, and where in the cell these molecules ended up. At the lower HU concentrations, tritium was found in viral DNA and in the dNTP pools. However, when the media was tested for the presence of label an interesting finding was made. When the tritiated purine ribonucleosides were used to label the deoxy pools, no evidence of excreted breakdown products like [^{3}H]dAdo or [^{3}H]dGuo was found. In contrast, when [^{3}H]Cyd was used to label the cells, more counts were present in the form of excreted dCyd and dUrd than were present in the viral DNA and dNTP pools combined (Slabaugh *et al.*, 1991; Table I).

These findings indicate that although the medium was changed at obvious times during the experiment, the very dynamic nature of dNTP metabolism facilitated the rapid flow of nucleotide into a cycle of dNTP anabolism and catabolism resulting in excretion of pyrimidine deoxyribonucleosides (dUrd and dCyd). Furhermore, these experiments support the findings made in other mammalian cells which suggest that the catabolism of the pyrimidine and purine deoxyribonucleotides culminates in significantly different end

products. To a large extent the pyrimidine dNTPs are degraded to the level of deoxyribonucleosides which are excreted in large quantities into the surrounding medium. A large fraction of the purine dNTPs are degraded to the nucleobase, which may then be further degraded or fed back into ribonucleotide metabolism.

Although it would have been quite interesting, and exciting, to have demonstrated that RNR was differentially sensitive to HU, my studies suggest that it is not. Therefore, an explanation centered around the substrate cycle hypothesis may be a plausible alternative to differential sensitivity. The following points are consistent with the substrate cycle hypothesis as an explanation for the HU-induced dNTP pool changes observed in vaccinia-infected BSC_{40} cells.

(i) HU inhibition of viral DNA replication was reversed by the addition of dAdo and EHNA. Presumably, dAdo was capable of reversing the block on replication because dATP was the smallest dNTP pool and therefore the "limiting reagent" for DNA synthesis. The fact that dAdo rescue was effective only in the presence of the deaminase inhibitor is a very important point. According to the substrate cycle explanation, the high level of ADA activity in mammalian cells plays a major role in the dATP pool depression seen in HU-treated cells. When the *de novo* synthesis is blocked the salvage pathway becomes an important source of dNTPs. Obviously, the ADA activity in vaccinia-infected cells is sufficiently high to deaminate the majority of dAdo present in the cell, or the addition of EHNA would not be required for the rescue. Therefore, when ADA is not inhibited, the deamination of dAdo effectively reduces the concentration, and hence the flux of this deoxyribonucleoside through the salvage pathway, to negligible levels. Furthermore, when dNTP levels were measured in HU-treated cells grown in the presence of dAdo and EHNA, the dATP pool was no longer depleted. Instead, under these conditions, the dATP pool remained at the level of the untreated control at all HU concentrations studied (Slabaugh *et al.*, 1991; Figure 6). Finally, the lack of purine deoxyribonucleosides in the

media of HU-treated and untreated cells is consistent with the high level of dAdo catabolism.

(ii) The dTTP pool was elevated by HU. This result is best explained as previously reported (Bianchi *et al.*, 1986a,b). Essentially, the dTTP pool increased because its utilization was blocked, and deamination of dCMP in combination with salvage synthesis continued to supply the pool. If deoxyribonucleosides equilibrate across the cell membrane in vaccinia-infected cells as they do in other cell types, then the high concentration of dCyd and dUrd detected in the culture media of these cells indicates that there should be a significant amount of intracellular pyrimidine deoxyribonucleosides available for phosphorylation by the salvage kinases.

Other factors may also contribute to the depressed dATP pool. For example, at the lower HU concentrations tested (0.5 and 1.0 mM), *in situ* assays demonstrated that ribonucleotide reduction continued to occur, albeit at significantly lower rates (Slabaugh *et al.*, 1991; Table I). In the mammalian form of RNR, rADP reduction is stimulated by dGTP. I have recently determined, using the four substrate assay, that the vaccinia enzyme behaves in a similar manner (Hendricks and Mathews, unpublished; see Chapter 4). Therefore, the HU-induced depression of the dGTP pool, a pool which is significantly underrepresented even in untreated cells (Mathews and Ji, 1992), will result in a lowered activation of the rADP-reducing activity of RNR and hence, a lower relative rate of dATP formation. Similarly, the elevated dTTP pool will stimulate the rGDP-reducing activity of RNR. This, along with the different catabolic pathways for dAdo and dGuo, may explain why the dGTP pool is not depleted to the same extent that the dATP pool is.

If the substrate cycle hypothesis is a valid explanation of the HU-induced dNTP pool changes, then other inhibitors which specifically target RNR should result in similar dNTP pool changes. Indeed, this is the case for the drug 2′-azidocytidine (N_3-Cyd). This nucleoside analog, after phosphorylation by a nucleoside kinase, is a suicide inhibitor of RNR which acts by scavenging the catalytically essential radical at the active site.

Exposure of 3T6 cells to N_3-Cyd results in changes in the dNTP pools which are remarkably similar to the changes observed in HU-treated cells (Åkerblom and Reichard, 1985). Like HU, treatment with N_3-Cyd results in elevated dTTP and greatly depressed dATP levels. In addition, both drugs decrease the dCTP pool to approximately the same extent. The only significant difference between the dNTPs after treatment with these drugs is the level of dGTP. Other RNR inhibitors have similar effects. Mimosine, a non-protein amino acid found in certain plants, is an iron chelator that has been shown to inhibit RNR *in vitro*. Like these other inhibitors of RNR, treatment of mammalian cells with mimosine results in a major reduction of the purine dNTP pools and an elevation of the dTTP pool (Dai *et al.*, 1994).

Why should dAdo be metabolized to such a great extent while the purine dNTPs are simply dephosphorylated and excreted? The answer may lie in the multiple roles that adenosine, and its nucleotides play in cellular metabolism. Adenosine acts as a neurotransmitter and is involved in the regulation of platelet and neutrophile functions, of blood flow in the heart and kidney, and of lipid biosynthesis in adipocytes (Gerlach and Becker, 1987). The excretion of dAdo by inappropriate cells, or at inappropriate times, could possibly wreak havoc on the signaling systems used by that organism. Therefore, since the progenitor of each cell type discussed in this chapter was once part of a multicellular organism, evolution has probably selected against the excretion of intact dAdo by these cells.

References

Adams, R. L. P., Berryman, S., and Thomson, A. (1971) *Biochem. Biophys. Acta* **248**, 455-462

Åkerblom, L., and Reichard, P. (1985) *J. Biol. Chem.* **260**, 9197-9202

Bianchi, V., Pontis, E., and Reichard, P. (1986a) *J. Biol. Chem.* **261**, 16037-16042

Bianchi, V., Pontis, E., and Reichard, P. (1986b) *PNAS* **83**, 986-990

Bianchi, V., Pontis, E. and Reichard, P. (1987) *Mol. Cell. Biol.* **7**, 4218-4224

Bianchi, V., Pontis, E. and Reichard, P. (1992) *Exp. Cell Research* **199**, 120-128

Bianchi, V., Ferraro, P., Borello, S., Bonvini, P., and Reichard, P. (1994) *J. Biol. Chem.* **269**, 16677-16683

Cheng, Y.-C. (1978) *Methods Enzymol.* **51**, 365-371

Covés, J., Niviére, V., Eschenbrenner, M., and Fontecave, M. (1993) *J. Biol. Chem.* **268**, 18604-18609

Daddona, P. E., and Kelley, W. N. (1977) *J. Biol Chem.* **252**, 110-115

Dai, Y., Gold, B., Vishwanatha, J. K., and Rhode, S. L. (1994) *Virology* **205**, 210-216

Ehrenberg, A., and Reichard, P. (1972) *J. Biol. Chem.* **247**, 3485-3488

Fontecave, M., Eliasson, R., and Reichard, P. (1989) *J. Biol. Chem.* **264**, 9164-9170

Garbett, K., Darnell, D. W., Klotz, I. M., and Williams, R. J. P. (1969) *Arch. Biochem. Biophy.* **135**, 419

Hendricks, S. P., and Mathews, C. K. (1997) *J. Biol. Chem.* **272**, 2861-2865

Howell, M. L., Sanders-Loehr, J., Loehr, T., Roseman, N. A., Mathews, C. K., and Slabaugh, M. B. (1992) *J. Biol. Chem.* **267**, 1705-1711

Hurley, M. C., Paletta, T. D., and Fox, I. H. (1983) *J. Biol. Chem.* **258**, 15021-15027

Karlsson, M., Sahlin, M., and Sjöberg, B.-M. (1992) *J. Biol. Chem.* **267**, 12622-12626

Kauppi, B., Nielson, B. B., Ramaswamy, S., Larson, I. J., Thelander, M., Thelander, L., and Eklund, H. (1996) *J. Mol. Biol.* **262**, 706-720

Land, E. J., Porter, G., and Strachan, E. (1961) *Trans. Faraday Soc.* **57**, 1885-1893

Mathews, C. K., and Ji, J. (1992) *Bioessays* **14**, 295-301

Nicander, B. and Reichard, P. (1985a) *J. Biol. Chem.* **260**, 5376-5381

Nicander, B. and Reichard, P. (1985b) *J. Biol. Chem.* **260**, 9216-9222

Nordlund, P., and Eklund, H. (1993) *J. Mol. Biol.* **232**, 123-164

Plagemann, G. W., and Erbe, J. (1973a) *J. Cell. Physiol.* **83**, 321-336

Plagemann, G. W., and Erbe, J. (1973b) *J. Cell. Physiol.* **83**, 337-344

Plagemann, G. W., Wohlheuter, R. M., and Woffendin, C. (1988) *Biochem. Biophys. Acta* **947**, 405-443

Reichard, P. (1988) *Ann. Rev. Biochem.* **57**, 349-374

Sarup, J. C., and Fridland, A. (1987) *Biochem.* **26**, 590-597

Skoog, L. and Nordenskjöld, B. (1971) *Eur. J. Biochem.* **19**, 81-89

Slabaugh, M. B., Howell, M. L., Wang, Y., and Mathews, C. K. (1991) *J. Virology* **83**, 2290-2298

Thelander, M., Gräslund, A., and Thelander, L. (1985) *J. Biol. Chem.* **260**, 2737-2741

Zannis, V., Doyle, D., and Martin, D. W. (1978) *J. Biol. Chem.* **253**, 504-510

Chapter 3

Regulation of T4 Phage Aerobic Ribonucleotide Reductase: Simultaneous Assay of the Four Activities

Stephen P. Hendricks and Christopher K. Mathews

Published in the *Journal of Biological Chemistry*
The American Society for Biochemistry and Molecular Biology, Inc.
Vol. 272, pp. 2861-2865, 1997

Summary

We have devised an assay procedure that permits simultaneous monitoring of the four activities of ribonucleotide reductase. Using this assay, we have compared the reduction of all four substrates by the T4 bacteriophage aerobic ribonucleotide reductase within different allosteric environments. Specifically, we compared the relative turnover rates of the enzyme when activated with "*in vivo*" concentrations of the known allosteric effectors versus activation by ATP alone. Consistent with the known allosteric properties of this form of ribonucleotide reductase, our results show that ATP does act as a general activator, although the rate of purine nucleotide reduction was approximately five percent of the rate for the pyrimidine nucleotides. However, addition of the allosteric effectors at their estimated physiological concentrations dramatically changed the relative rates of substrate reduction, creating a more "balanced" pool of products. Addition of the substrates at their respective "*in vivo*" concentrations further pushed rates of product formation towards a ratio similar to the base composition of the T4 genome. The similarity of the product profile produced under "*in vivo*" conditions to the genomic composition of T4 phage is discussed.

The first committed step in DNA biosynthesis occurs by direct reduction of the 2'-hydroxyl of ribonucleotides and is catalyzed by the enzyme ribonucleotide reductase. Because this single enzyme is responsible for the production of all four deoxyribonucleotides, and because these products are needed only at specific times in cell or viral life cycles, ribonucleotide reductase is highly regulated in both substrate specificity and overall activity.

The allosteric properties of the enzyme, as well as the kinetic parameters for all four rNDP substrates, are well characterized for the T4 phage aerobic ribonucleotide reductase (Berglund, 1972), and are similar to those of the prototypical enzyme from *Escherichia coli*. However, to our knowledge, no studies have been done to determine what the simultaneous turnover rates for each of the substrates are under different concentrations, and combinations, of the enzyme's allosteric effectors and substrates. Of particular interest to our laboratory is the relative rates of formation for each of the four products when the effector and substrate environment of the enzyme is designed to mimic the *in vivo* conditions as measured in T4 phage-infected *E. coli* (Mathews, 1972; Neuhard and Nygaard, 1987). In other words, when the known allosteric effectors and substrates are supplied together in a single reaction mixture at their estimated physiological or "*in vivo*" concentrations, what are the relative rates of formation for each of the products? This question is of particular interest, because *in vivo*, T4 ribonucleotide reductase functions as part of an enzyme complex (Mathews, 1993) and one must consider the possibility that intracellular reaction fluxes are controlled by protein-protein interactions.

Typically, ribonucleotide reductase has been assayed by using only one of the substrates because analysis of the simultaneous turnover of all four substrates by the enzyme was not possible with existing methods. The ability to follow the reduction of all substrates simultaneously and in a quantitative way, under various conditions, was the goal of this method development. We describe such an assay and its application to the T4

bacteriophage aerobic ribonucleotide reductase, in which the product profile was determined under different allosteric states.

The key requirement of this assay is the quantitative resolution of the dNDP products from the rNDP substrates and nucleoside triphosphate effectors (ATP, dATP, dGTP, and dTTP). This task is accomplished in two chromatographic steps. The first step involves separation of the deoxyribonucleotides from the ribonucleotides using boronate affinity chromatography. Molecules containing cis-diols readily bind to boronate affinity resins at basic pH by forming a complex between the vicinal alcohols of the ribose ring and boric acid functional groups. Thus, when a mixture of ribo- and deoxyribonucleotides is applied to a boronate column the deoxyribonucleotides pass through while the ribonucleotides are retained. This type of affinity chromatography is frequently used to separate dNTPs from rNTPs derived from cell lysates when doing dNTP pool assays (Shewach, 1992). In the second step, the boronate column eluate containing the deoxyribonucleotides is resolved into individual components by HPLC. The HPLC step utilizes a strong anion exchange column and an ammonium phosphate gradient to resolve the individual deoxyribonucleotides into quantifiable peaks.

Materials and Methods

Enzyme Assay Conditions— The enzyme assay procedure was modified from what we used previously (Slabaugh and Mathews, 1984). Briefly, assays were performed in 50 mM HEPES-KOH buffer (pH 8.2) containing: 5 mM magnesium chloride, 50 mM dithiothreitol, and 20 μM ferrous ammonium sulfate (prepared fresh). Assays done under "*in vivo*" conditions refer to enzyme reactions carried out with the following effector and/or substrate concentrations as measured in Mathews, 1972 and Neuhard and Nygaard, 1987: ATP, 2.7 mM; dATP, 175 μM; dTTP, 80 μM; dGTP, 125 μM; CDP, 80 μM; UDP, 90 μM; ADP, 250 μM; GDP, 130 μM. The concentration of the holoenzyme was typically

0.25 μM unless otherwise indicated. The volume of each aliquot removed for assay was 100 μl. The reaction was stopped by addition of 5 μl of 50% perchloric acid. Immediately after the addition of acid, the sample was vortexed and placed on ice. After 5 minutes on ice, KOH was added until the pH was between 8 and 9 (6-7 μl of 5 M KOH). The resulting suspension was then clarified by centrifugation and the supernatant recovered and analyzed by boronate affinity chromatography followed by HPLC, as described below.

Boronate Chromatography— Boronate affinity chromatography was performed essentially as described by Shewach, 1992. Briefly, hydrated Affi-Gel 601 (Bio-Rad) was packed into a 1-ml plastic tuberculin syringe fitted with a frit. The column was equilibrated with 50 mM NH_4HCO_3 buffer, pH 8.9, containing 15 mM $MgCl_2$ (buffer A). Precise volumes of concentrated NH_4HCO_3 and $MgCl_2$ solutions were added to the reaction mixture supernatant to 50 and 15 mM final concentrations, respectively, followed by addition of 100 μl of buffer A. The resulting ~200-μl sample was applied to the boronate column and the first 200 μl of eluate was discarded. The next 1.8 ml of eluate was collected while washing the column in buffer A. This volume of eluate was shown to contain <95% of the dNDPs present in the original sample (see Appendix V). It should also be noted that the rNDPs were retained by the boronate column better than the rNTPs. The 1.8-ml eluate was acidified to pH 3-4 with H_3PO_4 followed by HPLC analysis.

Ion-exchange HPLC analysis— Deoxyribonucleotide products were quantitated by HPLC using a Rainin HPLC system with detection at 260 nm. The boronate column eluate was loaded onto a 500-μl loop and injected onto a PartiSphere-10 SAX column (4.6 x 25 mm; Whatman LabSales) equilibrated in 0.15 M ammonium phosphate, pH 3.7. Deoxyribonucleotides were eluted with a biphasic gradient of ammonium phosphate buffer ranging in concentration from 0.15 to 0.80 M (pH 3.7) at a flow rate of 1.5 ml/min. The deoxyribonucleotides were identified on the basis of retention times and quantitated on the basis of peak area by comparison to authentic standards.

Induction and Purification of the T4 Ribonucleotide Reductase— E. coli strain MV1304 carrying the cloned genes for both subunits of the T4 aerobic ribonucleotide reductase was a gift from Dr. G. R. Greenberg's laboratory. Induction of the proteins and purification of the holoenzyme using dATP-sepharose affinity chromatography were performed as described in Tseng *et al.*, 1992.

RESULTS

Assay Method Validation— Figure 3.1 illustrates a typical HPLC chromatogram of a mixture of authentic deoxyribonucleotide standards. The HPLC method gives good resolution of all possible ribonucleotide reductase dNDP products as well as resolution of the dNTPs which may be added as allosteric effectors.

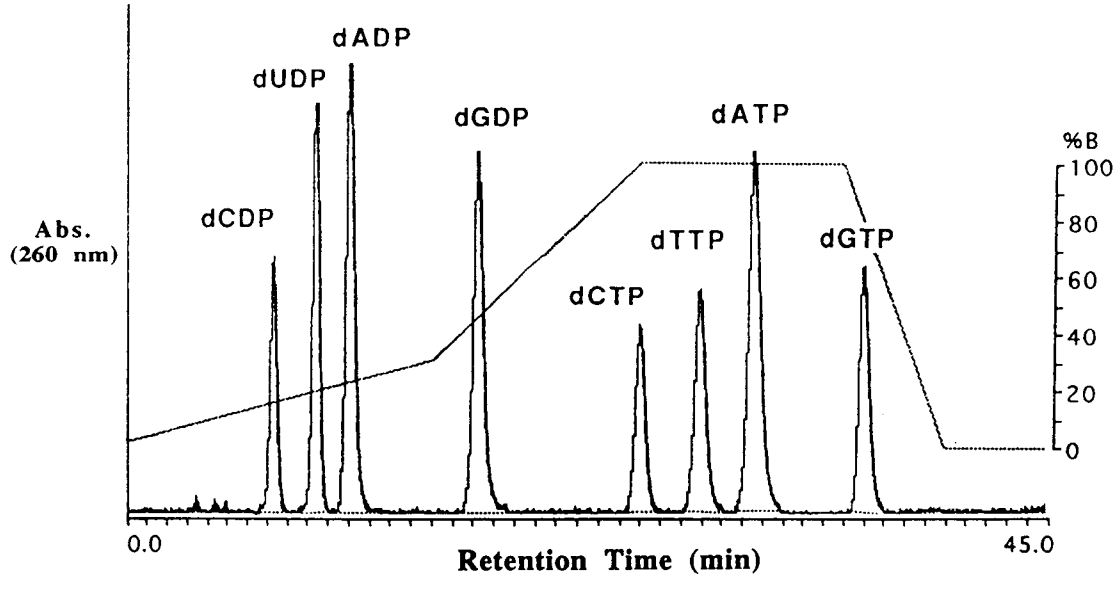

Figure 3.1 **Anion-exchange HPLC separation of dNDPs and dNTPs.** A mixture of 500 pmol each of dCDP, dUDP, dADP, dGDP, dCTP, dTTP, dATP, and dGTP in a volume of 500 µl was injected onto a PartiSphere 10 SAX column and eluted with a biphasic gradient of 0.15 to 0.8 M ammonium phosphate buffer at a flow rate of 1.5 ml/min.

In order to verify that the boronate column quantitatively retains ribonucleotides while allowing deoxyribonucleotides to elute freely, a mixture containing dCDP, dADP, dGDP, UDP, dGTP and ATP was prepared. One-half of the mixture was injected directly onto the HPLC column (see Figure 3.2A). The other half of the sample was applied to a boronate column, eluted as above, and then analyzed by HPLC (see Figure 3.2B). As is apparent from the chromatograms, the boronate column was extremely effective at binding ribonucleotides. This is demonstrated by the absence of UDP and ATP peaks in Figure 3.2B. Furthermore, comparison of the area under each of the deoxyribonucleotide peaks between the two chromatograms showed that at least 95% of each of the dNDPs was recovered after the boronate step.

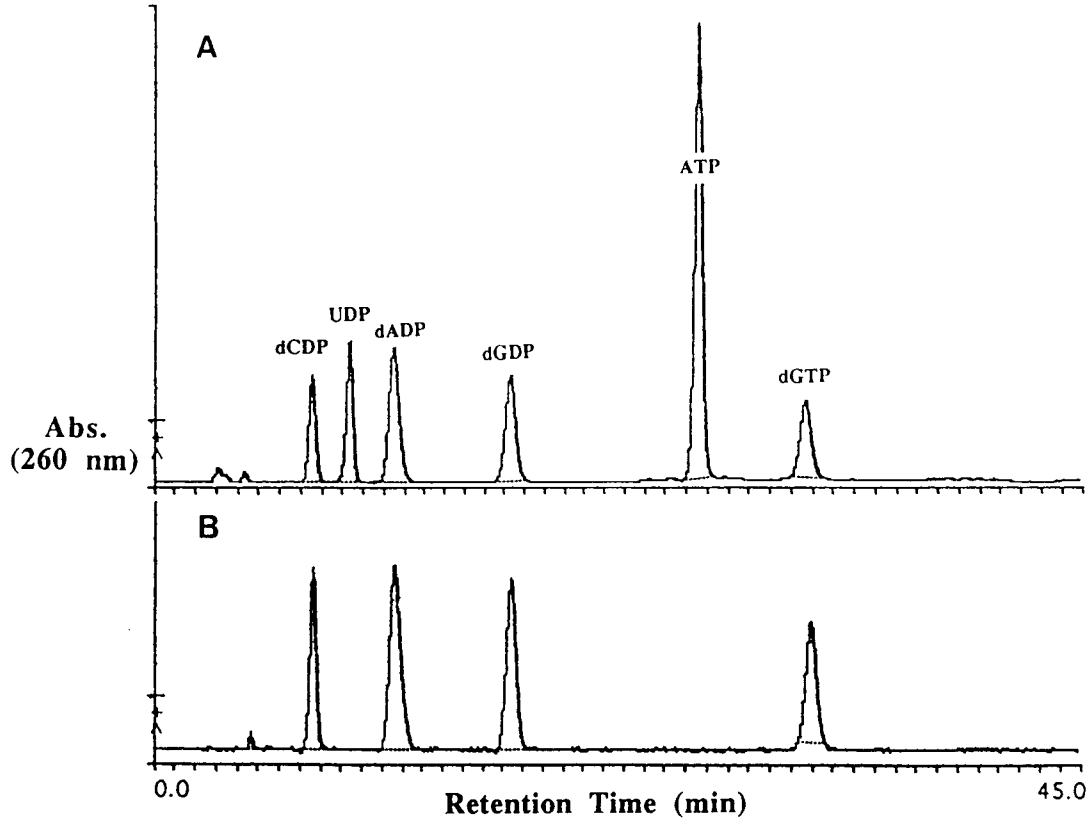

Figure 3.2 **HPLC Analysis of a mixture of deoxyribo- and ribonucleotides before and after boronate column chromatography.** *Panel* A, HPLC chromatogram of a mixture of dCDP, dADP, dGDP, UDP, dGTP (12.5 nmol each), and ATP (25 nmol). *Panel* B, HPLC analysis of the same mixture after removal of the ribonucleotides by boronate column chromatography.

To demonstrate that the method is linear with respect to enzyme concentration, assays were performed using a saturating concentration of CDP and five different enzyme concentrations ranging from 0 to 20 μg of protein. As Figure 3.3 illustrates, the assay is linear within the range of enzyme concentrations used in this study. Using these data from the linearity experiment, we calculated the turnover number for CDP reduction under conditions of saturating substrate to be 0.5 sec^{-1}. This value correlates well with the turnover number reported in the literature (Berglund, 1972) when DTT is the source of reducing equivalents for the T4 ribonucleotide reductase.

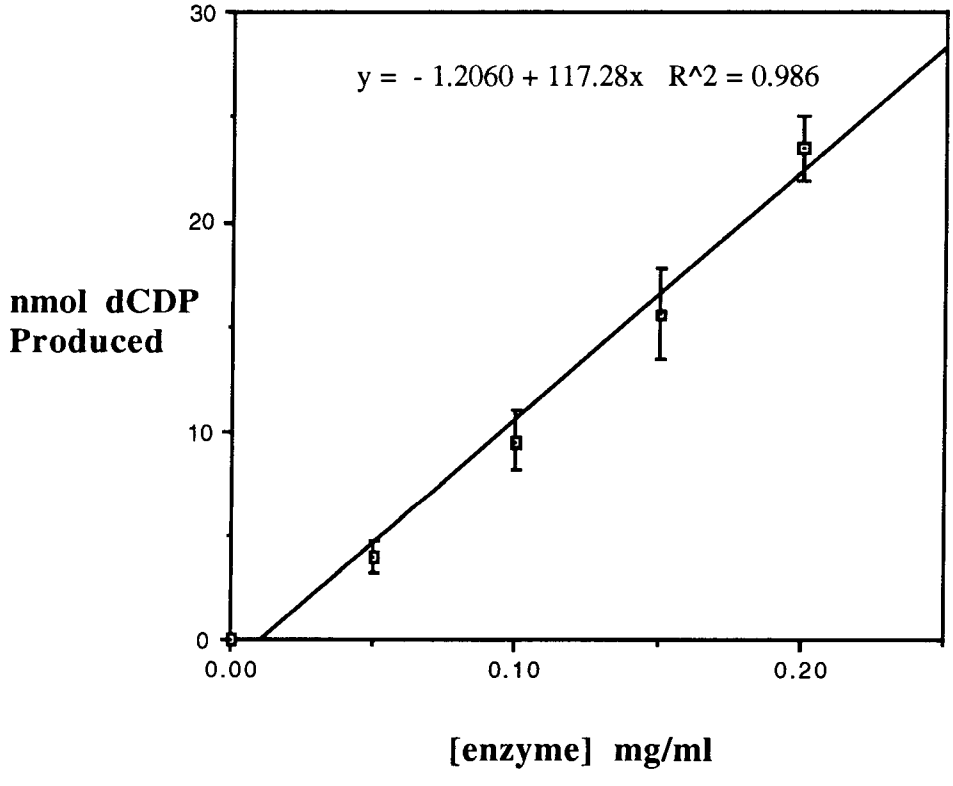

Figure 3.3 **Linearity of CDP reduction with respect to enzyme concentration.** Enzyme assay mixtures were incubated for 10 minutes at 37° C with varying final concentrations of T4 ribonucleotide reductase. CDP and ATP were added at 0.5 and 1.0 mM, respectively. Each data point represents the average of two separate determinations.

Measurement of the Simultaneous Reduction of all Four rNDP Substrates— Figure 3.4 shows the HPLC results of a typical ribonucleotide reductase assay with the reaction mixture incubated at 37° C and sampled at 5-minute intervals. In this particular experiment, the substrates and effectors were added at their "*in vivo*" concentrations, as defined in the Materials and Methods. As the chromatograms demonstrate, the formation of each of the four dNDP products can be followed quantitatively over time in a single reaction mixture.

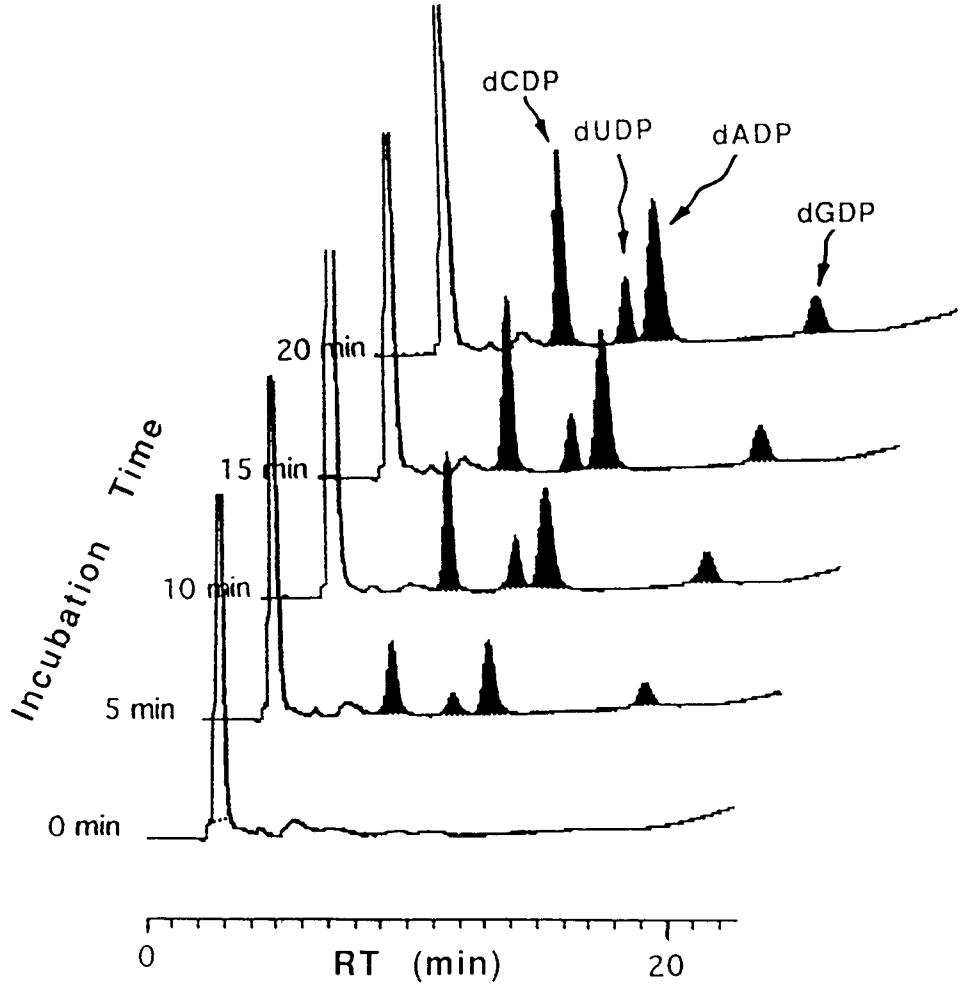

Figure 3.4 **HPLC analysis of product formation followed over time.** 100-µl aliquots were removed from the assay mixture at 5 minute intervals, subjected to boronate chromatography, and then analyzed by HPLC as described in the experimental procedures. In this particular example the assay mixture contained "*in vivo*" concentrations of allosteric effectors and substrates.

Figure 3.5 is a graphical representation of the same data after conversion of peak areas into nanomoles of the corresponding product. Using the initial rates of product formation, we calculated the percent of total product formed for each dNDP. These data, along with the percent of total for each product formed in assays done under different effector and/or substrate concentrations, are tabulated in Table 3.1.

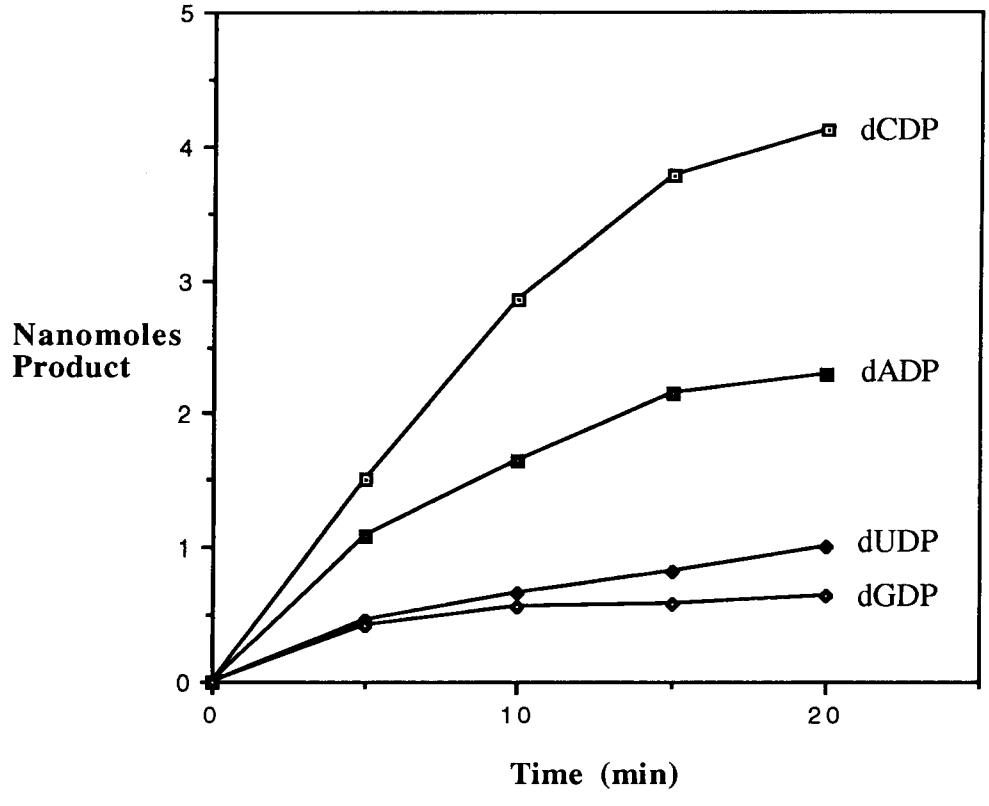

Figure 3.5 **Relative rates of formation of deoxyribonucleoside diphosphates.** Graphical representation of data from Figure 3.4 after conversion of peak areas to nmol product.

Table 3.1 *Relative rates of product formation by T4 ribonucleotide reductase*

assay conditions	% of total product formed			
	dCDP	**dUDP**	**dADP**	**dGDP**
ATP only in vivo substrates	85	11	4	>1
in vivo effectors equimolar substrates	48	17	28	7
in vivo effectors in vivo substrates	43	14	31	12
% of total nucleotides in T4 genome	18*	(32)**	32	18

*cytosine is present in T4 bacteriophage as 5-hydroxymethylcytosine

**32% of the T4 genomic composition is thymine

dTTP Inhibition of CDP Reduction— The T4 aerobic ribonucleotide reductase, unlike the enzyme from *E. coli*, is considered to be relatively insensitive to allosteric inhibition (Berglund, 1972). However, studies done in our laboratory, using crude extracts from T4-infected *E. coli*, have shown that CDP reductase activity is inhibited by dTTP *in situ*, but that this inhibition is lost upon purification of the enzyme (Ji *et al.*, 1991). The basis for the loss of feedback inhibition may involve a number of factors, including disruption of protein-protein interactions within the T4 enzyme complex, or, as suggested by Peter Reichard in a personal communication, loss of ATP during the purification process. Reichard's suggestion is based on the observation that, for the purified enzyme from *E. coli*, dTTP inhibition of CDP reduction occurs only when ATP is present at intracellular concentrations (Brown and Reichard, 1969). Using this new assay, we tested whether, in

the case of the T4 enzyme, the presence of ATP was sufficient to restore feedback inhibition by dTTP *in vitro*. Purified enzyme was mixed with either ATP and dTTP, or ATP alone, and the reduction of CDP was followed over time. Figure 3.6 shows the results of these experiments. As is evident by the similarity of the two lines, the addition of ATP does not sensitize the CDP reductase activity of the T4 enzyme to dTTP inhibition.

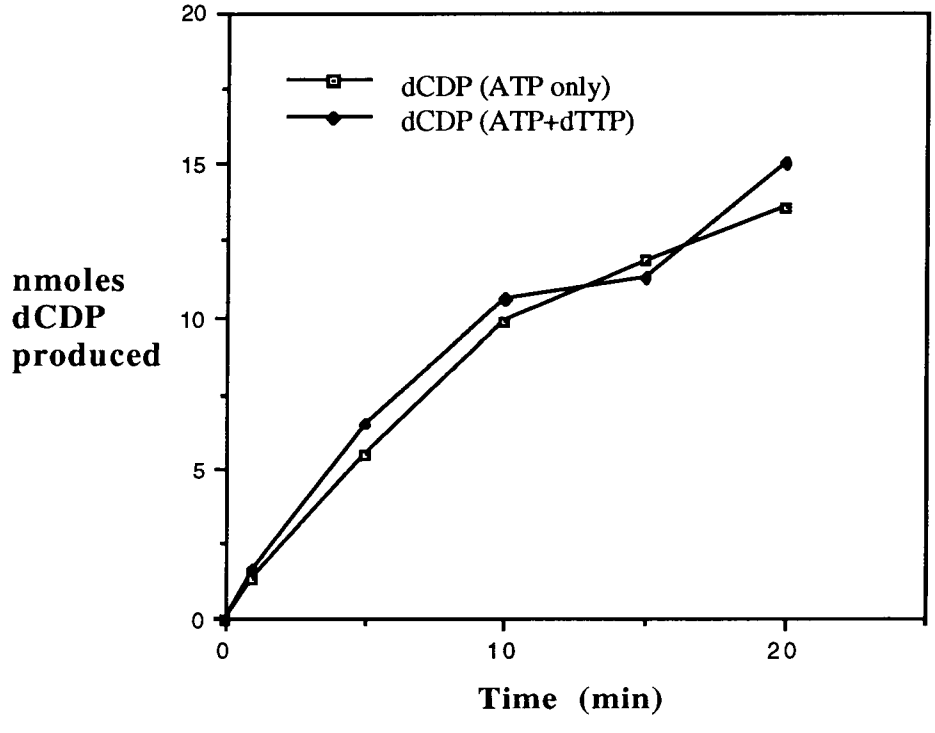

Figure 3.6 **dTTP inhibition of CDP reduction.** Purified T4 ribonucleotide reductase was incubated at 37° C with either ATP and dTTP (2.7 mM and 200 μM, respectively), or ATP alone (2.7 mM) and the reduction of CDP was followed over time. No significant difference in the rate of CDP reduction was evident in these experiments.

Discussion

This paper presents a novel method for the simultaneous assay of all four ribonucleotide reductase activities. More important, using this assay, we have determined how the simultaneous rates of these individual activities are influenced by the initial substrate concentrations and allosteric environment of the enzyme. To our knowledge, this represents the first study of this kind on ribonucleotide reductase and presents a new way of evaluating the role of the enzyme in regulating the levels of the DNA precursors.

Consistent with the known allosteric properties of the T4 aerobic ribonucleotide reductase (Berglund, 1972), our results show that ATP does act as a general allosteric activator for all four substrates, although pyrimidine nucleotide reduction greatly exceeded reduction of the purine nucleotides. When ATP was present as the only allosteric effector and the substrates were supplied at "*in vivo*" concentration levels, the reduction of GDP and ADP represented less than 5% of the total reaction flux (Table 3.1, row 1).

When the four ribonucleotide reductase activities were measured with the enzyme under "*in vivo*" allosteric conditions, dramatic changes in the product profile, or relative amounts of each product formed, were observed. When the "*in vivo*" levels of the nucleoside triphosphate effectors were supplied to the enzyme along with equimolar amounts of the four rNDP substrates (0.1 mM each), the percent of purine reduction increased to 35% of the total (Table 3.1, row 2). Even more interesting were the results obtained when both the effectors and the substrates were supplied to the enzyme at their respective "*in vivo*" concentrations (Table 3.1, row 3). Under these conditions, the amount of purine reduced increased to 43% of the total product formed, closely approaching the 50% expected in dsDNA. Of the purine nucleotide reduced in this experiment, dADP represented 31% of the total product formed. This is in surprisingly good agreement with the 32% adenine present in the T4 genome. The rate of formation of the other purine, dGDP, was lower than predicted from the genomic composition of guanine in T4 (12% vs. 18%). This was

true even though the K_m for GDP is almost identical to the K_m's for CDP and ADP when the prime effectors are present (Berglund, 1972). Low GDP reduction rates may simply be an inherent property of Class I ribonucleotide reductases and this may explain, at least in part, why the dGTP pools in many cell types are underrepresented (Mathews and Ji, 1992). It is also possible that the estimated "*in vivo*" effector and/or substrate concentrations used in these experiments do not faithfully represent the true concentrations sensed by the enzyme *in vivo*.

Formation of dCDP occurred at a much higher rate than that expected from its percent contribution to the T4 genome. This may be explained by the fact that a significant portion of the dCDP produced by ribonucleotide reductase is shuttled into the production of thymine nucleotides via deamination of the cytosine base. If ribonucleotide reductase does produce products in proportions relative to the proportions seen in the genome, then we would predict from these data, since all hydroxymethylcytosine nucleotide must come CDP reduction, that approximately one-half of the total dCDP produced under "*in vivo*" conditions, or approximately 21% of the total product produced, would be diverted into the thymine nucleotide pathway. The diverted dCDP, after the action of enzymes including dCMP deaminase, combined with the dUDP produced directly by ribonucleotide reductase, make up 35% of the total deoxyribonucleotide produced. This fits well with the 32% thymine present in the T4 genome. The flux of dCDP through dCMP deaminase predicted from these experiments suggests that roughly 65% of the total thymine pool results from cytosine deamination. This is remarkably close to thymine production in the T4 host, *E. coli*, in which 75% of the dTTP is derived from CDP reduction (Molgaard and Neuhard, 1983). The remaining portion of dCDP which is not shuttled into the thymine pathway represents 22% of the total amount of dNDP formed. The T4 genome is composed of 18% hydroxymethylcytosine. Therefore, the level of dCDP that we predict is not shuttled into thymine biosynthesis is sufficient to fulfill its contribution to the T4 genome.

The significance of this work is twofold. First, we describe a new assay procedure that is applicable to any ribonucleotide reductase, including the anaerobic rNTP reductases, which is relatively simple to carry out, and which permits simultaneous monitoring of the four activities of the enzyme. Since the creation of DNA precursor imbalances by drugs which specifically target ribonucleotide reductase are well documented (Bianchi *et al.*, 1986; Slabaugh *et al.*, 1991) and are important clinically (Lori *et al.*, 1994), the procedure should prove useful in evaluating therapeutically significant ribonucleotide reductase inhibitors. Second, we applied this assay to the T4 phage aerobic rNDP reductase, an enzyme whose allosteric control features are still not well understood. Berglund's original studies on the purified enzyme suggested that it is relatively insensitive to allosteric inhibition. More recently, our laboratory showed that *in vivo* and in crude preparations, the CDP reductase activity of the enzyme is sensitive to dTTP, suggesting the presence of regulatory factors that might be removed during enzyme purification. The present study, carried out with purified recombinant enzyme, shows that in the presence of near-physiological concentrations of substrates and effectors, the enzyme functions at relative rates that correspond closely to *in vivo* reaction fluxes. Thus, while the enzyme might be regulated in part by protein-protein interactions as part of its functioning within the dNTP synthetase complex, adequate information for modulating its four activities is built into the structure of the protein itself.

References

Berglund, O. (1972) *J. Biol. Chem.* **247**, 7270-7275

Berglund, O. (1972) *J. Biol. Chem.* **247**, 7276-7281

Bianchi, V., Pontis, E., and Reichard, P. (1986) *J. Biol. Chem.* **261**, 16037-16043

Brown, N. C., and Reichard, P. (1969) *J. Mol. Biol.* **46**, 39-43

Ji, J., Sargent, G. R., and Mathews, C. K. (1991) *J. Biol. Chem.* **266**, 16289-16292

Lori, F., Malykh, A., Cara, A., Sun, D., Weinstein, J. N., Lisziewicz, J., and Gallo, R. C. (1994) *Science* **266**, 801-805

Mathews, C. K. (1972) *J. Biol. Chem.* **247**, 7430-7438

Mathews, C. K. (1993) *J. Bacteriol.* **175**, 6377-6381

Mathews, C. K., and Ji, J. (1992) *Bioessays* **14**, 295-301

Molgaard, H., and Neuhard, J. (1983) *Metabolism of Nucleotides, Nucleosides, and Nucleobases in Microorganisms*, Academic Press, Inc (London), Ltd., London

Neuhard, J., and Nygaard, P. (1987) in *Escherichia coli and Salmonella typhimurium Cellular and Molecular Biology* (Neidhardt, F. C., Ingraham, J. L., Low, K. B., Magasanik, B., Schaechter, M., and Umbarger, H. E., eds) pp. 465-466, American Society for Microbiology, Washington DC

Shewach, D. S. (1992) *Anal. Biochem.* **206**, 178-182

Slabaugh, M. B., Howell, M. L., Wang, Y., and Mathews, C., K. (1991) *J. Virology* **65**, 2290-2298

Slabaugh, M. B., and Mathews, C. K. (1984) *J. Virol.* **52**, 501-506

Tseng, M.-J., Hilfinger, J. M., He, P., and Greenberg, G. R. (1992) *J. Bacteriol.* **174**, 5740-5744

Chapter 4

Allosteric Regulation of the Ribonucleoside Diphosphate Reductase from Vaccinia Virus

Stephen P. Hendricks and Christopher K. Mathews

Summary

This chapter describes experiments that examine the effects of nucleotide effectors and substrates on the relative turnover rates of the four activities of vaccinia virus ribonucleotide reductase (RNR). When individual nucleoside triphosphates were added to the vaccinia RNR, the substrate specificity and overall activity were modulated in a manner similar to the allosteric behavior of the mammalian enzymes. Specifically, dTTP activated rGDP reduction, dGTP activated rADP reduction, and ATP acted as a general allosteric activator. Furthermore, the four activities of the vaccinia RNR were strongly inhibited by dATP. This result is contrary to the allosteric behavior of RNR from other large DNA viruses, like T4 and herpes, which are relatively insensitive to dATP inhibition. These data indicate that the allosteric regulation of the vaccinia RNR closely resembles that of the host cell enzyme and is therefore a good model for the study of mammalian RNR allostery.

In addition to the effects of individual allosteric effectors, the influence of complex nucleotide environments on the relative rates of rNDP reduction were examined. For example, physiological mixtures of the known effectors and substrates were added to the assay mixture to determine how the vaccinia enzyme behaved under *in vivo*-like conditions. Similar to what was found for the T4 enzyme, these experiments indicate that the presence of physiological concentrations of the effectors and substrates promote the production of dNDPs in a ratio that approximates the nucleotide composition of the vaccinia genome.

Finally, this report includes two additional observations that are related to the regulation of RNR activity. Evidence is presented that the substrates, and possibly the products, of RNR are also involved in regulating enzyme activity. In addition, data are presented demonstrating that a chimeric form of RNR, composed of vaccinia R1 and mouse R2, is catalytically active. To my knowledge, this is the first report of an active chimeric RNR holoenzyme.

Introduction

The allosteric regulation of RNR is well characterized for several forms of the enzyme (Larsson and Reichard, 1966a,b; Berglund, 1972; Eriksson *et al.*, 1979; Chang and Cheng, 1979; Eliasson *et al.*, 1996). The three classes of RNR, although very different in structure, have very similar allosteric behavior in terms of substrate specificity. In all classes, ATP, and dATP when it is not inhibitory, activate reduction of the cytidine and uridine ribonucleotides. Reduction of adenosine and guanosine ribonucleotides are stimulated by dGTP and dTTP, respectively.

However, due primarily to the limitations of the traditional RNR assay method, only the isolated effects of individual allosteric effectors have been determined. With the advent of the four-substrate assay (Hendricks and Mathews, 1997), the effects of more complex nucleotide environments on substrate turnover rates can be examined. In addition, other factors that influence the relative turnover rates, such as protein-protein interactions, can be evaluated by this technique. This chapter describes the effects of different concentrations and combinations of nucleotide effectors and substrates on the vaccinia virus RNR, and further illustrates the utility of the four substrate assay.

Materials and Methods

Overexpression and Purification of Recombinant Subunits— Both subunits of vaccinia ribonucleotide reductase were previously cloned into IPTG-inducible pET expression vectors and were overexpressed as described (Slabaugh *et al.*, 1993; Howell *et al.*, 1992). The mouse R2 expression system was a gift from the laboratory of Lars Thelander, University of Umeå. Overexpression of the mouse R2 was performed according to the procedure used to express the vaccinia R2. The mouse R2 clone contains two selectable

markers encoding drug resistance gene products and therefore the addition of 25 μg/ml chloramphenicol was required in conjunction with 100 μg/ml ampicillin.

The purification procedure for the vaccinia R2 subunit was essentially as reported (Howell *et al.*, 1992) except for the incorporation of an additional radical reactivation step. Mouse R2 was purified by using the same procedure used to purify the vaccinia R2. Purification of the vaccinia R1 protein was performed using dATP-Sepharose affinity chromatography. Details for preparing dATP-Sepharose can be found in Appendix II. Routinely, 3-5 g of cells containing overexpressed vaccinia R1 was lysed in a French press and centrifuged at 12,000 rpm for 20 minutes. The clarified lysate was filtered and applied to a column packed with 1.0 ml of dATP-Sepharose resin previously equilibrated with buffer composed of 50 mM N-[2-hydroxyethyl]piperazine-N′-[2-ethanesulfonic acid] (HEPES), 100 mM KCl, and 1mM dithiothreitol (DTT), pH 8.2. After washing the column back to baseline with buffer (~100 ml), a 7.0 ml-wash of column buffer containing 5 mM ATP was used to elute any *E. coli* R1 or other bound proteins resulting from the expression system. Finally, the recombinant vaccinia R1 protein was eluted with column buffer containing 75 mM ATP. Centricon-30 centrifugation devices (No. 4209; Amicon Inc., Beverly, MA) were used to remove the ATP used in the elution step, and concentrate the purified R1. All steps of the purification were performed on ice or at 4° C.

Ribonucleotide Reductase Four-Substrate Assay— The assay is described in more detail in Chapter 3 (Hendricks and Mathews, 1997). Essentially, the technique is composed of two chromatographic steps. The first step, boronate affinity chromatography, separates the RNR products (dNDPs) from the substrates (rNDPs). In the second step of the assay, the dNDPs are resolved into individual nucleotides by high performance liquid chromatography (HPLC).

The concentrations of the vaccinia and mouse R2 proteins used in these experiments were 2 or 4 μM, as indicated. In all reactions, vaccinia R1 was added to 1 μM final concentration. ATP and DTT were present in all reaction mixtures at 2.5 mM and 50 mM,

respectively. The rNDP substrates were either added at equimolar (0.15 mM each) or *"in vivo"* concentrations. The *"in vivo"* concentrations for rCDP, rUDP, rADP, and rGDP were set to 50, 250, 600, and 100 μM, respectively. These values were based on the experimentally determined molar ratio of rNDPs measured in vaccinia-infected BSC_{40} cells (see below). The "*in vivo*" dNTP concentrations used in these assays were 15, 10 and 5 μM dATP, dTTP, and dGTP, respectively. These concentrations were based on dNTP measurements made in vaccinia-infected BSC_{40} cells (Slabaugh *et al.*, 1991) which were determined to be 15, 10, and 5 picomoles per 10^6 cells of dATP, dTTP, and dGTP, respectively. The volume of a vaccinia-infected BSC_{40} cell was not determined in these experiments. However, nucleated mammalian cell volumes range from approximately 1 to 3 picoliters per cell (Hauschka, 1973). For dATP, this corresponds to a concentration range of 5 to 15 μM. Various dNTP concentrations within this range were used in the "*in vivo*" studies and are defined in each experiment.

Measurement of rNDP levels in vaccinia-infected BSC_{40} cells— Monkey kidney BSC_{40} cells were infected with vaccinia virus strain WR as previously described (Slabaugh *et al.*, 1984). Cells were harvested 4 hours post infection so that the nucleotide pool measurements would reflect the levels that occur during peak viral DNA replication. Cell extracts were prepared by treating cells with 0.4 M aqueous perchloric acid (PCA). After 5 minutes on ice, the PCA-extracted cells were pelleted by centrifugation, and the supernatant neutralized with NaOH (neutralization with KOH resulted in a significant loss of nucleotides from the soluble fraction). The extract was lyophilized to dryness and resuspended in 75 mM $NH_4H_2PO_4$ buffer (pH 3.7) just prior to analysis. The total nucleotide extract was analyzed by HPLC using the anion exchange column and ammonium phosphate buffer system used in the four-substrate RNR assay. Peak identities were verified by "spiking" the extract with authentic standards. For a more detailed description of this procedure refer to Appendix III.

Results

Activation of the vaccinia RNR by the general allosteric effector, ATP— Figure 4.1 shows the HPLC results from a vaccinia virus RNR assay performed within an allosteric environment consisting only of the general activator, ATP. In this particular experiment, a reaction mixture containing 1 μM R1, 4 μM R2, 2.5 mM ATP, and the four rNDP substrates at 0.15 mM each, was sampled at 4 minute intervals and processed according to the assay procedure. As the chromatograms illustrate, within an allosteric environment consisting exclusively of ATP, the vaccinia RNR reduces primarily rCDP and rGDP. These conditions also gave the maximal rate of total rNDP reduction of all conditions used in this chapter. Typically, the specific activity of the vaccinia RNR, measured using the four-substrate assay, was on the order of 80 nmol dNDP·min^{-1}·mg R1^{-1}. The specific activity determined from the data shown in figure 4.1 was 77 nmol dNDP·min^{-1}·mg R1^{-1}. This corresponds to a turnover number of 12.4 min^{-1}.

Regulation of the vaccinia RNR by nucleoside triphosphate effectors — In order to determine if the vaccinia RNR is allosterically regulated like the other class I enzymes, the four-substrate assay was performed using a single dNTP and ATP, along with all four rNDP substrates. Figure 4.2 shows the HPLC results from these experiments. Table 4.1 is a qualitative summary of the allosteric effects of single dNTP effectors on the vaccinia RNR.

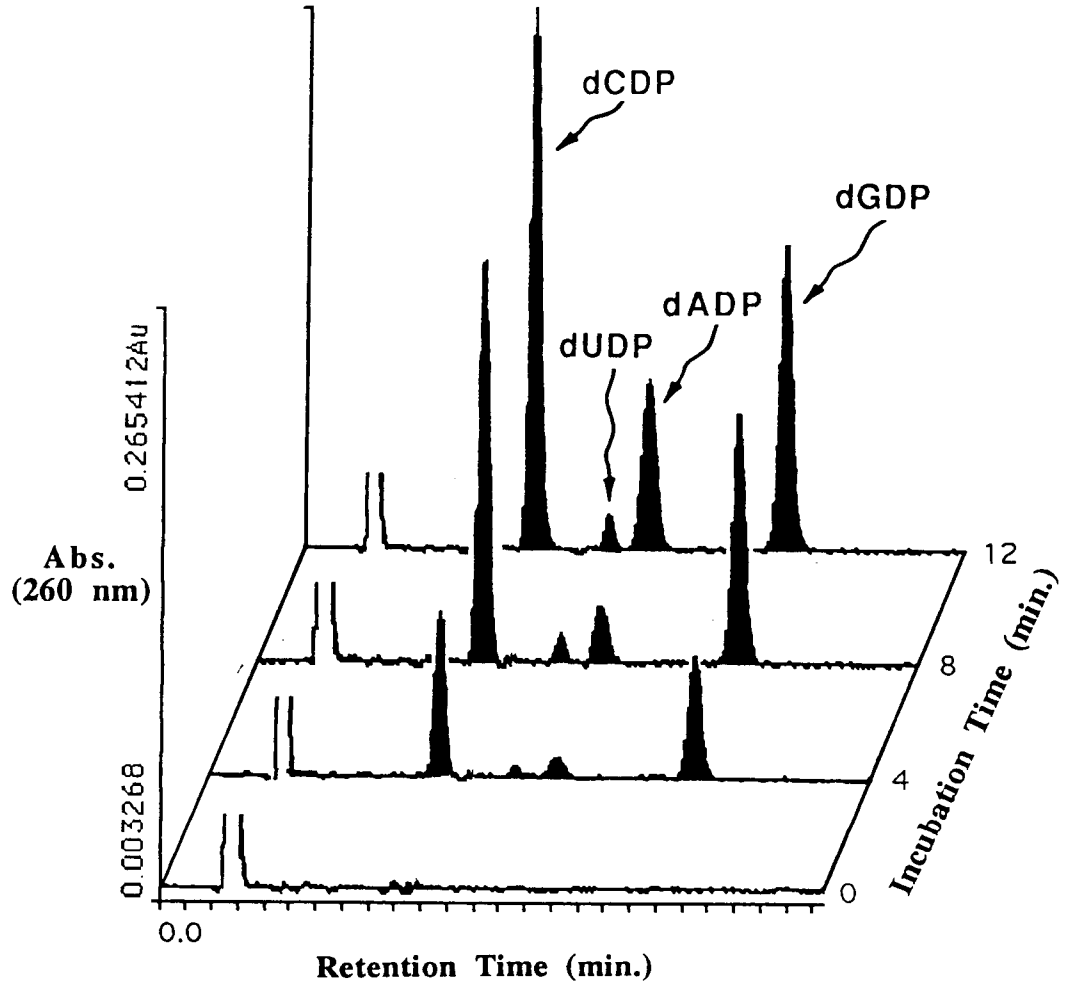

Figure 4.1 **ATP activation of the vaccinia ribonucleotide reductase measured using the four substrate assay.** In this experiment, 100-µl aliquots were removed from the reaction mixture at 4-minute intervals, subjected to boronate chromatography, and analyzed by HPLC as described in the "Materials and Methods" section. In this particular experiment, the four rNDP substrates were added to 0.15 mM each and ATP, the only nucleoside triphosphate effector present in the reaction mixture, was added to 2.5 mM.

Allosteric Effectors Present	Assay Result

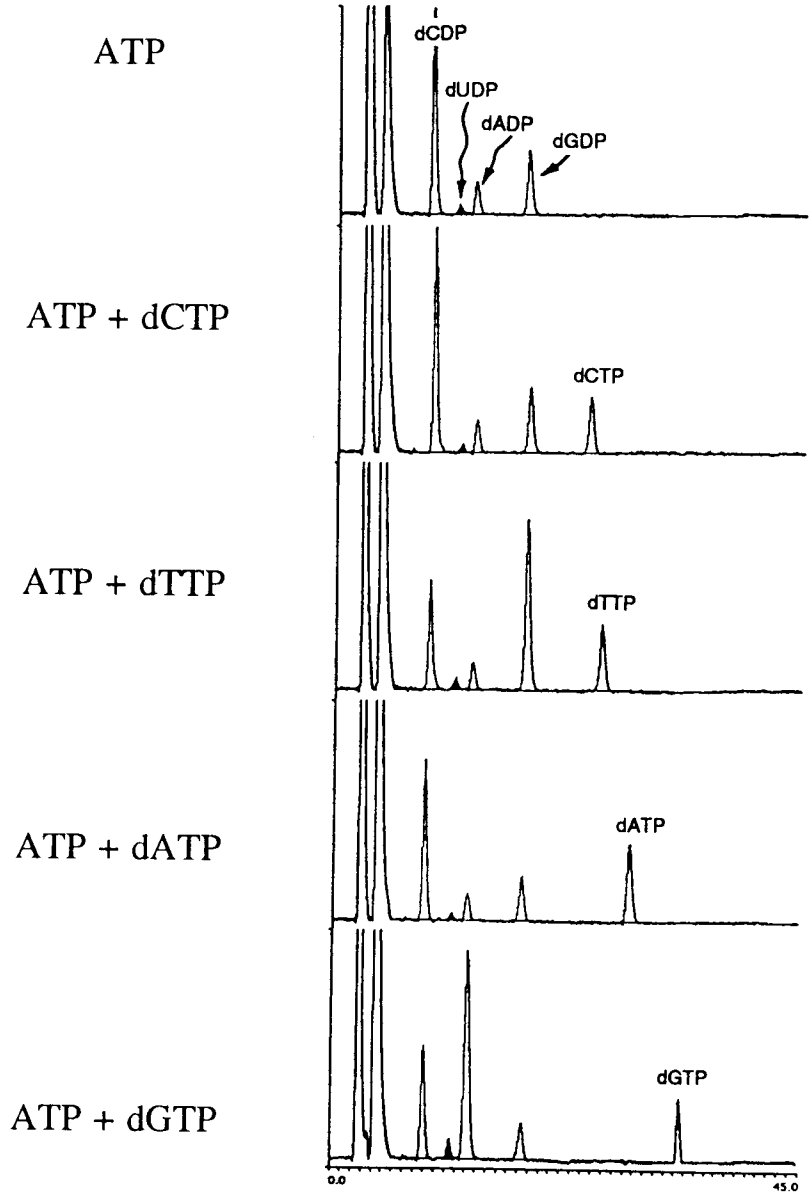

Figure 4.2 **Allosteric regulation of vaccinia virus ribonucleotide reductase by individual dNTPs.** All reaction mixtures contained ATP at 2.5 mM and all four rNDP substrates at 0.15 mM each. Individual dNTP effectors were added to a final concentration of 10 μM. Reaction mixtures was incubated at 37° C for 6 minutes.

Table 4.1 *Allosteric regulation of vaccinia ribonucleotide reductase by individual dNTPs*

dNTP (10 μM)	Activates† reduction of	Inhibits† reduction of
dCTP	no effect	no effect
dTTP	rGDP	rCDP and rADP
dGTP	rADP	rCDP
dATP	rCDP*	all

†The results summarized in this table represent changes that occur in rNDP turnover rates relative to the rates observed when the enzyme is stimulated by ATP only.

*Activation of rCDP reduction by dATP was evident only when ATP was not added to the reaction mixture. When dATP was added in conjunction with ATP (0.5 to 2.5 mM), all activities were inhibited relative to a control reaction containing only ATP.

Inhibition of the vaccinia RNR by dATP— Figure 4.3 shows the inhibitory effects on total RNR activity by the allosteric effector, dATP. From the inhibition curve, it is evident that only 50-60% of the potential reducing activity is utilized in the concentration range defined as "*in vivo*". These data indicate that the vaccinia RNR is inhibited by dATP similarly to the previously characterized mammalian RNRs.

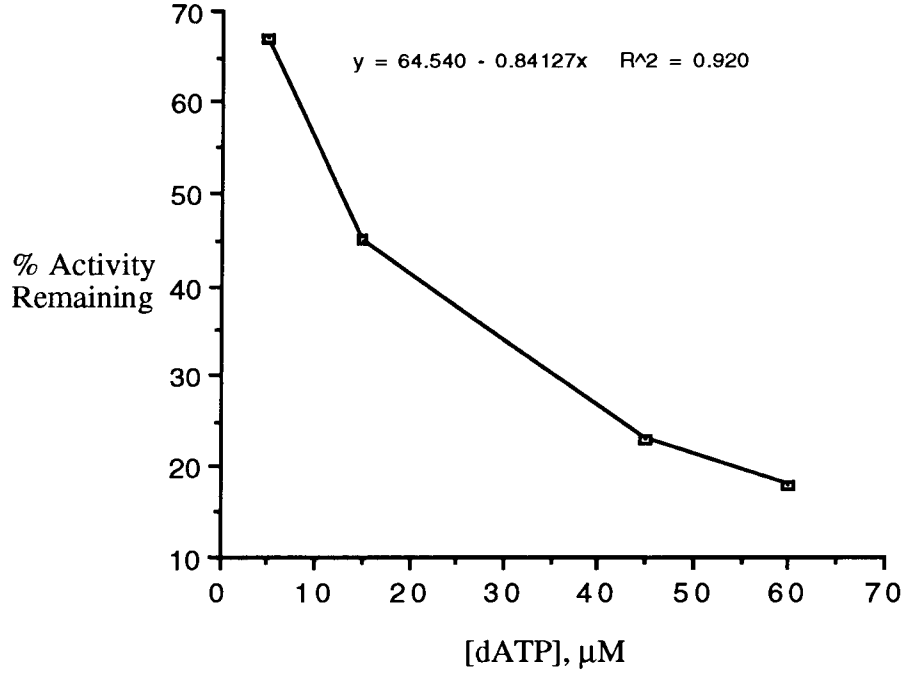

Figure 4.3 **Inhibition of the vaccinia RNR by dATP.** This graph shows the amount of total vaccinia RNR activity remaining after addition of dATP to the reaction mixture. The decrease in activity was calculated by comparing the total amount of rNDP reduced in the presence of 2.5 mM ATP with the amount reduced when the reaction contained 2.5 mM ATP plus dATP at the indicated concentration.

rNDP concentrations in vaccinia-infected BSC_{40} cells— The results of the rNDP measurements, reported as the average of two determinations, are listed in the second column from the left of Table 4.2. The HPLC method used to determine these values gives good baseline resolution of all rNDPs of interest (see Figure 3.1). In addition to retention times, peak identification was verified by "spiking" the extract with authentic samples. Therefore, the moles of each rNDP calculated from the peak areas in the chromatograms should be a reasonable measure of the actual concentrations. The only obvious contaminants that could lead to overestimation of the rNDPs are the corresponding dNDPs. In most cases, the rNDPs and the dNDPs coelute. However, for the purposes of this study, the contribution to peak area by the dNDPs is assumed to be negligible. This assumption is valid if one considers that the intracellular concentration of rNDPs exceeds that of the dNDPs by 100- to 1000-fold (Traut, 1994). From the rNDP concentrations determined by this method, an approximate molar ratio was calculated. This ratio is reported in the third column of Table 4.2. The calculation of the "*in vivo*" molar concentration of each rNDP from the picomole value determined in these experiments was complicated by the fact that the volume of a vaccinia-infected BSC_{40} cell was not determined. However, using a mid-range value of 2 picoliters per cell for the volume of a mammalian cell (Hauschka, 1973), the "*in vivo*" concentrations were calculated from the picomoles of rNDP/10^6 cells determined experimentally. These estimated concentrations, shown in the fourth column of Table 4.2, are remarkably close to the average concentration of rNDPs in mammalian cells reported in the literature. The standard deviation associated with each of the averaged literature values gives a sense of the extent to which the concentrations of the RNR substrates can vary within mammalian cells.

Table 4.2 *Ribonucleoside Diphosphate Concentrations in Vaccinia-infected BSC40 Cells*

rNDP	pmol rNDP /10^6 cells[1]	molar ratio	"in vivo" conc.[2] (μM)	ave. conc. (μM) from literature[3]
rCDP	98 ± 13	1	50	51 ± 17
rUDP	451 ± 39	5	250	163 ± 116
rADP	1196 ± 88	12	600	576 ± 449
rGDP	216 ± 29	2	100	94 ± 78

[1]Numbers reported in this column represent the average of two determinations. These results are reported as the mean ± (range/2)

[2]The volume of a vaccinia-infected BSC_{40} cell was not determined. Instead, in order to convert pmol rNDP/10^6 cells into "*in vivo*" molar concentrations, a mid-range value of 2 picoliters per cell was used.

[3]Traut, T. W. (1994) *Mol. Cell. Biochem.* **140**, 1-22. Average concentrations were calculated from at least 15 measurements made both in cultured mammalian cells and cells derived from whole animal tissues. Standard deviations are shown primarily to illustrate the large variance of rNDPs in animal cells.

Comparison of the product ratio formed under various nucleotide environments— Figure 4.4 shows the results of experiments in which the composition and concentrations of the substrates and allosteric effectors were varied in order to determine the influence of the total nucleotide environment on the relative turnover rates of the vaccinia RNR. The left hand column indicates the nucleotide effectors present in the reaction mixture and the center column gives the HPLC trace resulting from those conditions. The right hand column gives the percentage of the total product formed for each individual dNDP calculated from the peak area of the chromatogram and expressed as the molar ratio. In order to aid a comparison of the two forms of RNR, Table 4.3 summarizes the vaccinia results in a format similar to that used for the T4 enzyme (Hendricks and Mathews, 1977; see Chapter 3) . The last row of Table 4.3 shows the base composition of the vaccinia virus genome.

Nucleotide Environment (allosteric effectors and substrates)		% of total product formed (dCDP : dUDP : dADP : dGDP)
ATP equimolar rNDPs	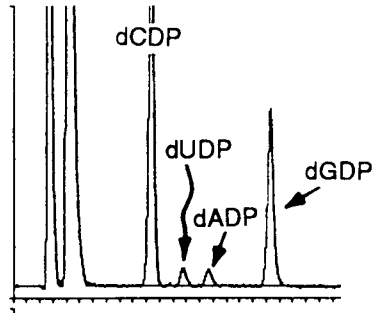	(76 : 3 : 2 : 19)
ATP *"in vivo"* rNDPs	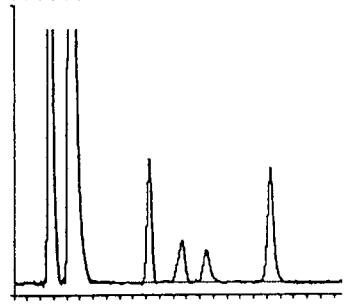	(49 : 15 : 8 : 28)
ATP *"in vivo"* dNTPs equimolar rNDPs	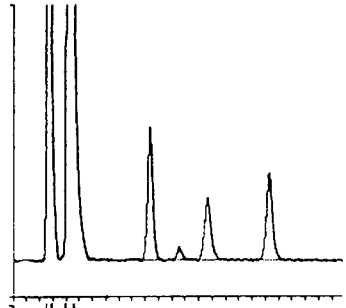	(60 : 3 : 15 : 22)
ATP *"in vivo"* dNTPs & rNDPs	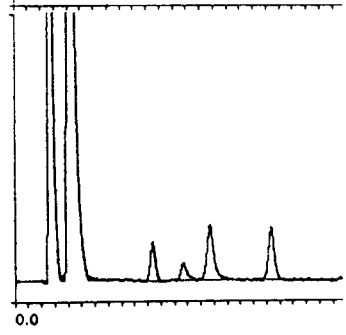	(34 : 12 : 29 : 26)

Figure 4.4 **Comparison of the four activities of the vaccinia RNR assayed under different allosteric environments.** ATP was present at 2.5 mM in all reaction mixtures. In the assay mixtures containing equimolar rNDPs, all four substrates were present at 0.15 mM each. Mixtures with *"in vivo"* dNTPs contained dATP, dTTP, and dGTP at 15, 10, and 5 μM , respectively, and those with *"in vivo"* rNDPs contained rCDP, rUDP, rADP, and rGDP at 50, 250, 600, and 100 μM , respectively.

Table 4.3 *Relative rates of product formation by vaccinia virus ribonucleotide reductase under different allosteric environments*

	percentage of total product formed as			
Assay conditions[1]	**dCDP**	**dUDP**	**dADP**	**dGDP**
ATP only equimolar substrates	76	3	2	19
ATP only *"in vivo"* substrates	49	15	8	28
"in vivo" effectors equimolar substrates	60	3	15	22
"in vivo" effectors *"in vivo"* substrates	34	12	29	26
% of total nucleotides in vaccinia's genome	17	(33)[2]	33	17

[1]All reaction mixtures contained ATP at 2.5 mM. Equimolar substrates were present at 0.15 mM. *"In vivo"* substrates levels were 50, 250, 600, and 100 μM, rCDP, rUDP, rADP, and rGDP, respectively. *"In vivo* " allosteric effector concentrations were 15, 10, and 5 μM dATP, dTTP, and dGTP, respectively.

[2]32% of vaccinia genomic composition is thymine.

Substrate inhibition of rADP reduction— It was of interest to determine whether the K_ms determined by traditional means, i.e. through the analysis of turnover rates for single substrates, were of the same magnitude as K_ms determined under physiological-like conditions using the four-substrate assay. The initial experimental design was to simply look at the turnover rates of the four substrates within an "*in vivo*" environment of nucleotide effectors and substrates. Specifically, a mixture of substrates was prepared in which the rNDPs were present at the molar ratio reported in Table 4.2. (1 : 5 : 12 : 2 ; rCDP : rUDP : rADP : rGDP). This mixture of rNDPs is referred to as a bioproportional substrate mixture. Reaction mixtures were prepared with identical concentrations of enzyme, ATP (2.5 mM), and dNTPs (dATP, 15 μM; dTTP, 10 μM; dGTP, 5 μM), and at the start of each assay a precise volume of the bioproportional substrate mixture was added. Each successive sample included a slightly larger volume of the substrate mixture.

Analogous to the determination of K_ms, these preliminary experiments were expected to yield the concentration at which the substrate saturates half of the potential binding sites. However, when the data from this experiment were analyzed, the unexpected result shown in Figure 4.5 was observed. Examination of the HPLC traces revealed that the production of dADP under these conditions is contrary to the normal Michaelis-Menten behavior initially expected. The data from Figure 4.5 were converted to graphical form to better illustrate the surprising result that reduction of rADP decreased as the bioproportional substrate concentrations were increased. These data are shown in Figure 4.6.

These results prompted me to repeat the experiment using the same conditions, except with a 10-fold increase in range of bioproportional substrate concentrations. Figure 4.7 shows the results of these experiments. As these data indicate, at these higher substrate concentrations, both the reduction of rADP and rGDP were inhibited as their concentrations increased.

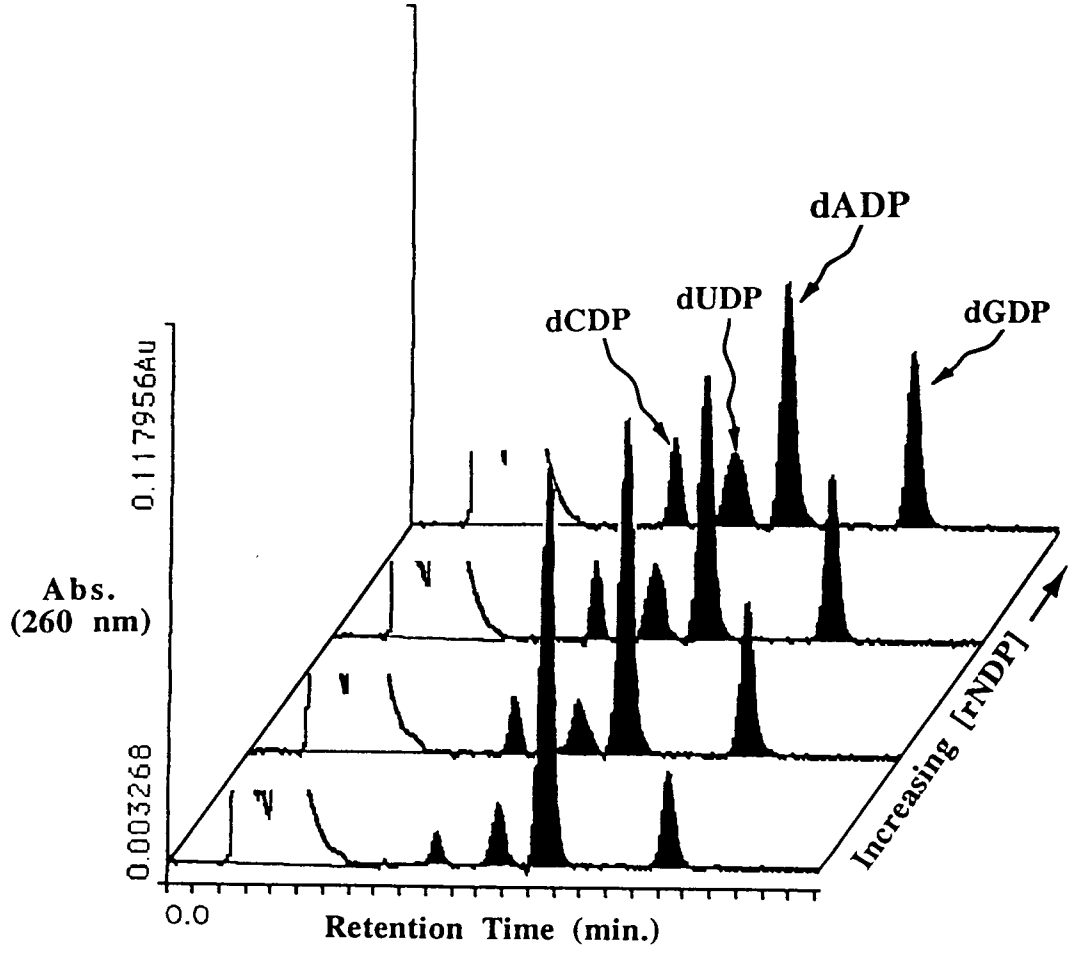

Figure 4.5 **HPLC results from assays containing different volumes of a bioproportional rNDP mix.** In these assays, the concentration of rNDP substrates were increased while the "bioproportional" molar ratio of the individual rNDPs was kept constant. This was accomplished by adding different volumes of a mixture containing the "*in vivo*" ratio of rNDPs (1 : 5 : 12 : 2 ; rCDP : rUDP : rADP : rGDP) to each reaction mixture. The concentrations of the nucleoside triphosphate effectors were set to "*in vivo*" levels (ATP, 2.5 mM; dATP, 15 μM; dTTP, 10 μM; and dGTP, 5 μM) and kept constant in all of these reactions.

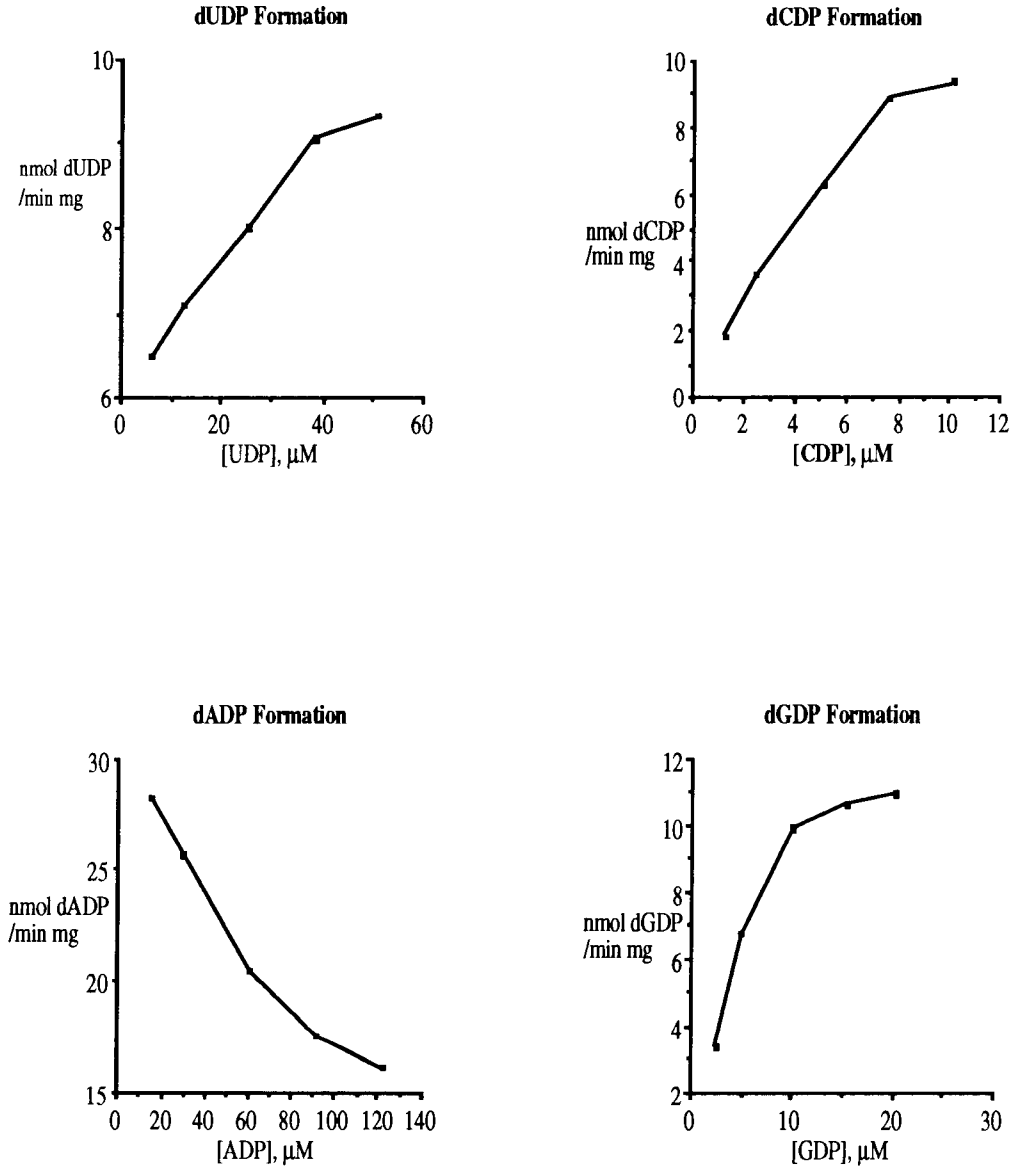

Figure 4.6 **Substrate inhibition of rADP reduction.** These graphs represent the data from Figure 4.5 after conversion of peak areas into nanomoles of dNDP formed. Although the formation of dUDP, dCDP, and dGDP behave according to normal Michaelis-Menten kinetics, dADP formation was inhibited as the substrate concentration increased.

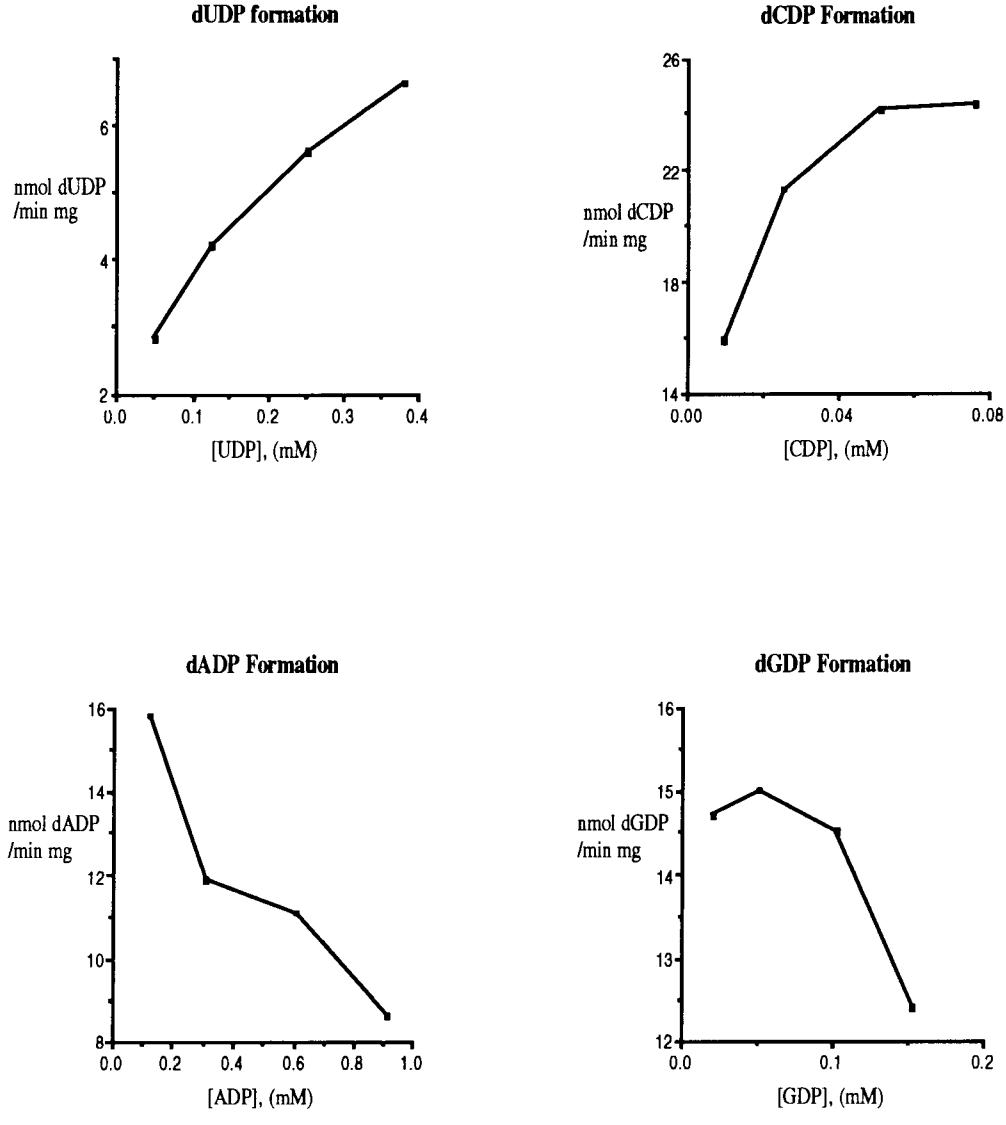

Figure 4.7 **Substrate inhibition of rADP and rGDP reduction.** The conditions used in this experiment are identical to those given in Figure 4.6 except that the "bioproportional" substrate mixture was added at a ten-fold higher concentration range.

Activity of a chimeric RNR holoenzyme— A mixed-species RNR was formed from the vaccinia R1 and mouse R2 proteins and assayed for activity using the four-substrate assay. Figure 4.8 shows the HPLC results from such an assay in which a reaction mixture containing vaccinia R1, mouse R2, ATP, and equimolar substrates was sampled at 3 minute intervals. Neither subunit showed activity when assayed alone (data not shown). The results from this experiment clearly indicate that this chimeric RNR is active. The specific activity calculated from these data was 48 nmol dNDP·min^{-1}·mg R1^{-1} which corresponds to a turnover number of 7.6 min^{-1}.

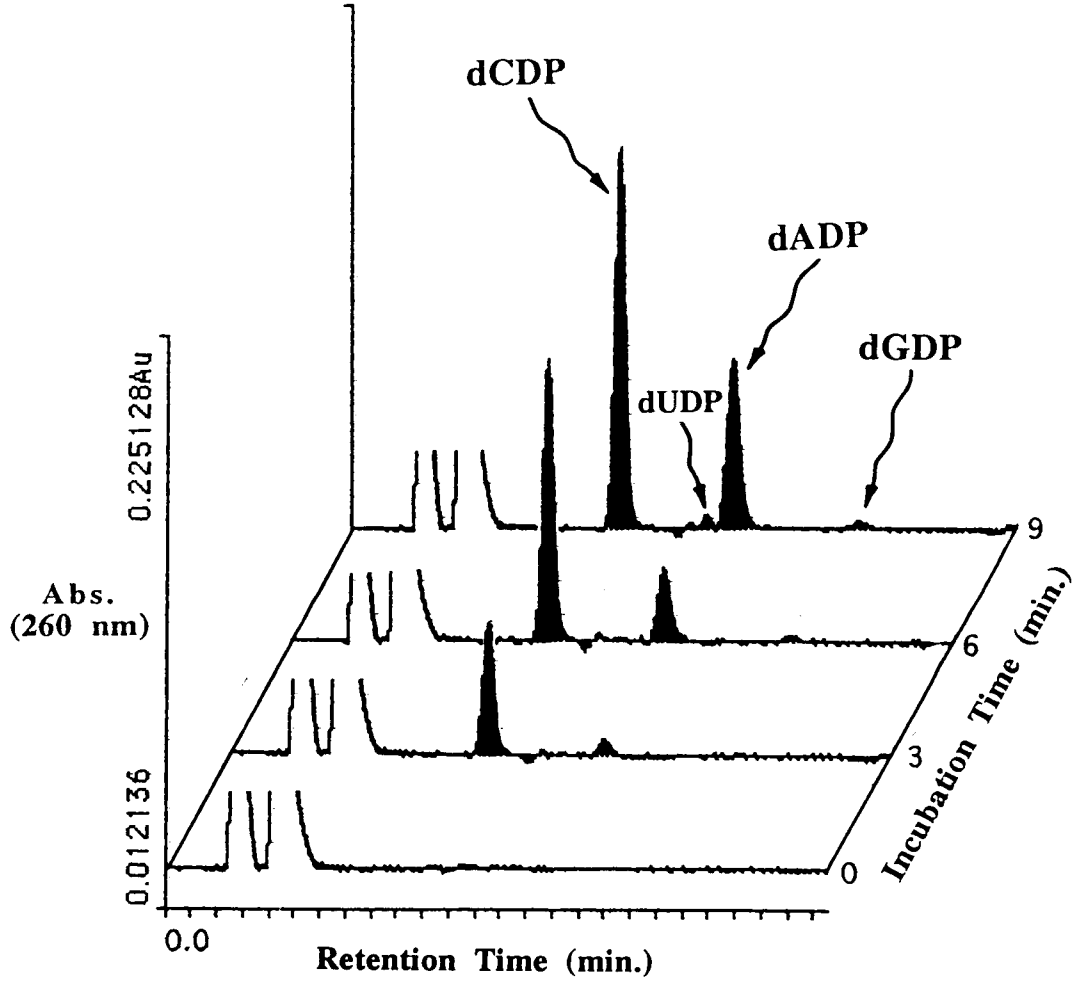

Figure 4.8 **Results from an assay of a vaccinia R1/mouse R2 chimera.** In this experiment, a reaction mixture containing 1 μM vaccinia R1, 4 μM mouse R2, 2.5 mM ATP, and equimolar substrates (0.15 mM each) was sampled at 3 minute intervals.

Discussion

Allosteric regulation of the vaccinia RNR— In this chapter, the isolated effects of single nucleoside triphosphates and the combined effects of complex nucleotide environments on the allosteric regulation of the vaccinia RNR was examined using the four-substrate assay. The vaccinia RNR was assayed in the presence of single dNTP effectors and the resulting product profile, or relative amounts of each dNDP formed, was compared to a control reaction containing only ATP. The results, depicted in Figure 4.2, indicate that the allosteric effectors modulate the activities of the vaccinia RNR similarly to the way they modulate the true mammalian enzymes. ATP acts a general activator of the mammalian and vaccinia RNRs and in the case of the vaccinia enzyme, ATP alone gave the highest turnover rate of all nucleotide effector combinations tested. Typically, the turnover number of ATP-activated vaccinia RNR was about 13 min^{-1}. This number is slightly lower than the values reported for the recombinant mouse and vaccinia enzymes of 24 and 18 min^{-1}, respectively, determined by the traditional single-substrate assay (Davis *et al.*, 1994; Slabaugh *et al.*, 1993).

From Figure 4.2, it is evident that dCTP has no effect on product formation by the vaccinia RNR. In no form of the enzyme has dCTP been shown to act as an allosteric modifier. In contrast, the addition of dTTP to the reaction mixture dramatically changed the product profile. From the HPLC trace in Figure 4.2 of the assay containing dTTP, the inhibition of rCDP reduction and stimulation of rGDP reduction is clearly evident. A similar effect is observed when dGTP is added to the reaction mixture, except in this case the reduction of rADP is stimulated rather than the reduction of rGDP. Addition of dATP to the reaction mixture didn't significantly change the ratio of dNDPs formed. Instead, it simply inhibited all reactions to approximately the same extent. Table 4.1 summarizes these results.

The potency of dATP as an inhibitor of vaccinia RNR is illustrated in Figure 4.3. An interesting aspect of this inhibition is the fact that a significant amount of the potential activity is lost under estimated physiological concentrations. This may reflect an inadequacy in the way that the "*in vivo*" molar concentrations were estimated, or may reflect the possibility that dNTP concentration gradients exist within the cell. This inhibition may also be an indication of how tightly the enzyme is regulated *in vivo*. The mammalian forms of RNR are inhibited by dATP to approximately the same extent as is the vaccinia enzyme. For example, the enzyme from calf thymus has 43% of the control activity at 10 μM dATP (Eriksson *et al.*, 1979). When dATP inhibition was evaluated in vaccinia-infected cell extracts, the viral-induced RNR activity was much more resistant to effects of this dNTP. In order to inhibit 50% of the activity in vaccinia-infected cell extracts, 100 μM dATP was required (Slabaugh et al., 1984). The discrepancy between the extent of dATP inhibition in extracts and purified enzyme may be explained by the presence of dATP-hydrolyzing enzymes present in the crude cell extracts.

The initial studies I did on the T4 and *E. coli* enzymes using the four substrate assay prematurely led me to believe that low rGDP-reducing activity was a general property of RNRs. When the T4 enzyme is measured under optimal conditions for rGDP reduction (ATP plus all of the dNTP allosteric effectors; Table 3.1), the highest rGDP-reducing activity measured was 12% of the total nucleotide produced. Similar levels of rGDP-reducing activity were observed for the *E. coli* enzyme (data not shown). In many cell types, the dGTP pool is severely underrepresented (Mathews and Ji, 1992). Therefore, the low production of dGDP by the T4 and *E. coli* enzymes led to speculation that a low rGDP-reducing activity may be common to all forms of RNR and that this may explain, at least in part, why the dGTP pool tends to be underrepresented in many cell types. For some reason, it may be that rGDP is just not a very good substrate for these forms of RNR. However, when the vaccinia RNR was assayed, this was not the case. Under all

conditions tested, the production of dGDP always exceeded the percent contribution that dGMP makes to the vaccinia genome.

In vivo, RNR is exposed to a complex ensemble of nucleotide effectors and substrates. In experiments similar to those performed on the T4 enzyme (see Chapter 3), the influence of different nucleotide environments on the relative rates of product formation was examined. Possibly the most significant observation made from these experiments is of the role that the relative substrate concentrations play in determining the product profile. As Figure 4.4 shows, the ratio of substrates is at least as important as the dNTP effectors in regulating the four turnover rates.

When the vaccinia RNR is assayed in the presence of *in vivo* concentrations of rNDPs and dNTPs, the ratio of dCDP, dUDP, dADP, and dGDP as the percentage of the total dNDP formed was 34 : 12 : 29 : 26, respectively. The percentage of dAMP in vaccinia DNA is 33% and therefore, under these conditions the production of dADP by the vaccinia RNR should adequately fill the need for this deoxyribonucleotide. The same is true for the reduction of rGDP, but, as mentioned above, in this case the enzyme appears to supply more than is actually needed for DNA synthesis. The percentage of dCMP in vaccinia DNA is 17%. Therefore, one-half of the dCDP formed by the vaccinia RNR will be used to fulfill the contribution that dCMP makes to the vaccinia genome. The remaining dCDP can be shuttled into thymidine nucleotide biosynthesis via dCMP deaminase (see Figure 1). The total amount of deoxyribonucleotide available for dTTP synthesis will be the sum of the deaminated dCMP (17%) and the dUDP produced from reduction of rUDP (12%). Thymidine nucleotides comprise 33% of the vaccinia genome. This percentage is reasonably close to the amount of deoxyribonucleotide available for dTTP synthesis by this analysis (29%). Thus, like the T4 enzyme, when exposed to substrates and effectors at their estimated *in vivo* concentrations, the RNR from vaccinia is programmed to produce dNDPs at relative rates that correspond closely to the composition of the respective nucleotides in vaccinia DNA.

The vaccinia and T4 RNRs have other regulatory features in common also. For example, the production of dUDP was always low regardless of which allosteric effectors were added to the reaction mixture. When ATP was the only allosteric effector present in the reaction mixture, the initial rate of formation of dUDP, as a percent of the total dNDP produced, was 11, 9, and 3%, for the T4, *E. coli*, and vaccinia enzymes, respectively (see Tables 3.1 and 4.3, *E. coli* data not shown). When the T4 and vaccinia RNRs are assayed in the presence of *"in vivo"* levels of substrates and allosteric effectors, the amount of dUDP formation increases, but only to 14, and 12% of the total product formed, respectively. The low production of dUDP by both the eukaryotic and prokaryotic forms of RNR is consistent with the results of *in vivo* studies on thymine metabolism which have shown that the majority of thymine nucleotides are generated from deamination of dCMP (Bianchi *et al.*, 1987; Møllgaard and Neuhard, 1983).

Why should deamination of dCMP be the major source of dTTP in the cell? Perhaps the low rUDP reducing activity of RNR has evolved as such in order to limit the production of dUTP. Recall that in eukaroytes, the production of dTTP via dCMP deamination bypasses the formation of dUTP because it produces dUMP, the substrate of thymidylate synthase, directly (see Figure 1). On the other hand, the dUDP produced from the reduction of rUDP is phosphorylated to dUTP and then cleaved by dUTPase to dUMP. Therefore, dCMP deamination may have evolved as the major pathway for the synthesis of dTTP in order to limit the intracellular concentration of dUTP.

Support for this hypothesis comes from studies on thymine metabolism. When thymidylate synthase is severely inhibited, dUTP accumulates in the cell, indicating that the system responsible for the degradation of this nucleotide can be overwhelmed. Furthermore, these cells die from a phenomenon known as "thymineless death" which, under these conditions, is thought to be due to the incorporation of uracil into DNA (Ingraham *et al.*, 1986).

Substrate inhibition of RNR activity— In an attempt to estimate the concentrations of half-saturation for each rNDP under *in vivo*-like conditions, the vaccinia RNR was assayed in the presence of different volumes of a particular mixture of rNDPs referred to as bioproportional substrates. This bioproportional substrate mixture was composed of the four rNDPs at the molar ratio shown in Table 4.2. When the results of these assays were analyzed, an unexpected observation was made. As the concentration of each substrate was increased in the reaction mixture through the addition of successively larger volumes of the bioproportional substrate mixture, the production of dADP was inhibited. In the concentration ranges used in the experiment depicted in Figure 4.5 and 4.6, the other activities behaved as expected. When the bioproportional substrate concentrations were elevated 10-fold from the concentrations used in the experiment in Figure 4.5, the inhibitory behavior expanded to include the reduction of rGDP. The results from this experiment are presented in graphical form in Figure 4.7.

This non Michaelis-Menten behavior is quite fascinating. If rNDPs were simply competing for the active site, the turnover rates would be expected to increase as the concentration of the substrate increased. Instead, the decrease in rADP reduction that occurs with increasing rNDP concentration indicates that the inhibition may be achieved through binding of rNDPs (or dNDPs) to one or both allosteric sites. Although the conventional dogma of RNR allostery presumes that only the triphosphates bind the allosteric sites, it seems reasonable that molecules as similar in structure as rADP and ATP, for example, could bind the same nucleotide binding site. In the bioproportional mixture, rADP is the most abundant substrate by as much as 12-fold. This biased rNDP ratio may facilitate the preferential binding of rADP to an allosteric site. In most forms of RNR, binding of the adenine-containing nucleotides to the specificity site stimulates reduction of the pyrimidine rNDPs at the expense of the purine substrates. If binding of rADP to the specificity site results in similar allosteric behavior, then the expected outcome would be stimulation of pyrimidine reduction at the expense of rADP reduction. Therefore, as the

concentration of rADP is increased, the rate of rADP reduction should decrease relative to the reduction of the other substrates. This hypothesis is also consistent with the inhibition of rGDP reduction observed at the higher levels of the bioproportional mixture.

Initially, I was concerned that the turnover number calculated from the results of the four-substrate assay was only about 75% of the value reported in Slabaugh *et al.*, 1993. I rationalized that competition between the substrates for active site binding might explain the lower turnover rate. Indeed, the results of assays done using bioproportional substrate levels clearly indicate that substrate inhibition does play a role in the activity of the vaccinia RNR. However, it appears that the form of this substrate inhibition is significantly more complex than I originally presumed.

Although the conventional belief is that RNR is regulated only by nucleoside triphosphates, regulation of ribonucleotide reductase activity by substrates and products does have precedence in the literature. Not surprisingly, competitive inhibition between alternate substrates has been shown to occur in several ribonucleotide reductase systems including the enzymes from calf thymus (Eriksson *et al.*, 1979), human lymphoblasts (Chang and Cheng, 1979), Ehrlich ascites cells (Cory *et al.*, 1985), and herpes simplex virus type I (Averett et al., 1983). However, noncompetitive inhibition by alternate substrates has also been demonstrated in several of these same systems.

Studies done using the human lymphoblast (Molt-4F) ribonucleotide reductase, purified from cultured cells, revealed that reduction of any of the rNDPs could be noncompetitively inhibited by other ribonucleoside diphosphates (Chang and Cheng, 1979). For example, rADP reduction was inhibited noncompetitively by all of the other substrates. The noncompetitive inhibition displayed by alternate substrates was observed even when these substrates shared a common allosteric activator. rCDP and rUDP, both of which are reduced when ATP is bound to the enzyme, could act as noncompetitive inhibitors of the reduction of each other.

The ribonucleotide reductase from herpes simplex virus type I (HSV-1) is also regulated by nucleoside diphosphates (Averett *et al.*, 1983). This ribonucleotide reductase is distinct from all other type I enzymes in that it is only weakly inhibited, and shows no activation by dNTPs. In addition, it does not appear to require the presence of the general activator, ATP, for activity. When competition experiments were performed with this enzyme, each rNDP substrate was a competitive inhibitor with respect to each other rNDP substrate. The inhibition constants (K_is) obtained for each alternate substrate as an inhibitor was in each case similar to the K_m of that rNDP as a substrate, consistent with the linear competitive model of inhibition in which substrate and inhibitor compete for the same binding site (Spector and Cleland, 1981).

The products of the HSV-1 ribonucleotide reductase (dNDPs) were also shown to be competitive inhibitors *versus* the substrates (rNDPs). However, in this case, the K_is for the dNDP products revealed a more complex pattern of inhibition. For example, the K_is for dCDP and dGDP as inhibitors of rCDP reduction were 4.8 and 9.0 μM, respectively. These values are of similar magnitude as the K_m for rCDP. In contrast, the K_i for dADP as an inhibitor of rCDP reduction was 140 μM, much greater than the K_m for rCDP. Thus, binding of dGDP or dCDP to the active site will have a much greater inhibitory effect on rCDP reduction than binding of dADP. Binding of dADP will presumably inhibit the reduction of a substrate other than rCDP. Thus, it appears that by inhibiting the reduction of specific substrates, the dNDPs are in effect promoting the reduction of the other substrates.

Although no evidence for allosteric control of the HSV-1 RNR exists, the relative turnover rates of the four substrates appear, instead, to be regulated by the levels of substrates and products. A model for the regulation of this form of ribonucleotide reductase is one in which the substrates compete for binding to the active site according to their relative concentrations and K_ms. The resulting deoxyribonucleotide products further compete with the substrates for binding to the active site. However, the inhibitory patterns

of the dNDPs are significantly different from the simple competitive inhibition observed when the substrates act as inhibitors. Although the dNDPs are believed to compete with substrate for binding to the active site, the inhibition constants are suggestive of a more sophisticated form of regulation in which the products direct reduction (through inhibition) of specific substrates in a way that may maintain the balance of products required for efficient viral DNA replication. With what is known about the relationship between dNTP pool imbalances and mutagenesis, it seems imperative that the four activities of this enzyme be regulated in some way such that an optimal level of all four products is maintained. In the herpes simplex I RNR, this regulation appears to be modulated by the substrates and products.

The RNR from Ehrlich ascites cells has been shown to be sensitive to regulation by both rNDPs and dNDPs (Cory *et al.*, 1985). In assays done on RNR purified from this mouse tumor cell line, it was found that the nucleoside diphosphates displayed similar allosteric modulation as their nucleoside triphosphate counterparts. For instance, rADP was found to activate rCDP reduction; dGDP activated rADP reduction; and rGDP reduction was activated by dTDP. The inhibitory pattern of regulation by the nucleoside diphosphates was also similar to the inhibition displayed by the nucleoside triphosphates. Like dATP, dADP inhibited the reduction of all four substrates. The chemical similarity of these two nucleotides suggests that dADP may also function as an inhibitor through binding to the activity site. Reduction of rUDP was inhibited by both dGDP and dTDP, and dGDP inhibited the reduction of rGDP. Analogous to the inhibition by dGTP and dTTP, these inhibitory effects may also be attributed to the binding of the deoxyribonucleoside diphosphate to one of the allosteric regulatory sites. Indeed, when the nature of the inhibition by these deoxyribonucleoside diphosphates was examined using Dixon plots (1/v vs [I]), it was found that the dNDPs were acting as noncompetitive inhibitors with respect to substrate, indicating that the inhibition was more complex than

simply competition for the substrate binding site. The K_i values in these experiments ranged from 5-100 μM, with the lowest values recorded when rUDP was the substrate.

Interestingly, of all four substrates, rUDP reduction by the Ehrlich tumor RNR was the most sensitive to the inhibitory effects of dNDPs. The inhibition of UDP reduction by dTDP, dGDP, and dADP was at least equal to that observed by dTTP, dGTP, and dATP, respectively. The K_i for dGDP, the most potent dNDP inhibitor of UDP reduction, was 5 μM, essentially the same value as the K_i for dGTP. Even dCDP significantly inhibited rUDP reduction while, as in the case of most ribonucleotide reductases, dCTP was found to be allosterically inert. These findings may be relevant to my studies on the vaccinia ribonucleotide reductase. I have been puzzled ever since I first assayed the vaccinia enzyme by the relatively low rate of rUDP turnover. With the data on the Ehrlich tumor ribonucleotide reductase in mind, I propose that one explanation for the low rUDP turnover may be due to the inhibitory effects of the newly formed dNDPs in the reaction mix. In the traditional assay performed with one substrate at a time, these dNDP inhibitory effects would not be seen.

Clearly, the regulation of ribonucleotide reductase activity by nucleoside diphosphates is an interesting *in vitro* phenomenon, but is this form of regulation physiologically relevant? Are the concentrations of these compounds in the cell high enough to play a significant role in regulating ribonucleotide reductase product formation? The concentrations of rNDPs in mammalian cells are, in general, 10-20 fold higher than the concentrations of dNTPs (Traut, 1994). Therefore, even though the effects of these nucleotides are less pronounced than those of their dNTP counterparts, their relatively high concentrations suggest that they may be capable of participating in the regulation of RNR.

The deoxyribonucleoside diphosphates, on the other hand, are normally present at extremely low concentrations. Typical concentrations for these nucleotides, when measurable, are in the 0.1-1 μM range (Traut, 1994). However, nucleotide labeling studies done in both HeLa and Chinese hamster ovary (CHO) cells have shown that

dNDPs are elevated during S-phase (Hordern and Henderson, 1982). Therefore, it seems possible that at critical times during the cell cycle when the rate of ribonucleotide reduction is greatly enhanced, the resultant increase in dNDPs may provide another level of control in maintaining a balanced supply of DNA precursors.

The model that I have formulated from my research, as well as research reported in the literature, is one in which the regulation of RNR is not quite as simple as once presumed. Although the dNTPs are important regulators of RNR, they are not the only nucleotides which must be considered if one desires a better understanding of the intricate *in vivo* regulation responsible for maintaining a balanced pool of the DNA precursors.

In this model, the regulation of RNR by nucleotides consists of three levels. At the first level are the substrates of RNR. These nucleotides compete with each other for binding to the active site according to their K_ms. In addition, in several cases, the substrates may also inhibit or activate reduction of alternate substrates through binding to the allosteric sites. The significant role that the relative substrate concentrations play in determining the relative turnover rates of the vaccinia and T4 bacteriophage enzymes is a conclusion from my research which has contributed greatly to the formulation of this model.

At the second level of regulation are the direct products of RNR, the dNDPs. These nucleotides may act to regulate RNR by binding either to the active site or the allosteric sites. In many cases, the K_i's of the dNDPs are of the same order of magnitude as the corresponding constants of the dNTPs indicating that they can compete effectively with the dNTPs for binding to the enzyme. Thus, at times during the cell or viral cycle when their concentrations are elevated, dNDPs may be just as potent regulators of RNR activity as the dNTPs. In fact, the effective concentration that RNR senses *in vivo* may be greater for the dNDPs than for the dNTPs. This assumption is justifiable if one considers that the dNDPs are the direct products of RNR and therefore will be in direct contact with the enzyme. The

dNTPs, on the other hand, are the products of one or more enzymes down the pathway and must "feed back" in order to act as effectors of RNR activity.

The third level of ribonucleotide reductase regulation, according to this model, is achieved by the final products of the deoxyribonucleotide biosynthetic pathway, the dNTPs. These nucleotides function to fine tune the relative turnover rates of RNR by inhibiting certain activities and activating others.

Obviously, these three levels of nucleotide regulation are intimately connected and act in conjunction to determine the final flux through RNR. Thus, the regulation of RNR via the substrates, the direct products of the RNR reaction, and the final products of the biosynthetic pathway initiated by RNR, results ultimately in a precisely regulated output of the DNA precursors.

The vaccinia-mouse RNR chimera— To assess whether a functional viral RNR was required for replication of the vaccinia genome, three insertionally inactivated vaccinia R1 mutants were prepared (Child *et al.*, 1990). Although the insertional inactivation of the R1 gene was shown to abolish viral RNR activity, all three mutant viruses replicated to levels comparable to wild-type virus in tissue culture cells. However, when the virulence of the mutants was examined in an animal model, it was found that lack of functional R1 produced viruses that were mildly attenuated. Approximately a 10-fold increase in the number of mutant viruses was needed to reach the lethal dose for 50% of a population of mice.

An obvious question which arises from this study is what is the *de novo* source of dNTPs for replication of the vaccinia genome in these mutants? Does this mutant rely on the host cell RNR activity, or does a chimeric form of RNR composed of host cell and vaccinia proteins function to provide deoxyribonucleotides? I tested the possibility that a chimeric form of RNR was functional by assaying proteins I had available, the vaccinia R1 and mouse R2. Figure 4.8 shows the results of a chimeric RNR assay. Based on these results, it appears that the mouse R2 can function as a radical source for the vaccinia R1.

The appropriate controls indicated that neither subunit had any detectable intrinsic activity of its own (data not shown). Furthermore, the specific activity of the chimera was on the same order of magnitude as that of the vaccinia holoenzyme (7.6 and 13 nmol min^{-1}, respectively) indicating that it is high enough to rule out residual *E. coli* RNR activity, resulting from the overexpression system. As a comparison, the chimeras formed from the T4 bacteriophage and *E. coli* proteins show no detectable activity (Berglund, 1972). To my knowledge, this represents the first report of an active chimeric RNR.

When one considers what is known about the interactions between R1 and R2, this result may not be so surprising. The large and small subunits of the Class I RNRs interact primarily through highly specific contacts formed between the R2 carboxy terminus and its corresponding binding site located on the R1 protein. The R2 carboxy terminus sequences are not conserved but are highly species-specific. In many cases, the formation of an active holoenzyme can be inhibited by short peptides with sequences similar to the penultimate C-terminal residues of R2. The last 12 residues of the mouse and human R2 proteins are identical, and the last 10 of these are virtually identical to the vaccinia protein. For purposes of comparison, the last 10 C-terminal residues of the R2 from mouse/human and vaccinia are shown below:

mouse/human	-E N S F T L D A D F-CO_2^-
vaccinia	-<u>D</u> N <u>H</u> F <u>S</u> L D <u>V</u> D F-CO_2^-

The underlined residues represent amino acids in the vaccinia R2 protein which differ from those of the mouse and human . All of the differences except one represent conservative substitutions.

Even more interesting than the fact that these proteins form an active enzyme, is the observation that the chimeric holoenzyme generates products at a significantly different ratio from that of the vaccinia RNR under identical nucleotide concentrations. Comparison

of Figure 4.1 and 4.8 illustrates this observation. When the four substrates are present at equimolar concentrations and ATP is the only added allosteric effector, the vaccinia holoenzyme primarily reduces rCDP and rGDP (Figure 4.1). In contrast, under similar conditions the vaccinia R1 and mouse R2 chimera prefers rCDP and rADP as substrates for reduction. The reduction of rGDP by the chimeric enzyme is very low, and as evident in Figure 4.8, the production of dGDP is detectable only at the later time points of the reaction. Therefore, ATP activation of these two holoenzyme forms results in distinctly different substrate preferences.

There are at least two possible models which may explain the different product profiles generated by these two holoenzyme forms. One possible source for the different substrate specificities may result from a slight noncomplementarity between the interacting surfaces of vaccinia R1 and mouse R2. Clearly the complementarity between these surfaces is sufficient to drive formation of the heterotetramer, or such high RNR activity would not be observed. However, if the interacting surfaces in the chimeric enzyme do not complement each other in the same way that they do in the holoenzyme formed by subunits from a single species, then formation of the chimeric enzyme may drive minor structural changes in one or both of the subunits. The structural changes induced by the formation of the chimera may result in a perturbation of the R1 allosteric sites, altering the allosteric effects of ATP on substrate specificity. The dramatic effects that nucleotide effectors have on RNR activity indicate that the substrate specificity is exquisitely sensitive to minor structural changes in R1. Therefore, the perturbation of R1 structure that may result from the interaction of dimer surfaces with inexact complementarities may explain the observed differences in substrate specificities between the wild-type and chimeric enzymes.

A second possible explanation for the different substrate specificities is contrary to the presumption that the only function of R2 is to serve as a radical storage site for R1. The R1 subunit is generally referred to as the "business end" of the holoenzyme because it contains the active site, where ribonucleotide reduction occurs, and presumably the two

allosteric sites. Therefore, it is normally assumed that the specificity of the holoenzyme is an inherent property of R1 protein, exclusively. On the other hand, since R2 is thought to serve primarily as a radical storage site, the function of this protein is frequently compared to that of a cofactor.

However, it is possible that the R2 protein also contributes to the allosteric regulation of RNR by physically forming part of an allosteric binding site. If this is true, then the R2 from a different, but closely related, species may physically alter the structure , and hence the function, of that allosteric site. Since limited knowledge about the structure of the allosteric sites of RNR exists, a contribution by the R2 protein to the formation of these sites cannot be ruled out. Indeed, the activity site is thought to be formed by the N-terminus of the R1 protomer. In the crystal structure, the last resolvable N-terminal residues are located in the region adjacent to the binding site for the R2 C terminus. Furthermore, the contribution of R2 to the formation of an allosteric site is consistent with the poor efficiency at which nucleotides specifically label the isolated R1 protein in cross-linking and crystallography studies (Eriksson *et al.*, 1986; Uhlin and Eklund, 1994). Localization and structural characterization of the allosteric sites of RNR will serve to test this hypothesis. However, this structural information will probably not be available until the crystal structure of the holoenzyme has been solved.

References

Averett, D. R., Lubbers, C., Elion, G. B., and Spector, T (1983) *J. Biol. Chem.* **258**, 9831-9838

Bianchi, V., Pontis, E., and Reichard, P. (1987) *Mol. Cell. Biol.* **7**, 4218-4224

Berglund, O. (1972) *J. Biol. Chem.* **247**, 7276-7281

Chang C.-H., and Cheng, Y.-c. (1979) *Cancer Res.* **39**, 5081-5086

Child, S. J., Palumbo, G. J., Buller, M. L., and Hruby, D. E. (1990) *Virology* **174**, 625-629

Cory, J. D., Rey, D. A., Carter, G. C., and Bacon, P. E. (1985) *J. Biol. Chem.* **260**, 12001-12007

Davis, R., Thelander, M., Mann, G. J., Behraven, G., Soucy, F., Beaulieu, P., Lavaslée, P., Gräslund, A., and Thelander, L. (1994) *J. Biol. Chem.* **269**, 23171-23176

Eliasson, R., Pontis, E., Jordan, A., and Reichard, P. (1996) *J. Biol. Chem.* **271**, 26582-26587

Eriksson, S., Sjöberg, B.-M., Jörnvall, H., and Carlquist, M. (1986) *J. Biol Chem.* **18**, 2948-2952

Eriksson, S., Thelander, L., and Åkerman, M. (1979) *Biochemistry* **18**, 2948-2952

Hauschka, P. V. (1973) *Meth. Cell Biol.* **7**, 361-462

Hendricks, S. P., and Mathews, C. K. (1997) *J. Biol. Chem.* **272**, 2861-2865

Hordern, J., and Henderson, J. F. (1982) *Can. J. Biochem.* **60**, 422-433

Howell, M. L., Sanders-Loehr, J., Loehr, T. M., Roseman, N. A., Mathews, C. K., and Slabaugh, M. B. (1992) *J. Biol. Chem.* **267**, 1705-1711

Ingraham, H. A., Tseng, B. Y., and Goulian, M. (1986) *Biochemistry* **25**, 3225-3230

Larsson, A., and Reichard, P. (1966a) *J. Biol. Chem.* **241**, 2533-2539

Larsson, A., and Reichard, P. (1966b) *J. Biol. Chem.* **241**, 2540-2549

Mathews, C. K., and Ji, J. (1992) *BioEssays* **14**, 295-301

Møllgaard, H., and Neuhard, J. (1983) *Metabolism of Nucleotides, Nucleosides, and Nucleobases in Microorganisms* Academic Press, Inc. (London), Ltd. London, 149-198

Slabaugh, M. B., Davis, R. E., Roseman, N. A. and Mathews, C. K. (1993) *J. Biol. Chem.* **268**, 17803-17810

Slabaugh, M. B., Howell, M. L., Wang, Y., and Mathews, C. K. (1991) *J. Vir.* **65**, 2290-2298

Slabaugh, M. B., Johnson, T. L., and Mathews, C. K. (1984) *J. Vir.* **52**, 507-514

Spector, T., and Cleland, W. W. (1981) *Biochem. Pharmacol.* **30**, 1-7

Traut, T. (1994) *Mol. Cell. Biochem.* **140**, 1-22

Uhlin, U., and Eklund, H. (1994) *Nature* **370**, 533-539

Concluding Remarks

Since my first exposure to biochemistry, I have been intrigued by the relationship between protein structure and function. This intrigue was the primary driving force that led me to study ribonucleotide reductase (RNR). From the perspective of structure/function relationships, I cannot think of a more interesting enzyme than RNR.

I joined the Mathews laboratory to study how the regulatory state of RNR affects the sensitivity of the enzyme to the inhibitor hydroxyurea, a clinically-significant drug that targets the catalytically essential radical of RNR. This work led me to explore further the intricate pattern of regulation that fine tunes the relative flux rates of this enzyme and has culminated in a new model for the control of RNR activity.

My thesis project was to test the possibility that the individual activities of the vaccinia virus RNR may be differentially sensitive to hydroxyurea. The initial approach I used to address this question involved measurement of the radical/iron-oxo decay rates under different allosteric conditions. These experiments led to the conclusion that the susceptibility of RNR is directly correlated to the activity level of the enzyme. Activation of RNR by the addition of effectors increased the sensitivity of the enzyme to hydroxyurea. Addition of substrate to the activated enzyme, further increased the sensitivity. However, technical difficulties associated with the method made it difficult to say with much confidence whether or not the individual activities were differentially sensitive to the inhibitor.

It is often quoted that, "Necessity is the Mother of invention." This is a concept that certainly applies in the case of my research. The lack of reproducibility of the radical/iron-oxo decay measurements incited me to approach the question from a different perspective. Instead of following the chromophore decay directly, I decided to follow the radical destruction as a function of the relative enzyme activities. This approach led to the development of the RNR four-substrate assay, a novel procedure that has proved

invaluable in investigating the inhibitory effects of hydroxyurea, as well as other aspects of RNR regulation. The results obtained by use of the four-substrate assay indicate that all four activities of vaccinia RNR are equally susceptible to hydroxyurea inhibition.

The development of the four-substrate assay dramatically increased the scope of my project by prompting us to ask questions regarding the regulation of RNR that either were unanswerable by the traditional one-substrate assay, or that had not been previously considered. For example, using the four-substrate assay to measure the activities of the T4 phage RNR, we asked what the relative substrate turnover rates would be in a reaction mixture containing the known allosteric effectors and substrates, at their estimated *in vivo* concentrations. Although it is assumed that under these conditions RNR will generate appropriate levels of the four products, it had never been demonstrated experimentally. The studies conducted using the four-substrate assay indicate that the T4 RNR, when functioning within an *in vivo*-like nucleotide environment, generates the four products in a ratio that approximates the nucleotide composition of the T4 genome. Similar results were found for the RNR encoded by vaccinia virus.

The studies I have done on the vaccinia and T4 RNRs suggest that much of the regulatory functions of these proteins have been retained, even though these viruses are vastly separated by evolution. For example, the modulation of substrate specificity by the allosteric effectors is very similar for both of these forms of RNR. Furthermore, both the T4 and vaccinia RNRs reduce uridine diphosphate at very low rates, an observation that is consistent with *in vivo* thymine metabolism.

However, other aspects of the regulation of these enzymes are significantly different. One of the biggest distinctions in the way these RNRs are regulated is in their response to deoxyadenosine triphosphate (dATP). At 50 μM dATP approximately 50% of the vaccinia enzyme activity, present in reaction mixtures without dATP is inhibited. At 15 μM, the estimated physiological concentration of dATP in vaccinia-infected cells, approximately

20% of the vaccinia enzyme activity is inhibited. In contrast, no indication of dATP inhibition of the T4 RNR was observed at the concentrations used in my experiments.

The rate of guanosine diphosphate (rGDP) reduction is also significantly different for these eukaryotic and prokaryotic viral forms of RNR. When ATP is the only allosteric activator present in the reaction mixture, the T4 enzyme reduces very little rGDP. As the nucleotide environment approaches the estimated physiological concentrations of effectors and substrates, the rate of rGDP reduction increases significantly. However, although it gets close, the rate never quite reaches what is expected based on the contribution that deoxyguanosine nucleotides make to the T4 genome. The vaccinia enzyme behaves conversely. The rate of rGDP reduction under non-physiological nucleotide concentrations is well above what is expected from the guanine content of vaccinia DNA. As the nucleotide effectors and substrates approach estimated physiological concentrations, the rate of rGDP reduction decreases. However, under the conditions used in my experiments, rGDP reduction always remains higher than expected.

This observation may be related to an area of research that is of particular interest to the Mathews laboratory, oxidative damage of deoxyguanosine nucleotides. It has been proposed that the deoxyguanosine triphosphate pool is underrepresented in mammalian cells because it is particularly prone to oxidative damage. If this theory proves to be valid, then it is possible that the high rate of rGDP reduction by the mammalian form of RNR may be a mechanism that has evolved to counteract the depletion of deoxyguanosine nucleotides resulting from oxidative damage. At this point, however, this explanation for the high rate of rGDP reduction by the mammalian form of RNR is pure speculation.

Another unexpected observation that was made using the four-substrate assay was the important role that substrate concentrations play in regulating the activities of RNR. For both forms of RNR used in my studies, the product output best approximated the genomic composition when both the allosteric effectors and substrates were present in the reaction mixture at near physiological concentrations. Furthermore, the inhibitory phenomena

observed when different amounts of the "bioproportional substrate" mixture (see Chapter 4) were added to the reaction mixtures exemplifies the potential role that substrates play in regulation of the activities of RNR.

The results from these studies have changed my thinking in regards to the regulation of RNR. Instead of the triphosphate nucleotides being the main small-molecule determinants of RNR activity, my studies suggest that the substrates, and perhaps the products, also play a significant role in the control of reduction rates. In this model, the level of each RNR activity is intricately controlled by a complex interplay of nucleoside triphosphate effectors, substrates, and products. This interplay may be in the form of competition between nucleotides for binding to the allosteric sites, or the active site, or both. Hopefully, subsequent studies will unravel the details of what appears to be a very complicated regulatory scheme. I would expect nothing less than a highly sophisticated pattern of regulation from such a extraordinary enzyme as ribonucleotide reductase.

Bibliography

Adams, R. L. P., Berryman, S., and Thompson, A. (1971) *Biochem. Biophys. Acta* **240**, 455-462

Åkerblom, L., and Reichard, P. (1985) *J. Biol. Chem.* **260**, 9197-9202

Atkin, C. L., Thelander, L., Reichard, P., and Lang, G. (1973) *J. Biol. Chem.* **248**, 7464-7472

Ator, M.A., Stubbe, J. A., and Spector, T (1986) *J. Biol. Chem.* **261**, 3595-3599

Averett, D. R., Lubbers, C., Elion, G. B., and Spector, T (1983) *J. Biol. Chem.* **258**, 9831-9838

Backes, G., Sahlin, M., Sjöberg, B.-M., Loehr, T. M., and Sanders-Loehr, J. (1989) *Biochemistry* **28**, 1923-1929

Berglund, O. (1972) *J. Biol. Chem.* **247**, 7270-7275

Berglund, O., and Sjöberg, B.-M. (1978) *J. Biol. Chem.* **254**, 253-254

Bianchi, V., Ferraro, P., Borello, S., Bonvini, P., and Reichard, P. (1994) *J. Biol. Chem.* **269**, 16677-16683

Bianchi, V., Pontis, E., and Reichard, P. (1986a) *J. Biol. Chem.* **261**, 16037-16042

Bianchi, V., Pontis, E., and Reichard, P. (1986b) *PNAS* **83**, 986-990

Bianchi, V., Pontis, E. and Reichard, P. (1987) *Mol. Cell. Biol.* **7**, 4218-4224

Bianchi, V., Pontis, E. and Reichard, P. (1992) *Exp. Cell Research* **199**, 120-128

Blakley, R. L. and Barker, H. A. (1964) *Biochim. Biophys. Res. Commun.* **16**, 301

Bolin, R. W., Robinson, W. A., Sutherland, J., and Hamman, R. F. (1982) *Cancer* **50**, 1683-1686

Bollinger, J.M., Edmonson, D.E., Huynh, B. H., Filley, J., Norton, J.R., and Stubbe, J. (1991) *Science* **253**, 292-298

Booker, S., Licht, S., Broderick, J. and Stubbe, J. (1994) *Biochemistry* **33**, 12676-12685

Brown, N. C., Eliasson, R., Reichard, P., and Thelander, L. (1969) *Eur. J. Biochem.* **9**, 512-518

Brown. N. C. and Reichard, P. (1969a) *J. Mol. Biol.*, **46**, 25-38

Brown. N. C. and Reichard, P. (1969b) *J. Mol. Biol.*, **46**, 39-55

Caras, I. W., and Martin, D. W. J. (1988) *Mol. Cell Biol.* **8**, 2698-2704

Chan, A. K., Lichfield, D. W., and Wright, J. A. (1993) *Biochemistry*, **32**, 12835-12840

Chang C.-H., and Cheng, Y.-C. (1979) *Cancer Res.* **39**, 5081-5086

Chen, A. K., Bhan, A., Hopper, S., Abrams, R., and Frazen, J. S. (1977) *Biochemistry* **13**, 654-661

Cheng, Y.-C. (1978) *Methods Enzymol.* **51**, 365-371

Child, S. J., Palumbo, G. J., Buller, M. L., and Hruby, D. E. (1990) *Virology* **174**, 625-629

Climent, I., Sjöberg, B.-M., and Huang, C. Y. (1992) *Biochemistry* **31**, 4801-4807

Cori, J. D., Lasate, L., and Sato, A. (1981) *Biochem. Pharm.* **30**, 979-984

Cori, J. D., Rey, D. A., Carter, G. C., and Bacon, P. E. (1985) *J. Biol. Chem.* **260**, 12001-12007

Covés, J., Niviére, V., Eschenbrenner, M., and Fontecave, M. (1993) *J. Biol. Chem.* **268**, 18604-18609

Daddona, P. E., and Kelley, W. N. (1977) *J. Biol Chem.* **252**, 110-115

Dai, Y., Gold, B., Vishwanatha, J. K., and Rhode, S. L. (1994) *Virology* **205**, 210-216

Davis, R., Thelander, M., Mann, G. J., Behraven, G., Soucy, F., Beaulieu, P., Lavaslée, P., Gräslund, A., and Thelander, L. (1994) *J. Biol. Chem.* **269**, 23171-23176

Drake, J. (1991) *Proc. Natl. Acad. Sci. USA* **88**, 7160-7164

Dresler, W. F. C., and Stein, R. (1869) *Justus Liebigs Ann. Chem. Pharmacol.* **150**, 242-252

Ehrenberg, A., and Reichard, P. (1972) *J. Biol. Chem.* **247**, 3485-3488

Ekberg, M. Sahlin, M., Eriksson, M., and Sjöberg, B.-M. (1996) *J. Biol. Chem.* **271**, 20655-20659

Eliasson, R., Pontis, E., Jordan, A., and Reichard, P. (1996) *J. Biol. Chem.* **271**, 26582-26587

Eliasson, R., Pontis, E., Sun, X., and Reichard, P. (1994) *J. Biol. Chem.* **269**, 26052-26057

Eriksson, S., Sjöberg, B.-M., Jörnvall, H., and Carlquist, M. (1986) *J. Biol. Chem.* **261**, 1878-1882

Eriksson, S., Thelander, L., and Äkerman, M. (1979) *Biochemistry* **18**, 2948-2952

Fontecave, M., Eliasson, P., and Reichard, P. (1989) *Proc. Natl. Sci. U.S.A.* **86**, 2147-2153

Fontecave, M., Eliasson, R., and Reichard, P. (1989) *J. Biol. Chem.* **264**, 9164-9170

Fontecave, M., Nordlund, P., Eklund, H., and Reichard, P. (1992) *Adv. Enzymol. Relat. Areas Mol. Biol.* **65**, 147-183

Fox, B. G., Surerus, K. K., Münck, E., and Lipscomb, J. P. (1989) *J. Biol. Chem.* **263**, 10553

Frenkel, E. P., Skinner, W. N., and Smiley, J. D. (1964) *Cancer Chemother. Rep.* **40**, 19-22

Gao, W.-Y., Cara, A., Gallo, R. C., and Lori, F. (1993) *Proc. Natl. Acad. Sci. USA* **90**,825

Garbett, K., Darnell, D. W., Klotz, I. M., and Williams, R. J. P. (1969) *Arch. Biochem. Biophys.* **135**, 419

Hamilton, J. A., Tamao, Y., Blakley, R. L. and Coffman, R. E. (1972) *Biochemistry* **11**, 4696-4705

Hauschka, P. V. (1973) *Meth. Cell Biol.* **7**, 361-462

Hendricks, S. P., and Mathews, C. K. (1997) *J. Biol. Chem.* **272**, 2861-2865

Holmgren, A. (1988) *Bioch. Soc. Trans.* **16**, 95-96

Hordern, J., and Henderson, J. F. (1982) *Can. J. Biochem.* **60**, 422-433

Howell, M. L., Sanders-Loehr, J., Loehr, T., Roseman, N. A., Mathews, C. K., and Slabaugh, M. B. (1992) *J. Biol. Chem.* **267**, 1705-1711

Hurley, M. C., Paletta, T. D., and Fox, I. H. (1983) *J. Biol. Chem.* **258**, 15021-15027

Ingraham, H. A., Tseng, B. Y., and Goulian, M. (1986) *Biochemistry* **25**, 3225-3230

Ji, J., Sargent, G. R., and Mathews, C. K. (1991) *J. Biol. Chem.* **266**, 16289-16292

Jordan, A., Pontis, E., Atta, M., Krook, M., Gilbert, I., Barbé, J., and Reichard P. (1994) *Proc. Natl. Acad. Sci. U.S.A.* **91**, 12892-12896

Jordan, A., Pontis, E., Åslund, F., Hellman, U., Gilbert, I., and Reichard P. (1996) *J. Biol. Chem.* **271**, 8779-8785

Karlsson, M., Sahlin, M., and Sjöberg, B.-M. (1992) *J. Biol. Chem.* **267**, 12622-12626

Kauppi, B., Nielsen, B. B., Ramaswamy, S., Larsen, I. K., Thelander, M., Thelander, L., and Eklund, H. (1996) *J. Mol. Biol.*, **262**, 706-720

Kjöller-Larson, I., Sjöberg, B.-M., and Thelander, L. (1982) *Eur. J. Biochem.* **125**, 75-81

Kunz, B. A., Kohalmi, S. E., Kunkel, T. A., Mathews, C. K., McIntosh, E. M., and Reidy, J. A. (1994) *Mutat. Res.* **318**, 1-64

Land, E. J., Porter, G., and Strachan, E. (1961) *Trans. Faraday Soc.* **57**, 1885-1893

LaPlante, S. R., Aubry, N., Moss, N., and Liuzzi, M. (1993) *J. Cell. Biochem.* **S17C**, 307

Larsson, A., and Reichard, P. (1966a) *J. Biol. Chem.* **241**, 2533-2539

Larsson, A., and Reichard, P. (1966b) *J. Biol. Chem.* **241**, 2540-2549

Lehman, I. R., Bessman, M. J., Simms, E. S., and Kornberg, A. (1958) *J. Biol. Chem.* **233**, 163-170

Liuzzi, M., Deziel, R., Moss., N., Beaulieu, P., Bonneau, A. M., Bousquet, C., Chafouleas, J. G., Garneau, M., Jaramillo, J., Krogrud, R. L., Lagace, L., McCollum, R. S., Nawoot, S. and Guindon, Y. (1994) *Nature* **372**, 695-698

Lori, F., Maly, K. H., Cara, A., Sun, D., Weinstein, J. N., Lisziewicy, J., and Gallo, R. C. (1994) *Science* **266**, 801-805

Lycksell, P. O., Ingemarson, R., Davis, R., Gräslund, A., and Thelander, L. (1994) *Biochemistry* **33**, 2838-2842

Mann, G. J., Gräslund, A., Ochiai, E. I., Ingemarson, R., and Thelander, L. (1991) *Biochemistry* **30**, 1939-1947

Mao, S. S., Holler, T. P., Bollinger, J. M., Yu, G. X., Johnston, M. I., and Stubbe, J. (1992b) *Biochemistry* **31**, 9744-9751

Mao, S. S., Holler,T. P., Yu, G. X., Bollinger, J. M., Booker, S., Johnston, M. I., and Stubbe, J. (1992a) *Biochemistry* **31**, 9733-9743

Mao, S. S., Yu, G. X., Chalfoun, D., and Stubbe, J. (1992c) *Biochemistry* **31**, 9752-9759

Mathews, C. K. (1972) *J. Biol. Chem.* **247**, 7430-7438

Mathews, C. K. (1993) *J. Bacteriol.* **175**, 6377-6381

Mathews, C. K. and Ji, J. (1992) *Bioessays* **14**, 295-301

McDonald, C. J. (1981) *Pharmacol.Ther.* **14**, 1-24

Menage, S., Brennan, B. A., Juarez-Garcia, C., Münck, E., and Que, L. (1990) *J. Am. Chem. Soc.* **112**, 6423-6425

Møllgaard, H., and Neuhard, J. (1983) *Metabolism of Nucleotides, Nucleosides, and Nucleobases in Microorganisms* Academic Press, Inc. (London), Ltd. London, 149-198

Moore, E. C. and Hurlbert, R. B. (1985) *Pharmac. Ther.* **27**, 167-196

Morgan, J. S., Creasey, D. C., and Wright, J. A. (1986) *Biochem. Biophys. Res. Commun.* **134**, 1254-1257

Neuhard, J. (1967) *Biochem. Biophys. Acta* **145**, 1-6

Neuhard, J., and Nygaard, P. (1987) in *Escherichia coli and Salmonella typhimurium Cellular and Molecular Biology* (Neidhardt, F. C., Ingraham, J. L., Low, K. B., Magasanik, B., Schaechter, M., and Umbarger, H. E., eds) pp. 465-466, American Society for Microbiology, Washington DC

Nicander, B. and Reichard, P. (1985a) *J. Biol. Chem.* **260**, 5376-5381

Nicander, B. and Reichard, P. (1985b) *J. Biol. Chem.* **260**, 9216-9222

Nordlund, P., Sjöberg, B.-M., and Eklund, H. (1990) *Nature* **345**, 593-598

Nordlund, P., and Eklund, H. (1993) *J. Mol. Biol.* **232**, 123-164

Nyholm, S., Thelander, L., and Gräslund, A. (1993) *Biochemistry* **32**, 11569-11574

Ochiai, E.-I., Mann, G. J., Gräslund, A., and Thelander, L. (1990) *J. Biol. Chem.* **265**, 15758-15761

Ollagnier, S., Mulliez, E., Gaillard, J., Eliasson, R., Fontecave, M., and Reichard, P. (1996) *J. Biol. Chem.* **271**, 9410-9416

Petersson, L., Gräslund, A., Ehrenberg, A., Sjöberg, B.-M., and Reichard, P. (1980) *J. Biol. Chem.* **255**. 6706-6712

Plagemann, G. W., and Erbe, J. (1973a) *J. Cell. Physiol.* **83**, 321-336

Plagemann, G. W., and Erbe, J. (1973b) *J. Cell. Physiol.* **83**, 337-344

Plagemann, G. W., Wohlheuter, R. M., and Woffendin, C. (1988) *Biochem. Biophys. Acta* **947**, 405-443

Pontius, B. W. (1993) *Trends Biochem. Sci.* **18**, 181-186

Pötsch, S., Sahlin, M., Langelier, Y., Gräslund, A., and Lassmann, G. (1995) *FEBS Letters* **374**, 95-99

Reichard, P. (1958) *Biochim. Biophys. Acta* **27**, 434-435

Reichard, P. (1988) *Ann. Rev. Biochem.* **57**, 349-374

Reichard, P. (1993) *Science* **260**, 1773-1777

Rosenthal, F., Wislicki, L., and Koller, L. (1928) *Klin. Wochstr.* **7**, 972-977

Sahlin, M., Gräslund, A., Petersson, L., Ehrenberg, A., and Sjöberg, B.-M. (1989) *Biochemistry* **28**, 2618-2625

Sahlin, M., Petersson, L., Gräslund, A., Ehrenberg, A., and Sjöberg, B.-M., and Thelander, L. (1987) *Biochemistry* **26**, 5541-5548

Sanders-Loehr, J. (1989) in *Iron Carriers and Iron Proteins* (Loehr, T. M., ed) pp. 375-466, VHC Publishers Inc., New York

Sarup, J. C., and Fridland, A. (1987) *Biochem.* **26**, 590-597

Sather, M. R. Weber, C. E., Preston, J. D., Lyman, G. H., and Sleight, S. M. (1978) *Cancer Chemotherapeutic Agents: Handbook of Clinical Data* 69-71, G.K. Hall & Co.; Boston

Shewach, D. S. (1992) *Anal. Biochem.* **206**, 178-182

Sjöberg, B.-M. (1994) *Structure* **2**, 793-796

Sjöberg, B.-M., Karlsson, M., Jörnvall, H. (1987) *J. Biol. Chem.* **262**, 9736-9743

Sjöberg, B.-M., Loehr, T. M., and Sanders-Loehr, J. (1982) *Biochemistry* **21**,96-102

Sjöberg, B.-M., Reichard, P., Gräslund, A., and Ehrenberg, A (1977) *J. Biol. Chem.* **252**, 536-541

Skoog, L., and Nordenskjöld, B. (1971) *Eur. J. Biochem.* **19**, 81-89

Slabaugh, M. B., Howell, M. L., Wang, Y., and Mathews, C. K. (1991) *J. Virol.* **65**, 2290-2298

Slabaugh, M. B., and Mathews, C. K. (1984) *J. Virol.* **52**, 501-506

Slabaugh, M. B., Roseman, N., Davis, R., and Mathews, C. K. (1988) *J.Virol.* **62**, 519-527

Spector, T., and Cleland, W. W. (1981) *Biochem. Pharmacol.* **30**, 1-7

Stock, C. C., Clarke, D. A., Philips, F. S., Barclay, R. K., and Myron, S. A. (1960) *Cancer Res.* **20**, 193-382

Stubbe, J. A., and Ackles, D (1980) *J. Biol. Chem.* **255**, 8027-8030

Stubbe, J. A., Ator, M. A., and Krenitsky, T (1983a) *J. Biol. Chem.* **258**, 1625-1630

Stubbe, J. A., and Kozarich, J. W. (1980) *J. Am. Chem. Soc.* **102**, 2505-2507

Stubbe, J. A., Smith, G. and Blakley, R. L. (1983b) *J. Biol. Chem.* **258**, 1619-1624

Tagger, A. Y., Boux, J., and Wright, J. A. (1987) *Biochem. Cell. Biol.* **65**, 925-929

Tamao, Y. and Blakley, R. L. (1973) *Biochemistry* **12**, 24-34

Tengelsen, L. A., Slabaugh, M. B., Bibler, J. K., and Hruby, D. E. (1988) *Virology* **164**, 121-131

Thelander, L. (1973) *J. Biol. Chem.* **248**, 4591-4601

Thelander, L. (1974) *J. Biol. Chem.* **249**, 4858-4862

Thelander, L., Larsson, A., Hobbs, J., and Eckstein, F. (1976) *J. Biol. Chem.* **251**, 1398-1405

Thelander, L., and Gräslund, A. (1994). Ribonucleotide reductase in mammalian systems. In *Metal Ions in Biological Systems* (Sigel, H. and Sigel, A., eds), pp. 109-129, Marcel Dekker, Inc., New York.

Thelander, M., Gräslund, A., and Thelander, L. (1985) *J. Biol. Chem.* **260**, 2737-2741

Timson, J. (1975) *Mutat. Res.* **32**, 115-131

Traut, T. (1994) *Mol. Cell. Biochem.* **140**, 1-22

Tseng, M.-J., Hilfinger, J. M., He, P., and Greenberg, G. R. (1992) *J. Bacteriol.* **174**, 5740-5744

Uhlin, U. and Eklund, H. (1994) *Nature* **370**, 533-539

Uhlin, U. and Eklund, H. (1996) *J. Mol. Biol.* **262**, 358-369

Uhlin, U., Uhlin, T., and Eklund, H. (1993) *FEBS Letters* **336**, 148-152

von Döbeln, U. and Reichard, P. (1976) *J. Biol. Chem.* **251**, 3616-3622

Young, P., Öhmann, M., Xu, M. Q., Shub, D. A., and Sjöberg, B.-M. (1994) *J. Biol. Chem.* **269**, 20229-20232

Young, P., Andersson, J., Sahlin, M., and Sjöberg, B.-M. (1996) *J. Biol. Chem.* **271**, 20770-20775

Zannis, V., Doyle, D., and Martin, D. W. (1978) *J. Biol. Chem.* **253**, 504-510

Appendices

Appendix I

RNR Four-Substrate Assay Procedure

Preparation of the reaction mixture

Reaction mixture volumes are 100 µl per point. Routinely, reactions are performed in 50 mM HEPES buffer (pH 8.2) containing 0.1 M KCl, 50 mM DTT, and 4 µM $Fe(NH_4)_2(SO_4)$. 1.0 µM R1 and a molar excess of R2 are a typical protein concentrations. Substrates and effectors are added to the reaction mixture at the desired concentrations at the start of the reaction.

1. After the addition of substrate, the reaction mixture is incubated in a water bath for a specific amount of time.
2. Reactions are quenched by the addition of 5 µl of 50% perchloric acid (PCA). After addition of PCA, samples are vortexed and placed on ice. After 5 minutes on ice, the reaction mixture is neutralized by the addition of 1M NaOH (~28 µl).
3. Add 5 µl of 1M NH_4HCO_3 (pH 8.9) and 1.5 µM of 0.1 M $MgCl_2$ to each sample and transfer to Nanospin device, or equivalent, to remove protein. Centrifuge for 6 minutes at 15000 rpm. Add 100 µl of boronate column buffer (see below) to sample and centrifuge again for 6 minutes.
4. Remove filtrate from Nanospin tube and apply to boronate column.

Boronate chromatography

Ribonucleotides are removed from the sample by boronate chromatography on Bio-Rad Affi-gel 601. Deoxyribonucleotides do not bind to the column and are collected in the flow-through. To prepare the column resin, weigh out 0.17 to 0.18 gm of Affi-gel 601

and resuspend in 1.5 ml of column buffer. Allow to swell ~30 min. prior to filling column.

1. Apply sample to a column constructed from a 1.0 ml tuberculin syringe containing 1.0 ml of Affi-gel 601 preequilibrated with buffer containing 50 mM NH_4HCO_3 and 15 mM $MgCl_2$ (pH 8.9). Discard the first 200 µl of eluate.
2. Elute deoxyribonucleotides by washing column with column buffer while collecting a 1.8 ml fraction.
4. Acidify the boronate column eluate to pH 3-4 prior to HPLC analysis.

   note: Affi-gel resin can be regenerated and reused many times. To regenerate, wash column extensively (20-30 ml) with 0.1 M sodiumtetraborate (borax) (pH 8.9). Reequilibrate with 20to 30 ml of 50 mM NH_4HCO_3, 15 mM $MgCl_2$ (pH 8.9) buffer prior to use. Store column at 4° C. Column can be reused as many as 20 times without loss of performance.

HPLC analysis

The dNDP products and dNTP effectors are separated and quantitated by anion-exchange HPLC on a Partisphere-10 SAX column (4.6 mm x 25 cm, Whatman) with detection at 260 nm. Column is equilibrated in 0.075 M monobasic ammonium phosphate (pH to 3.7 with H_3PO_4), and deoxyribonucleotides are eluted with a biphasic gradient of monobasic ammonium phosphate ranging in concentration from 0.075 to 1.0 M (pH 3.7) at a flow rate of 1.5 ml/min. dNDP quantities are determined by peak areas and are calculated from the response factors obtained from authentic standards. See Appendix V for validation of the four-substrate assay.

Appendix II

Preparation of γ-phosphate linked dATP-sepharose

Required Reagents

i) 2'-deoxyadenosine-5'-(γ-aminophenyl)-triphosphate
USB catalog no. 77121

ii) Cyanogenbromide activated Sepharose 4B
Pharmacia Biotech (code no. 17-0430-01)

Procedure

1. 7.5 g of Sepharose 4B was suspended in 2 mM HCl and poured onto a scintered glass funnel. The resin contained in the funnel was then washed with ~ 2 liters of 2 mM HCl over a 15-20 minute period.
2. The ligand (γ-aminophenyl dATP) was dissolved in 40 ml coupling buffer (0.1 M NaHCO3, 0.5 M NaCl, pH 8.3) and the absorbance of a 10X dilution at 260 nm was recorded.
3. After the HCl wash of the Sepharose is finished, the resin was then washed with several hundred milliliters of coupling buffer and added to the ligand solution.
4. The suspension was rotated, or rocked (do not use magnetic stirring), for 3 hours at room temperature.
5. After coupling for 3 h, the gel was allowed to settle and the absorbance at 260 nm of a 10X dilution of the supernatant was recorded (this allows the coupling efficiency to be calculated; >90 % coupling is normally seen).
5. Supernatant was decanted and the resin was resuspended in 0.1 M Tris-HCl, pH 8.3, and rotated overnight at 4 deg. C (this blocks unreacted active sites).

6. Resin was washed in alteration 3 times with 0.1 M acetate, 0.5 M NaCl, pH 4.0 and 0.1 M Tris-HCl, 0.5 M NaCl, pH 8.3. Store in refrigerator in Tris buffer containing NaN_3.

note: This resin goes a long way. For a 1-2 liter culture of overexpressed R1 I usually pour a 1.0 ml column. The column can be re-used approximately ten times.

Appendix III

Procedure for dNDP & dNTP analysis of whole cell extracts

Extraction

The following extraction procedure is adapted from E. Muller (1994) *J. Biol. Chem.* **269**, 24466-24471. The procedure described below was used for extracting BSC_{40} cells and yeast. The procedure should also be useful for extracting other types of cells, with minor modifications.

1. 3 plates BSC_{40} cells (~10^7 cells/plate) or 100 ml of yeast cells grown to 50-100 Klett units (~2 x 10^7 cells/ml).
2. Remove 1.0 ml for quantification of cell number.
3. Pour cells into graduated cylinder, record volume, and harvest cells by rapid filtration on nylon membranes (47 mm x 0.8 μm, Schleicher & Schuell, or equivalent). For cultured cells grown on plates: wash the cells with ice-cold PBS, scrape cells with rubber policeman into a centrifuge tube, add 10 ml PBS per plate to resuspend cells, centrifuge at low speed to pellet cells. Resuspend cells again in known volume of PBS, remove aliquot for determination of cell number, and centrifuge again at low speed to pellet cells. In order to extract enough dNTPs for analysis from cultured cells, 3 plates of approximately 10^6 cells/plate are required for each determination.
4. Place nylon filter, cell-side down, onto a crystallization dish containing 2.0 ml of ice-cold 10% trichloroacetic acid (TCA). Swirl plate gently on ice for 10 minutes. In the case of cells scraped from plates, resuspend the washed pellet containing 3 plate equivalents of cells in 2.0 ml of ice-cold water. Once suspended, add 2.0 ml of 10% TCA and place on ice for 5 min., swirling occasionally.

5. When extracting yeast, transfer the filter and solution to a 50-ml conical tube and vortex. Place on ice for an additional 20 minutes.
6. Centrifuge extract to pellet cell debris and collect supernatant containing dNTPs.
7. Neutralize TCA extract with 3.3 ml cold Freon-amine reagent. Freon-amine reagent is prepared by mixing 2.2 ml of N-trioctylamine with 7.8 ml Freon (store in refrigerator and use within a couple days). Vortex the neutralized solution, centrifuge to separate phases and transfer the **upper** phase to a new tube. Check pH. If pH > 6, go to step 8. If pH < 6, extract again with Freon-amine reagent.
8. Lyophilize extract to dryness.

Boronate chromatography

Ribonucleotides are removed from the extract by boronate chromatography on Bio-Rad Affi-gel 601. Deoxyribonucleotides do not bind to the column and are collected in the flow-through.

1. Resuspend lyophilized extract in 0.9 ml H_2O, add 100 µl 1.0 M ammonium acetate (pH 8.8). Adjust pH to 8.8 if necessary and centrifuge if any insoluble material remains.
2. Apply sample to a 1 x 5 cm column of Affi-gel 601 pre equilibrated with 0.1 M ammonium acetate (pH 8.8).
3. Elute dNTPs by washing column with 0.1 M ammonium acetate (pH 8.8). Collect 1.0 or 2.0 ml fractions. Pool fractions containing UV absorbing material (260 nm).
4. Lyophilize pooled fractions to dryness.

note: Affi-gel resin can be regenerated and reused many times. To regenerate, wash column extensively with 0.1 M sodiumtetraborate (borax) (pH 8.8). Reequilibrate with ammonium acetate buffer prior to use. Store column at 4° C.

HPLC analysis

For more detail on HPLC analysis see Hendricks, S.P., & Mathews, C.K. (1997) *J. Biol. Chem.* **272**, 2861-2865. dNTPs are separated and quantitated by anion-exchange HPLC on a Partisphere-10 SAX column (4.6 mm x 25 cm, Whatman) with detection at 260 nm. Column is equilibrated in 0.075 M monobasic ammonium phosphate (pH 3.7), and dNTPs are eluted with a biphasic gradient of monobasic ammonium phosphate ranging in concentration from 0.075 to 1.0 M (pH 3.7) at a flow rate of 1.5 ml/min. Prior to HPLC analysis, the boronate eluate must be treated with periodate to remove any contaminating ribonucleotides which may have eluted through boronate column.

1. Resuspend sample in 80 µl of H_2O. Add 16 µl 0.5 M $NaIO_4$ (prepared fresh). Vortex and incubate at 37° C in the dark for 2 minutes.
2. Add 20 µl 4 M CH_3NH_2-HCl (freshly prepared and neutralized to pH 7 with ammonium hydroxide). Vortex and incubate at 37° C for 30 minutes.
3. Add 4 µl 1M rhamnose to quench remaining periodate.
4. Adjust pH of sample to match pH of HPLC mobile phase (pH 3.7) with phosphoric acid and inject a reasonable portion onto the HPLC ("reasonable" depends on HPLC system and detection limit, as well as extraction efficiency. Generally you should have enough dNTPs in the yeast extract to do 2 to 4 injections. Extracts from cultured mammalian cells may only contain enough dNTPs for 1 or 2 injections).

Appendix IV

Measurement of *Escherichia coli* RNR Activity by Use of the Four-Substrate Assay:

Application of the Method to the Measurement of Nucleoside Diphosphate Kinase Activity and Inhibition of ADP Reduction by 5′-adenylylimidodiphosphate

The R1 and R2 subunits of the ribonucleotide reductase from *Escherichia coli* were provided by the laboratory of Britt-Marie Sjöberg, Stockholm University, Sweden. The results of assays done using the *E. coli* holoenzyme illustrate that the four-substrate assay may also be useful for the measurement of nucleoside diphosphate kinase (NDPK) activity, as well the activities of other enzymes involved in the biosynthesis of deoxyribonucleotides, and can be used to investigate potential kinetic coupling between these enzymes. Furthermore, the results of experiments included in this appendix illustrate the utility of this assay in evaluating the effects of nucleotide effector analogues on the regulation of ribonucleotide reductase.

Reaction conditions

The reaction mixture was prepared essentially as described in Appendix I. The reaction buffer in these experiments was composed of 50 mM HEPES (pH 7.6), 15 mM MgCl, and 50 mM DTT. ATP was added to a final concentration of 2.0 mM. Protein concentrations in the reaction mixture were 3.0 and 4.5 μM, R1 and R2, respectively, and were based on the published molar extinction coefficients (R1: $e_{(280\text{-}310\ nm)}$ = 180,000 $M^{-1}cm^{-1}$, and R2: $e_{(280\text{-}310\ nm)}$ = 120,000 $M^{-1}cm^{-1}$; Karlsson *et al.*, (1992) *J. Biol. Chem.* **267**, 12622). The four NDP substrates were added to the reaction mixture at equimolar concentrations (0.15 mM each) at time = 0. In these experiments, the reactions were quenched at the times indicated by the addition of 5 μl 1M hydroxyurea followed by immediate immersion into

liquid nitrogen (note that this is significantly different from the routine method used to quench the reaction and was used only in a limited number of experiments).

Results

Figure A4.1 shows the results from one of the *E. coli* ribonucleotide reductase assays done using the four substrate assay. What is obvious from this figure is that this particular preparation of *E. coli* RNR was contaminated with a high level of NDPK-like activity. This was corroborated by SDS-PAGE analysis of the individual subunits (gel not shown) which demonstrated the presence of many bands other than those corresponding to the R1 and R2 proteins.

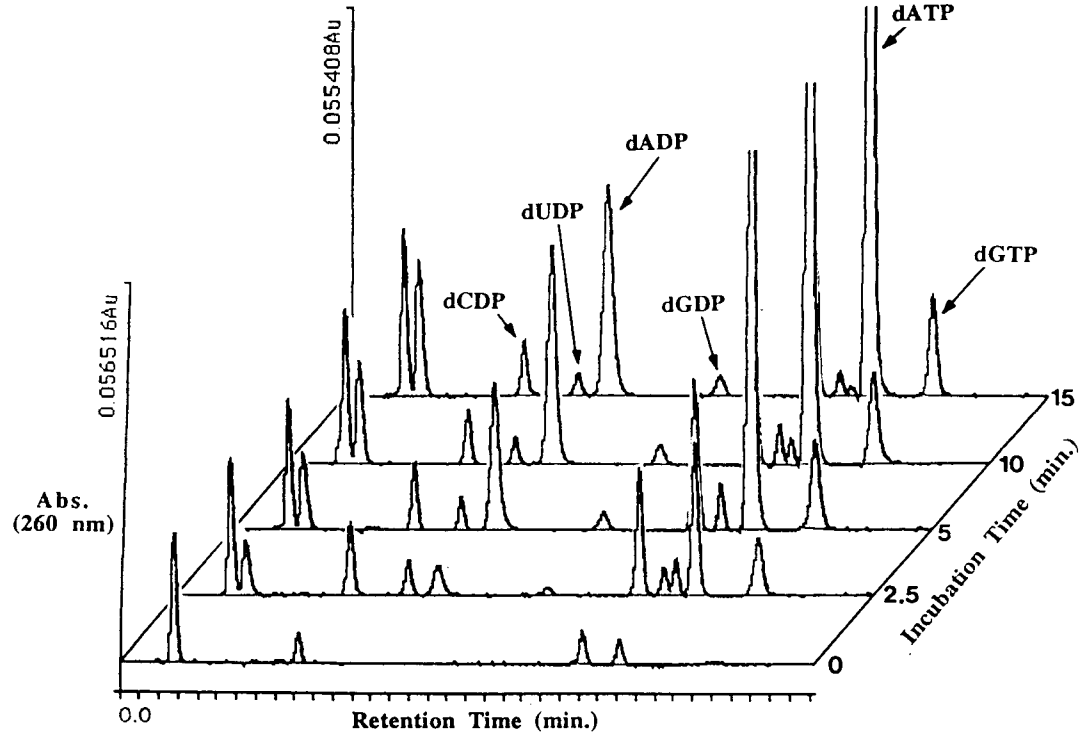

Figure A4.1 **Analysis of the *E. coli* RNR activity as analyzed by the four-substrate assay.** In this experiment, ATP was the only allosteric effector added to the reaction mixture. The substrates were present at equimolar concentrations.

In the context of the biosynthesis of deoxyribonucleotides, NDPK catalyzes the following general reaction:

$$ATP + dNDP \rightleftharpoons ADP + dNTP$$

Since the reaction mixture contained a relatively high concentration of ATP (as compared to the substrate concentrations), there will be plenty of nucleoside triphosphate available to serve as a phosphate donor for the production of dNTPs. As dNDPs are produced in the reaction catalyzed by *E. coli* RNR, they will undergo phosphorylation to the corresponding dNTP by the contaminating NDPK-like activity. This partially explains why dCDP, for example, increases in concentration after 2.5 minutes and then appears to decrease at later time points. The increase in dCTP which occurs over time corroborates this point. In contrast, the dADP peak increased steadily over time. This is explained by considering the NDPK-catalyzed reaction shown above. As ATP is dephosphorylated, ADP is produced. Therefore, the supply of this particular RNR substrate will be maintained in the reaction mixture during the entire course of the experiment, while the other substrates, CDP, UDP, and GDP, will be depleted over time due to the RNR and NDPK-like activities.

Although the RNR preparation used in these experiments was contaminated with an NDPK-like activity, the following qualitative conclusions regarding the regulation of the *E. coli* RNR can be made:

i) Like the other forms of RNR examined in my research, when ATP was the only nucleoside triphosphate effector added to the reaction mixture, the *E. coli* enzyme primarily reduced CDP. In contrast, the reduction of UDP was minimal.

ii) Similar to the T4 RNR, but unlike the vaccinia RNR, GDP reduction by the *E. coli* enzyme was low compared to the reduction of the other substrates.

In order to obtain more information about the regulation of the *E. coli* RNR, I decided to use a non-hydrolyzable ATP analogue, 5′-adenylylimidodiphosphate (AMP-PNP), to activate the enzyme. AMP-PNP has been used previously to activate RNR in cell extracts containing high levels of ATPase activity (Slabaugh *et al.*, 1991). With the assumption that this ATP analogue should not be capable of functioning as a phosphate donor for NDPK, the contaminating NDPK-like activity should be negligible in the presence of AMP-PNP. Figure A4.2 shows the results of the *E. coli* RNR assay performed in the presence of AMP-PNP.

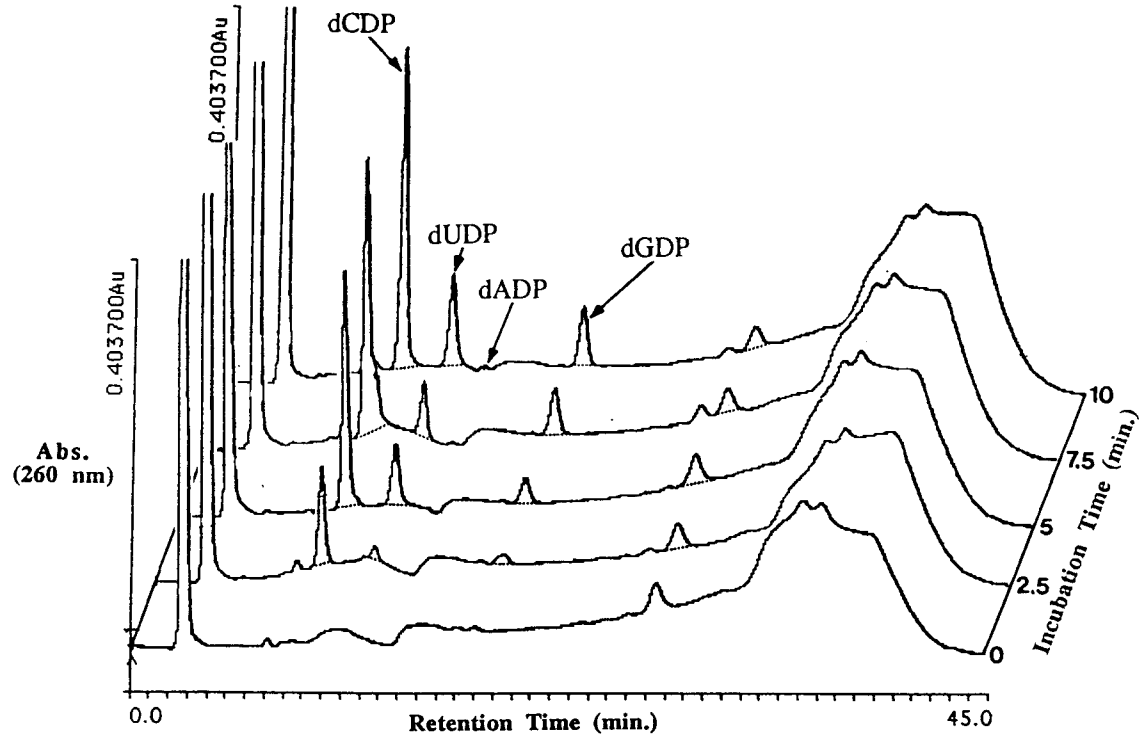

Figure A4.2 **Activation of the E. coli RNR by AMP-PNP.** The conditions used in these experiments were identical to those of Figure A4.1, except that ATP was replaced with AMP-PNP (1 mM).

As predicted, the substitution of AMP-PNP for ATP in the reaction mixture decreased the formation of dNTPs to negligible levels. However, the results also indicate that AMP-PNP does not activate RNR in the same way that ATP does. When AMP-PNP was added to the reaction mixture, the reduction of ADP was completely inhibited, while the rates of formation of the other products were approximately the same as the rates observed when ATP was used as the allosteric activator.

The inhibitory effect of AMP-PNP on the reduction of ADP does not appear to be limited to the *E. coli* RNR. Similar results were obtained when the vaccinia RNR was assayed in the presence of AMP-PNP (data not shown; see SPH notebook #7, page 20).

Appendix V

Ribonucleotide Reductase Four-Substrate Assay Method Validation

The method validation procedure described in this appendix is used to verify that the ribonucleotide reductase four-substrate assay is functioning properly. This validation procedure, or a modification of this procedure, should be performed whenever the results of an experiment are in question, or when a new batch of boronate column resin is purchased. Furthermore, it is recommended that this validation procedure be performed by persons using the assay method for the first time.

Validation procedure

To evaluate the performance of the HPLC system, and to determine, or verify, the response factors and retention times for each nucleotide, a sample containing each of the deoxyribonucleotides of interest is prepared, using good analytical technique, and analyzed according to the HPLC method described in Appendix I. Figure A5.1 shows a typical HPLC analysis of deoxyribonucleotide authentic standards. In this example, precise volumes of carefully prepared nucleotide stock solutions were added to HPLC buffer A to give a final concentration of 0.6 μM each. 500 μl of this nucleotide mixture was injected onto a Partisil 10 SAX column and separated using an $NH_4H_2PO_4$ gradient (0.075 to 1.0 M, pH 3.7).

From these data, the response factors, or the peak area corresponding to 1.0 mole of a particular nucleotide, can be determined for each species by dividing the peak area by the number of moles injected. These values are then used to calculate the moles of dNDP formed in the assay from the peak areas corresponding to each product. The absolute value of these response factors will vary as the detector lamp ages (or with different detectors)

and therefore, should be determined for each set of experiments. Of course, the retention times of the standards need to be determined each time fresh buffer is prepared. This is an obvious time to also determine the response factors.

Date: Sun, Mar 22, 1998 7:01 PM
Data: sph.03-22MAR98-008

Sample: Method Validation:

deoxyribonucleotide authentic std. mix (6/23/97 stock)
300 picomoles each injected

Processing File: steve's process
Method: sph.03
Inject Vol: 500
Sampling Int: 0.3 Seconds

Chromatogram:

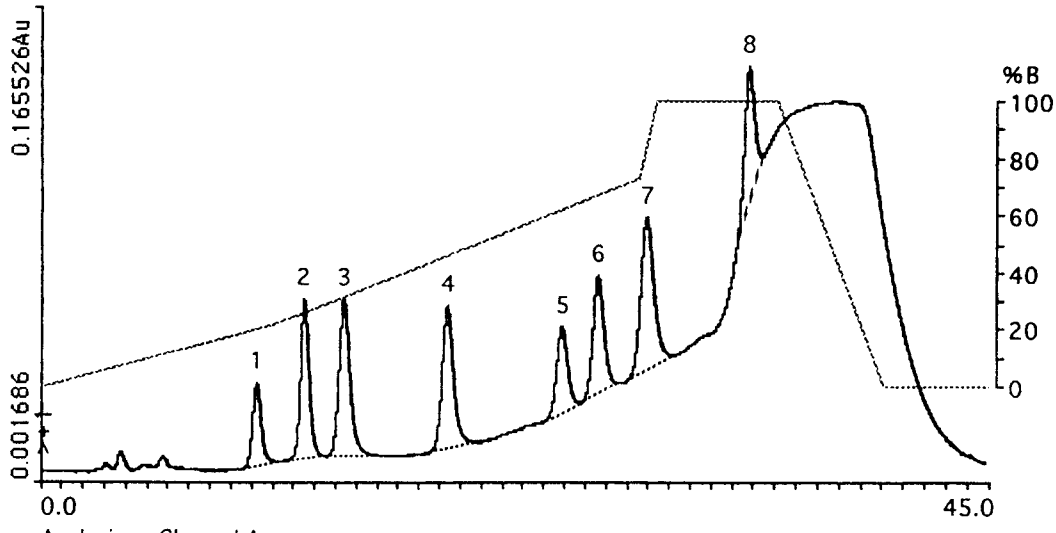

Analysis: Channel A

Peak No.	Time	Type	Height(Au)	Area(μV-sec)
1	10.245	*N	0.029146	440173
2	12.520	*N	0.055250	782497
3	14.395	*N	0.055032	1021196
4	19.360	*N	0.049450	953333
5	24.860	*N	0.029786	544219
6	26.605	*N	0.041428	753570
7	28.915	*N	0.053176	1135116
8	33.750	*N	0.046444	700281

Figure A5.1 **HPLC chromatogram of the deoxyribonucleotide authentic standards.** Peak identities are: Peak No. 1, dCDP; 2, dUDP; 3, dADP; 4, dGDP; 5, dCTP; 6, dTTP; 7, dATP; and 8, dGTP.

To evaluate the performance of the boronate column chromatography for each of the four ribonucleotide reductase reactions, two solutions are prepared, each of which contains two NDPs and two dNDPs of different nucleobase identity. In the example shown in this appendix, mixture 1 contained CDP, ADP, dUDP, and dGDP, and mixture 2 contained the converse of mixture 1, dCDP, dADP, UDP, and GDP. The concentrations of the nucleotides should be set to levels similar to what would be present in a typical reaction mixture. In addition, all other components present in the reaction mixture, excluding the enzyme, should be added to the sample. In the following example, the nucleotides were added to a final concentration of 0.1 mM each in HEPES buffer containing 2 mM $MgCl_2$ (pH 8.2). A 100-µl aliquot (the same volume as the reaction mixture used in the assay) of mixture 1 was added to 1.7 ml of boronate column buffer (50 mM NH_4HCO_3, 15 mM $MgCl_2$, pH 8.9). The sample was diluted in this way in order to mimic the sample dilution that occurs as a result of the boronate chromatography step. After acidification to pH 3-4 with H_3PO_4, 500 µl of this "pre-boronate" sample was injected onto the column. Figure A5.2 shows the results of the HPLC analysis of mixture 1 prior to boronate column chromatography.

To determine the retention of ribonucleotides and recovery of deoxyribonucleotides from the boronate chromatography step, another aliquot of mixture 1 was treated identically to that of an actual assay sample, and the HPLC results compared to the those of the "pre-boronate" sample. To 100 µl of mixture 1, 5 µl of 1 M NH_4HCO_3, pH 8.9, and 1.5 µl 1M $MgCl_2$ were added, followed by the addition of 100 µl of boronate column buffer. The resulting ~200-µl sample was applied to a 1.0 ml boronate column and washed with column buffer while collecting 1.8 ml of eluate (see Appendix I for more detail). The boronate column eluate was acidified, as above, prior to the injection of 500 µl onto the column.

Figure A5.3 shows the results from the HPLC analysis of the "post-boronate" sample. Comparison of the HPLC results obtained from the pre- and post-boronate column samples

allows the efficiency of the boronate chromatography step to be assessed. In this particular example, no UDP or GDP was detected in the post-boronate sample, indicating the effectiveness of the boronate resin at removing ribonucleoside diphosphates. Furthermore, the area counts corresponding to the dCDP and dADP peaks in the post-boronate sample can be compared to the corresponding peak areas in the pre-boronate sample to determine the recovery of deoxyribonucleotides after boronate chromatography. In this particular example, 95.2 and 95.8% of dCDP and dUDP, respectively, were recovered from the boronate column.

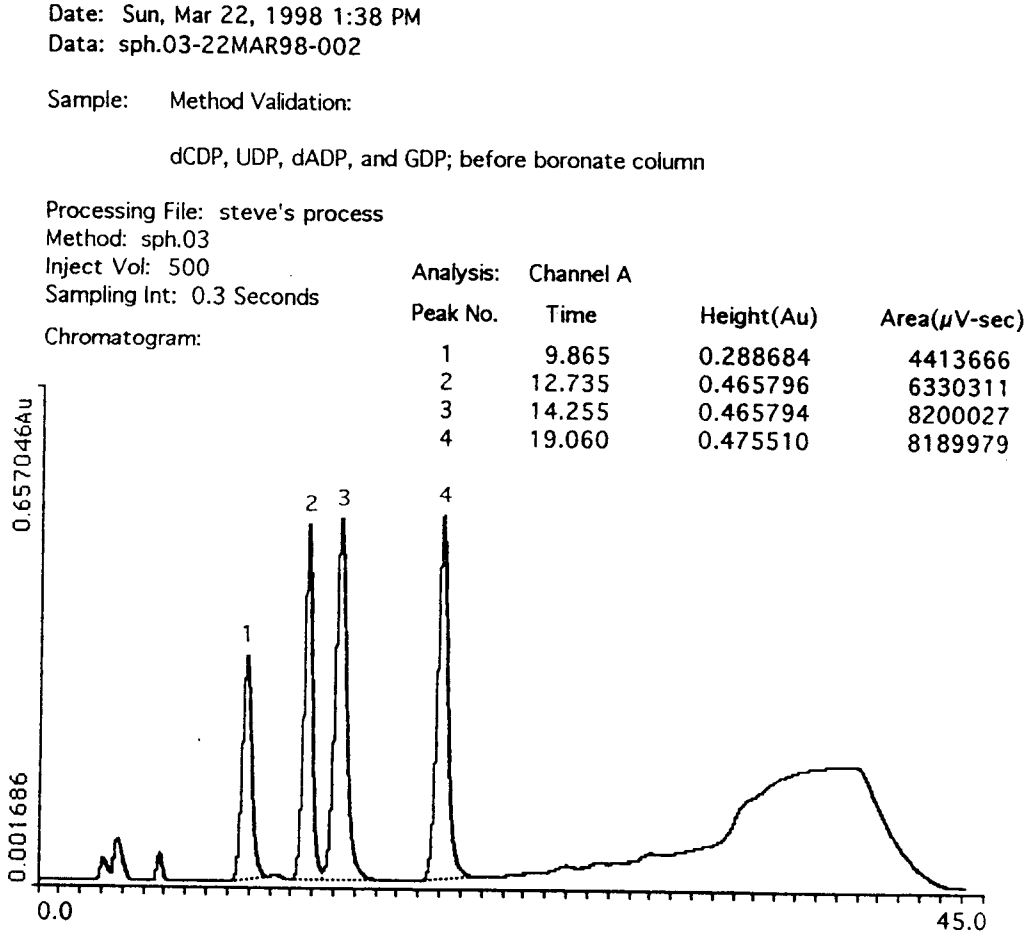

Figure A5.2 **HPLC analysis of nucleotide mixture 1 prior to boronate chromatography**. Peak identities are as follows: Peak No. 1, dCDP; 2, UDP; 3, dADP; and 4, GDP.

Date: Sun, Mar 22, 1998 2:27 PM
Data: sph.03-22MAR98-003

Sample: Method Validation:

dCDP, UDP, dADP, and GDP; after boronate column

Processing File: steve's process
Method: sph.03
Inject Vol: 500
Sampling Int: 0.3 Seconds

Chromatogram:

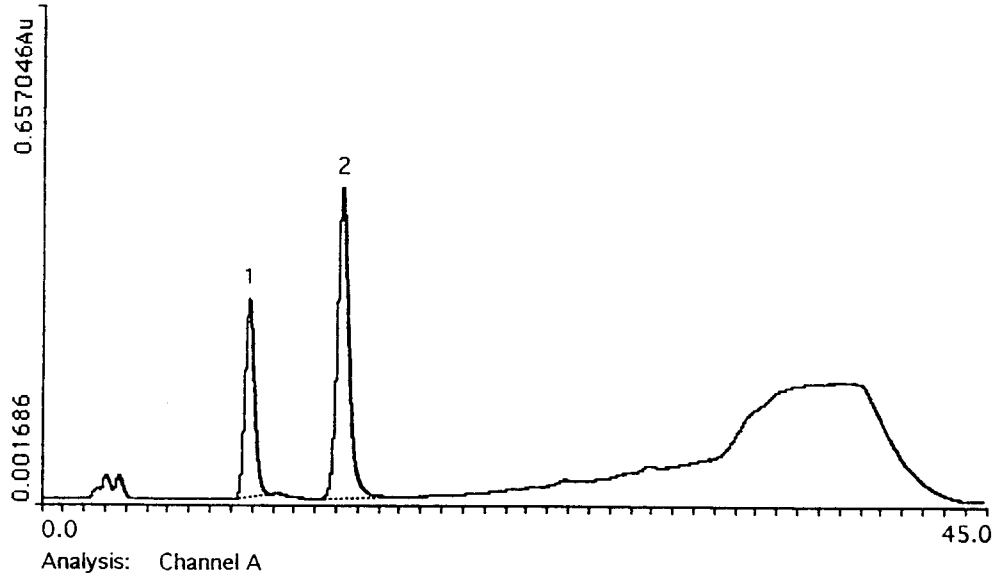

Analysis: Channel A

Peak No.	Time	Type	Height(Au)	Area(μV-sec)
1	9.850	*N	0.266600	4202976
2	14.260	*N	0.413940	7856406

Figure A5.3 **HPLC analysis of nucleotide mixture 1 following boronate chromatography**. Peak identities are: Peak No. 1, dCDP; and 2, dADP.

A similar analysis of the pre- and post-boronate column HPLC results of mixture 2 will allow the performance of the boronate column chromatography to be evaluated in terms of the other four nucleotides of interest. Figures A5.4 and A5.5 show the HPLC analyses of the pre- and post-boronate column samples, respectively, prepared from nucleotide mixture 2. Again, the HPLC chromatogram corresponding to the post-boronate sample showed no indication of the presence of ribonucleoside diphosphates. Recovery of the dNDPs present in mixture 2 from the boronate column were calculated to be 99.1 % for dUDP, and 94.2 % for dGDP. The recovery of dUDP is probably overestimated in this example because of the fact that dUDP and ADP are not completely resolved, making the dUDP peak area difficult to accurately determine.

One more important point regarding the repeatability and accuracy of the four-substrate assay should be made here. The method has a built-in mechanism by which the proper functioning of the assay can be evaluated in each and every sample. As Figure A5.6 illustrates, the HPLC method used in the assay gives resolution of ADP and dADP. At concentrations lower than those shown in this example, these peaks are baseline resolved. If the boronate chromatography doesn't function efficiently, substrate will leak through the column and be collected in the initial eluate containing the products of the reaction catalyzed by ribonucleotide reductase. Because the substrate, ADP, is resolved from the product, dADP, the presence of a doublet at the relative retention time of dADP should alert the researcher to the fact that the boronate column step may not be functioning properly. Furthermore, as is illustrated in Figure A5.4, ADP is also resolved from the product dUDP. Therefore, if ADP does leak through the boronate column, the absorbance due to this substrate will be distinguishable from the absorbance arising from products. Although it is not shown in Figure A5.6, GDP and dGDP are also resolved by the HPLC method. This gives the assay procedure another built-in check on the performance of the method. Interestingly, the pyrimidine ribonucleotides and the corresponding deoxyribonucleotides are not resolved under these HPLC conditions.

Date: Sun, Mar 22, 1998 3:28 PM
Data: sph.03-22MAR98-004

Sample: Method Validation:

CDP, dUDP, ADP, and dGDP; before boronate column

Processing File: steve's process
Method: sph.03
Inject Vol: 500
Sampling Int: 0.3 Seconds

Chromatogram:

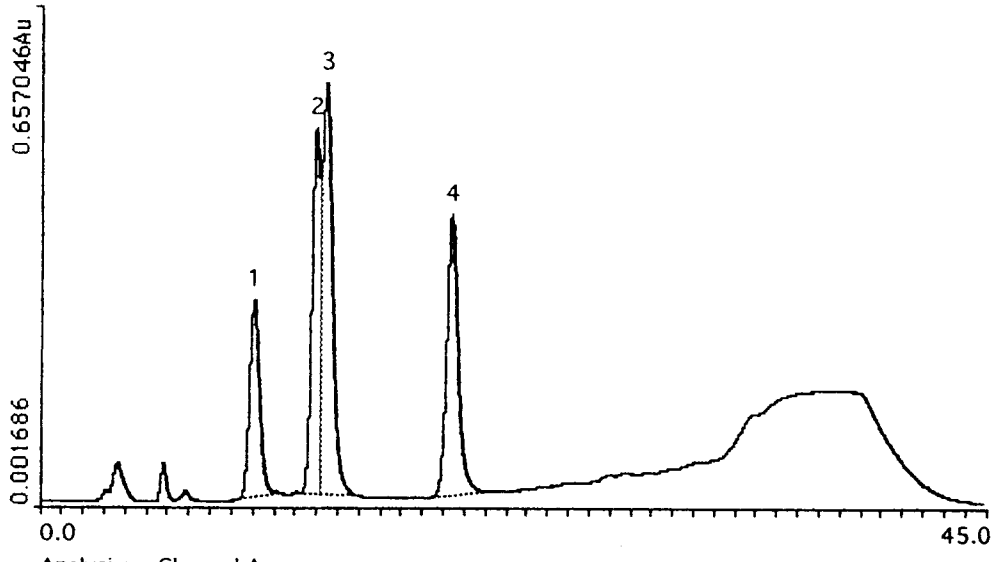

Analysis: Channel A

Peak No.	Time	Type	Height(Au)	Area(μV-sec)
1	10.060	*N	0.264578	4408601
2	12.945	*N1	0.480544	6128723
3	13.440	*N2	0.540250	9376769
4	19.385	*N	0.365222	6569200

Figure A5.4 **HPLC analysis of nucleotide mixture 2 prior to boronate chromatography**. Peak identities are: Peak No. 1, CDP; 2, dUDP; 3, ADP; and 4, dGDP.

Date: Sun, Mar 22, 1998 4:16 PM
Data: sph.03-22MAR98-005

Sample: Method Validation:

CDP, dUDP, ADP, and dGDP; after boronate column
(started collecting after sample completely entered gel)

Processing File: steve's process
Method: sph.03
Inject Vol: 500
Sampling Int: 0.3 Seconds

Chromatogram:

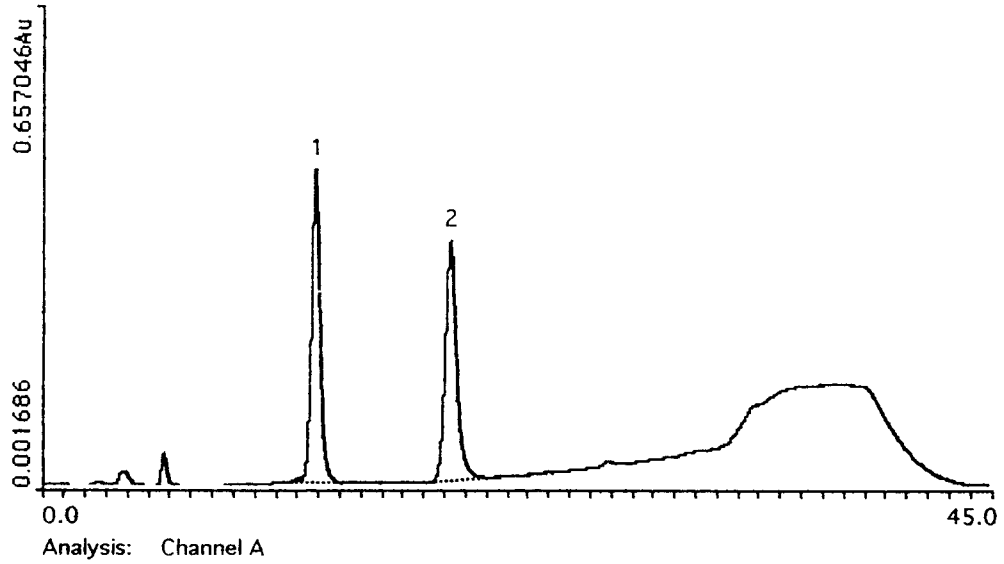

Analysis: Channel A

Peak No.	Time	Type	Height(Au)	Area(μV-sec)
1	12.830	*N	0.429562	6074434
2	19.255	*N	0.328770	6189619

Figure A5.5 **HPLC analysis of nucleotide mixture 2 following boronate chromatography**. Peak identities are: Peak No. 1, dUDP; and 2, dGDP.

Date: Sun, Mar 22, 1998 5:21 PM
Data: sph.03-22MAR98-006

Sample: Method Validation:

500 picomoles of dADP and ADP injected

Processing File: steve's process
Method: sph.03
Inject Vol: 500
Sampling Int: 0.3 Seconds

Chromatogram:

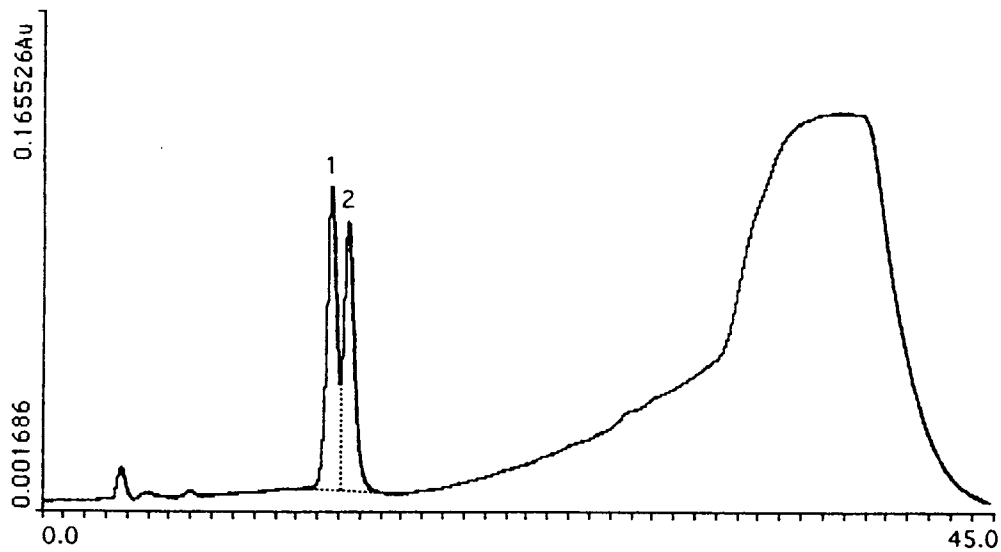

Analysis: Channel A

Peak No.	Time	Type	Height(Au)	Area(μV-sec)
1	13.630	*N1	0.100594	1641971
2	14.435	*N2	0.089252	1612548

Figure A5.6 **HPLC chromatogram showing partial resolution of ADP and dADP.** Under the HPLC conditions used in the four-substrate assay, ADP elutes just prior to dADP.